

**STUDY OF SYNCHRONISATION AND CONTROL
OF CHAOS IN DIRECTLY MODULATED
SEMICONDUCTOR LASERS**

Bindu. V



**INTERNATIONAL SCHOOL OF PHOTONICS
COCHIN UNIVERSITY OF SCIENCE AND TECHNOLOGY**

G8535

**STUDY OF SYNCHRONISATION AND CONTROL OF CHAOS IN
DIRECTLY MODULATED SEMICONDUCTOR LASERS**

Bindu.V

Thesis submitted
in partial fulfilment of the requirements
for the Degree of
Doctor of Philosophy



**International School of Photonics
Cochin University of Science and Technology
Kochi - 682 022, India**

DECEMBER 2002

G 8 535

Study of Synchronisation and Control of Chaos in Directly Modulated Semiconductor Lasers
Ph. D Thesis

Author

Bindu.V

*Research Fellow, International School of Photonics,
Cochin University of Science and Technology
Kochi- 682 022, India
e-mail:bindumurali@eth.net*

Research Advisor

R
531.8 : 535.374
BIN

Prof. (Dr.) V.M.Nandakumaran

Head of the Department

*International School of Photonics,
Cochin University of Science and Technology
Kochi - 682 022, India*

*International School of Photonics
Cochin University of Science and Technology
Kochi-682 022, India.*

December 2002

International School of Photonics

A CENTRE OF HIGHER LEARNING DEDICATED TO THE SCIENCE AND TECHNOLOGY OF PHOTONICS

Cochin University of Science and Technology

Kochi - 682 022, INDIA

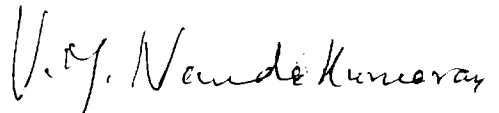
Dr. V. M. Nandakumaran

December 26, 2002

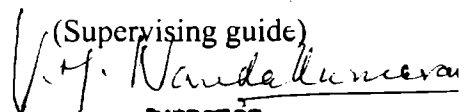
Professor & Head

CERTIFICATE

This is to certify that the work presented in the thesis entitled ***Synchronisation and Control of Chaos in Directly Modulated Semiconductor Lasers*** is based on the bonafide research work carried out by Bindu.V. under my guidance at the International School of Photonics, Cochin University of Science and Technology, Kochi – 682 022 and that no part thereof has been included in any other thesis submitted previously for the award of any Degree.



V. M. Nandakumaran

(Supervising guide)


DIRECTOR
International School of Photonics
Cochin University of
Science & Technology
Cochin - 682 022

DECLARATION

Certified that the work presented in the thesis entitled *Synchronisation and Control of Chaos in Directly Modulated Semiconductor Lasers* is based on the original work carried out by me under the guidance of Prof. (Dr.) V. M. Nandakumaran, Director, International School of Photonics, Cochin University of Science and Technology, Kochi – 682 022 and that no part thereof has been included in any other thesis submitted previously for the award of any Degree.

Kochi – 682 022

December 26, 2002



Bindu.V

Acknowledgements

I wish to place on record my deep sense of gratitude to Prof. V.M.Nandakumaran, Director, International School of Photonics, Cochin University of Science and Technology for his constant guidance and intellectual support which immensely helped me in completing my research work and submission of thesis in time.

I have received guidance, help and support, both intellectual and material, from Prof. C.P.Girijavallabhan, Prof. V.P.N.Nampoori, and Prof.. P.Radhakrishnan, all members of the faculty of the Department, which immensely helped me to carry out my research programmes in the right perspective. I express my sincere thanks to them.

The financial assistance received from Cochin University of Science and Technology and the Institutional facilities made available for carrying out the research programme are gratefully acknowledged.

I have great pleasure to convey my sense of appreciation to all fellow scholars of ISP and other friends for their help during the course of my work.

Bindu.V

Research Publications

1. Numerical studies on bi-directional coupled directly modulated semiconductor lasers. **V. Bindu** & V. M. Nandakumaran. Phys. Lett. A. **277** (2000) 345
2. Chaotic encryption using long wavelength semiconductor lasers. **V. Bindu** & V. M. Nandakumaran. J. Opt. A. Pure & Appl. Opt. **4** (2002) 115
3. Synchronisation of directly modulated semiconductor lasers through bi-directional coupling. **V. Bindu** & V. M. Nandakumaran. International Conference on Laser Materials and Devices (1999).
4. Synchronisation of directly modulated semiconductor laser using variable feedback method. **V. Bindu** & V. M. Nandakumaran. National Laser Symposium (1999)
5. Synchronisation of chaotic semiconductor laser array using a uni-directional closed loop coupling. **V. Bindu** & V. M. Nandakumaran. National Laser Symposium (2000).
6. Control of chaos in coupled array of semiconductor lasers. **V. Bindu** & V. M. Nandakumaran. International Conference on Stochastic Optimization and Adaptation. (2000)
7. Synchronisation of an array of chaotic semiconductor lasers. **V. Bindu** & V. M. Nandakumaran. Recent Advances in Nonlinear Dynamics, (2002)

PREFACE

Chaos is a subject of topical interest and, studied in great detail in relation to its relevance in almost all branches of science, which include physical, chemical, and biological fields. Chaos in the literal sense signifies *utter confusion*, but the scientific community has differentiated chaos as deterministic chaos and white noise. Deterministic chaos implies the complex behaviour of systems, which are governed by deterministic laws. Behaviour of such systems often become unpredictable in the long run. This unpredictability arises from the sensitivity of the system to its initial conditions. The essential requirement for '*sensitivity to initial condition*' is nonlinearity of the system. The only method for determining the future of such systems is numerically simulating its final state from a set of initial conditions.

Synchronisation and control are two aspects of chaotic dynamics. During the last decade there took place extensive studies leading to remarkable developments in the field of synchronisation of chaotic systems. Similarly control of chaotic lasers has also been an important topic of research. Synchronisation and control of chaotic semiconductor lasers assume great significance because of their potential use in communication systems and in designing high power sources. Semiconductor lasers because of their attributes such as compactness, reliability, low cost, efficiency, direct modulation capability and, above all, their characteristic output wavelength that fall in the

minimum loss and dispersion window of optical fibers, are ideal candidates for the above applications.

Various methods have been employed for achieving synchronisation and control of chaos. The methods used are different types of couplings such as uni-directional coupling, bi-directional coupling and feedback methods such as proportional feedback, variable feedback and occasional proportional feedback. Variants of these schemes are also in use. The emphasis in our studies was on the aspects of synchronisation and control of chaotic semiconductor lasers employing various types of coupling and feedback schemes.

Various aspects of our studies and, the results and conclusions are presented in eight chapters.

Chapter 1 outlines the general aspects of chaos in dynamical systems and provides a review of the relevant literature. Various mathematical tools and quantitative measures used in the characterisation of chaotic systems are described briefly. Different routes taken by a system to enter into chaotic regime are also discussed. The conditions necessary for chaos to occur in dynamical systems and the identifying characteristics of a chaotic system also are briefly described. Further, this chapter also delineates general characteristics of lasers and chaos in lasers with specific reference to semiconductor lasers. The mechanisms by which semiconductor lasers undergo transitions to the chaotic regime are also discussed.

Chapter 2 deals with synchronisation of chaotic systems in general. The different methods of synchronisation like drive response scheme, coupling scheme and feedback methods are described with the help of schematic diagrams. Various types of synchronisation in chaotic systems such as complete synchronisation, generalised synchronisation, phase synchronisation, lag synchronisation, exact synchronisation, practical synchronisation, partial synchronisation and almost synchronisation are reviewed. Special emphasis has been laid on the synchronisation aspects in chaotic laser systems. The different methods adopted for the synchronisation of chaotic Nd:YAG lasers, CO₂ lasers and semiconductor lasers are detailed. Control of chaos in dynamical systems with reference to laser systems is also discussed.

Chapter 3 covers a brief description of the laser model that we used for our numerical studies and its general dynamical properties. This chapter contains descriptions of rate equations governing the dynamics of directly modulated semiconductor lasers. Effects of modulation depth, modulation frequency, and nonlinear gain reduction factor on the output dynamics are explained. The period doubling route taken by this system to enter chaotic regime and the reverse period doubling route to enter stable regime are described. The parameter values that are used for our numerical studies are included at the end of this chapter.

Chapter 4 contains descriptions on the results of our numerical study on the use of uni-directional and bi-directional coupling schemes for synchronisation of two directly modulated chaotic semiconductor lasers and the types of synchronisation that could be achieved. Coupling schemes are described using schematic diagrams. Results of the studies on the effect of coupling strength on the output dynamics also are discussed. Bi-directional coupling scheme can give exact synchronisation between the two lasers whereas the uni-directional coupling can induce only practical synchronisation. The bi-directional coupling can provide synchronisation over a wider range of coupling strength compared to the uni-directional coupling. In addition, bi-directional coupling could achieve control over the synchronised chaotic outputs of the two semiconductor lasers and suppress the double peak nature of its output for large values of coupling strengths.

In Chapter 5 we present the results of numerical study of synchronisation of two chaotic semiconductor lasers using a variable feedback technique. In this method one of the lasers that are to be synchronised operate as the drive system and the other operate as the response system for synchronising it with the drive. The difference between the output of the response system and that of the drive system is calculated at each time step. A feedback current that is proportional to a small fraction of this difference is fed to the input of the response system. The range of feedback fraction value for which the two lasers are synchronised and the type of synchronisation achieved are investigated. The results of this study show that the variable feedback method can induce exact synchronisation

between the two lasers only when the value of feedback fraction is higher than a critical value.

Chapter 6 contains the results of the numerical study on the use of the various techniques discussed above, for use in secure communication system using two directly modulated chaotic semiconductor lasers. The best method for coupling for this application is investigated. The results indicate that uni-directional scheme and variable feedback scheme cannot provide proper recovery of the encoded message. For achieving this purpose a new scheme called Proportional Integral scheme was, therefore, devised. Using this technique analog and digital messages are transmitted and recovered successfully.

In Chapter 7 we present the results of the numerical study of synchronisation of one-dimensional and two-dimensional arrays of chaotic directly modulated semiconductor lasers. Eight different linear arrays are simulated numerically with the number of elements varying from three to ten. Different methods such as open loop coupling, closed loop coupling, global coupling and nearest neighbour coupling are used for synchronisation of one-dimensional array, with different number of elements. The results show that there is strong dependence of the synchronisation and output dynamics of the array elements on the number of elements in an array and also on the type of coupling used. Open loop coupling is the least effective in synchronising an array of directly modulated semiconductor lasers. Closed loop coupling is found to be very sensitive to the number of elements present in an array. This scheme could

achieve synchronisation between the chaotic outputs for low values of coupling strengths and control over the synchronised chaotic outputs for higher coupling strengths only for arrays having even number of elements. No synchronisation or control of chaos could be achieved using this scheme with odd number of elements in the array. Global coupling scheme is effective in synchronising all the elements in arrays with even and odd number of elements. This scheme is also effective in controlling the chaotic outputs and, the coupling strength needed for synchronising the outputs decreases as the number of elements in the array increases. In the nearest neighbour coupling scheme the outer and inner laser pairs get synchronised separately, but does not synchronise with each other even for large coupling values for e.g. in the case of an array with four elements, first and fourth lasers will get synchronised with each other. Similarly the second and third lasers will also get synchronised separately. However there is no observable synchronisation between the first and second or, first and third or, second and fourth lasers and, the third and fourth lasers in the array. In the case of one-dimensional array all these schemes except the open loop coupling the output undergoes reverse period doubling and achieves stable period one cycle nature for strong coupling strengths. The two dimensional array is coupled using the nearest neighbour coupling scheme. In this case synchronisation can be achieved between all laser pairs. For strong coupling strengths the synchronised outputs undergo reverse period doubling and become stable one cycle. Suppression of the double peak structure can be obtained for higher values of coupling strengths in the case of one-dimensional and two-dimensional arrays.

Chapter 8 is the concluding part of the thesis and contains summary and conclusion of the whole work. The overall outcome of this work is that, the type of coupling or feedback that will be suitable for a particular system is to be found out by more of a trial and error method. The particular application for which we are using the system should also be of major concern while designing a coupling or feedback scheme. The dependence of synchronisation properties and other dynamical properties on the coupling strength also should be taken into consideration while designing the scheme and its application. It is to be noted that the existing methods will have to be modified appropriately, when using it for different applications.

CONTENTS

1. Chaos and Lasers – An Overview	1
1.1 Chaos in Dynamical Systems	2
1.1.1 What is a Chaotic System?	2
1.1.2 Conditions necessary for Chaos	4
1.1.3 Characteristics of a Chaotic System	5
1.1.4 Tools for the Study of Chaos	5
Phase Space	6
Poincaré Section	6
Power Spectrum	6
1.1.5 Roots to Chaos	6
1.1.5.1 Period Doubling	7
1.1.5.2 Quasiperiodic Route	10
1.1.5.3 Intermittency	11
1.1.6 Quantitative Measures of Chaos	12
1.1.6.1 Lyapunov Exponent	12
1.1.6.2 Correlation Function	13
1.1.6.4 Attractor Dimension	14
1.2 Lasers	15
1.2.1 Chaos in lasers	19

2. Synchronisation and Control of Chaos	23
2.1 Synchronisation of Chaotic Systems	24
2.1.1 Methods of Synchronisation	26
2.1.1.1 Drive-Response Scheme	26
2.1.1.2 Coupling Scheme	27
Occasional Coupling	27
Variable Feedback	29
Linear Feedback Control	30
2.1.2 Types of Synchronisation	30
2.1.2.1 Generalised Synchronisation	30
2.1.2.2 Phase Synchronisation	31
2.1.2.3 Lag Synchronisation	31
2.1.2.4 Exact Synchronisation	32
2.1.2.5 Practical Synchronisation	32
2.1.2.6 Complete Synchronisation	32
2.1.2.7 Partial Synchronisation	33
2.1.2.8 Almost Synchronisation	33
2.2 Synchronisation of Chaotic Laser Systems	34
2.3 Control of Chaotic Systems	35
3. Laser Model and its Dynamical Properties	37
3.1 Laser Model	38
4. Effect of Uni-Directional and Bi-Directional Couplings on Synchronisation of Two Directly Modulated Semiconductor Lasers	45

4.1	Introduction	46
4.2	Uni-Directional Coupling Scheme	47
	4.2.1 Coupling Scheme	47
	4.2.2 Numerical Analysis and Results	49
4.3	Bi-Directional Coupling	54
	4.3.1 Coupling Scheme	54
	4.3.2 Numerical Analysis and Results	56
5.	Variable Feedback Method for Synchronisation of Two Directly Modulated Semiconductor Lasers	67
5.1	Introduction	68
5.2	Variable Feedback Scheme	68
	5.2.1 Numerical Analysis and Results	70
6.	Chaotic Encryption using Long Wavelength Directly Modulated Semiconductor Lasers	75
6.1	Introduction	76
6.2	Chaotic Encryption	76
6.3	Message Encoding and Decoding	78
7.	Synchronisation and Control of Chaos in One-Dimensional and Two-Dimensional Arrays of Directly Modulated Semiconductor Lasers	91
7.1	Introduction	92
7.2	One-Dimensional Array	93
	7.1.1 Open Loop Coupling Scheme	94
	7.1.1.1 Numerical Analysis and Results	96
	7.1.2 Closed Loop Coupling	101
	7.1.2.1 Numerical Analysis and Results	103

Arrays With Even Number of Elements	103
Arrays with Odd Number of Elements	109
7.1.3 Global Coupling Scheme	111
7.1.3.1 Numerical Analysis and Results	113
7.1.4 Nearest Neighbour Coupling Scheme	117
7.1.4.1 Numerical Analysis and Results	119
7.2 Two Dimensional Array	124
7.2.1 Numerical Analysis and Results	126
8. Summary and Conclusion	131
9. References	137

CHAOS AND LASERS – AN OVERVIEW

This chapter briefly describes chaos in dynamical systems and various mathematical tools and quantitative measures used in the characterisation of chaotic systems. Related literature on the subject has been reviewed. General characteristics of lasers and, chaos in lasers with specific reference to semiconductor lasers also are discussed.

1.1 CHAOS IN DYNAMICAL SYSTEMS

Chaotic phenomena are abundant in nature and they have played important roles in the evolutionary processes of dynamical systems. What was considered as unwanted noise in the past centuries has now developed into a branch of science with its application in diverse fields such as lasers, chemical reactions, mechanical structures, fluid dynamics, neural networks, biological rhythms, earthquakes and share market fluctuations. Interest in the study of chaos and its importance grew at a rapid pace after 1963, when Lorenz^[1] published his numerical work on convection model and, discussed its implications on weather predictions. The word chaos means a state of utter confusion or disorder. However, for the last few decades the word chaos in scientific literature is used in the sense of '*Deterministic Chaos*'. In the present scientific scenario, wherein nonlinearity has become the rule rather than exception, chaos has made its presence felt in all dynamical processes extending from the swinging of a pendulum to planetary motion, the fluctuations in ECG/EEG signals, eruption of epidemics and many more. It is therefore not surprising that chaotic dynamics is now considered responsible for the fluctuations in the share market thus making its impact in economic scenario as well!

1.1.1 WHAT IS A CHAOTIC SYSTEM?

Any system that develops in time in a non-trivial manner may be considered a dynamical system. Dynamical systems are normally regulated by system

parameters and when these parameters change, the properties of the system also change^[2]. Even though all dynamical systems evolve according to some deterministic system of equations, for certain parameter values the evolution of most of the nonlinear dynamical systems appears random and becomes unpredictable. In other words, if the determining equations are nonlinear, then under some conditions the solution becomes sensitive to initial conditions as well as parametric changes and hence unpredictable.

A system whose temporal or spatial evolution seems random, but is really deterministic, i.e. obeys some definite evolutionary equation, can be called a chaotic system. By terming a system chaotic, the implication is about the uncertainty in the long-term predictability of that system. In a linear system, the distance between two initially close states will be preserved or will increase linearly during the evolution. However, in a system governed by chaotic dynamics, this feature will be absent and the distance between the initial states will diverge exponentially as the systems evolve. Thus the unpredictability of a chaotic system arises from its instability against small perturbations. This is also called sensitive dependence on the initial conditions, which leads to an exponential growth of any errors in specifying the initial conditions. Thus the state of the system becomes essentially unknown after a finite time. Henri Poincaré (1854 - 1912), a prominent mathematician and theoretical astronomer who studied the dynamical systems, was one of the first to recognise this phenomenon. He described it as follows.

'... it may happen that small difference in the initial conditions produce very great ones in the final phenomenon. A small error in the former will produce an enormous error in the latter. Predictions become impossible, and we have the fortuitous phenomenon.'^[3]

1.1.2 CONDITIONS NECESSARY FOR CHAOS

The conditions necessary for chaos to occur in any dynamical system are^[4]

- i) The system has at least three independent dynamical variables
- ii) The equations of motions are nonlinear.

Such equations can be generally written as

$$\frac{d\bar{X}}{dt} = \bar{F}(\bar{X}, \mu) \quad (1.1)$$

where $\bar{X} = (x_1, x_2, \dots, x_n)$, x_1, x_2, \dots, x_n are dynamical variables and $\bar{F} = (F_1, F_2, \dots, F_n)$, F_1, F_2, \dots, F_n are the source functions. According to the first condition n should be at least three. Nonlinear equations of motion for such a system should contain some nonlinear term that couples the independent variables. This defines a continuous time dynamical system. One can also consider discrete time dynamical systems. Here the equations are of the form

$$\bar{X}_{n+1} = F_{\mu}(\bar{X}_n) \quad (1.2)$$

where n refers to discrete values of time.

In (1.1) and (1.2) μ stands for a set of control parameters (usually one or two) that can be varied. The asymptotic behaviour of the system depends on the value of these parameters.

1.1.3 CHARACTERISTICS OF A CHAOTIC SYSTEM

In the light of the above discussions, we can arrive at the conclusion that chaotic dynamics would have some general characteristics. The identifying characteristics of a chaotic system can be described as the following

- i) Chaos occurs only in nonlinear deterministic dynamical systems
- ii) Chaos occurs neither because of uncontrolled external forces like noise, nor because of large number of degrees of freedom, but because of the inherent nonlinearity of the system that induce sensitivity to initial conditions.
- iii) There is a certain order in chaos.

Presence of chaos implies that long-term predictions are meaningless, but short-term predictions can be fruitful.

1.1.4 TOOLS FOR THE STUDY OF CHAOS

The mathematical tools generally used in identifying chaotic behaviour of dynamical systems are phase space, Poincaré section and the power spectrum^[4].

- ***Phase space***

Phase space is the mathematical space of the dynamical variables of a system with orthogonal coordinates representing each of the variables needed to specify the instantaneous state of the system.

- ***Poincaré section***

Poincaré section is a means of simplifying phase space diagrams of complicated systems. It is constructed by viewing the phase space diagram stroboscopically in such a way that the motion is observed periodically. This reconstructs the continuous time evolution of the phase space with discrete time mapping.

- ***Power spectrum***

Power spectrum is defined as the Fourier transform of the autocorrelation function of a time series. This is computed using Fourier analysis and it displays the frequency composition of the time variation of the dynamical variables

1.1.5 ROUTES TO CHAOS

Loss of long-range coherence in time produces chaos in any system. All nonlinear dissipative dynamical systems have one common feature. No matter

from which initial conditions the system starts, its trajectories in phase space converge or settle down to a subspace in the phase space. This subspace can be called an attractor of the system. This is true for systems in the chaotic as well nonchaotic regimes. Chaotic behaviour manifests only under certain conditions, which depend on the parameter values of the system. There are certain parameters called the control parameters, which govern the changes in the behaviour of dynamical systems. When the control parameter changes, the attractor of the system also undergoes some change. Usually these changes will be small like a slight shift of the fixed point or, a small change in the form of the attractor. However, for some critical values of the control parameter, the attractor undergoes radical changes, which would result in sharp modifications of the system dynamics². Any discontinuous qualitative change in the behaviour of a system is called bifurcation. There are several routes through which dynamical systems enter the chaotic regime. These vary according to the system and also the point of entry, i.e. the parameter values. The same system can use one route for one set of parameter values and another route for another set of parameter values. The most common routes to chaos are period doubling, quasiperiodicity and intermittency.

1.1.5.1 PERIOD DOUBLING

Period doubling is considered one of the most common routes to chaos, as for example,

in the one-humped quadratic maps. This is also called Feigenbaum route to chaos. We shall consider the common and simplest example of a chaotic

system, the logistic equation, which is a discrete dynamical system. It can be presented as^[5,6]

$$X_{n+1} = \lambda \times X_n \times (1 - X_n) \quad : \quad 0 \leq \lambda \leq 4$$

$$0 \leq X \leq 1 \quad (1.4)$$

This equation was originally devised by Verhulst in 1845 in the form of differential equation for modelling population growth subject to limited resources and was later considered in the discretised form by Robert May in 1976^[7]. This equation is now widely used as a simple example of a chaotic system. In the equation (1.4), X_n represents population in the n th year and X_{n+1} that in the $(n+1)^{\text{th}}$ year. λ is the control parameter, which decides the dynamics of the system. It can represent the sudden bursts of epidemics or drought or such other incidents. For $\lambda < 1$, whatever be the initial conditions, if we start within the boundary of 0 and 1, X_{n+1} asymptotically settles down to 0. This point in the phase space is called stable fixed point, which acts as an attractor. The interval 0 -1 can be called the basin of attraction of this attractor. On increasing λ , this stable fixed point becomes unstable and a new fixed point arises depending on the value of λ . At $\lambda=3$, the stable fixed point disappears and a new set of two fixed points appear i.e. for $\lambda=3$, as $n \rightarrow \infty$, alternate iterates oscillate between two stable fixed points. This phenomenon where a set of 2^n fixed points in the phase space of a system disappear and a new set of 2^{n+1} fixed points arise is called a period doubling bifurcation or a pitchfork bifurcation. This is the basic mechanism of period doubling route. At $\lambda = 3.4$, this set

becomes unstable and gets replaced by a new set of 4 fixed points. This is called a period 4 orbit. At $\lambda = 3.569$, the period becomes infinite, which means that a particular iterate value never repeats. At this point the system becomes chaotic. The sequence by which the above system becomes chaotic is called the period doubling route to chaos. For $3.57 \leq \lambda \leq 4$, there are periodic windows which interrupt the chaotic behaviour. These are shown in Fig 1.1

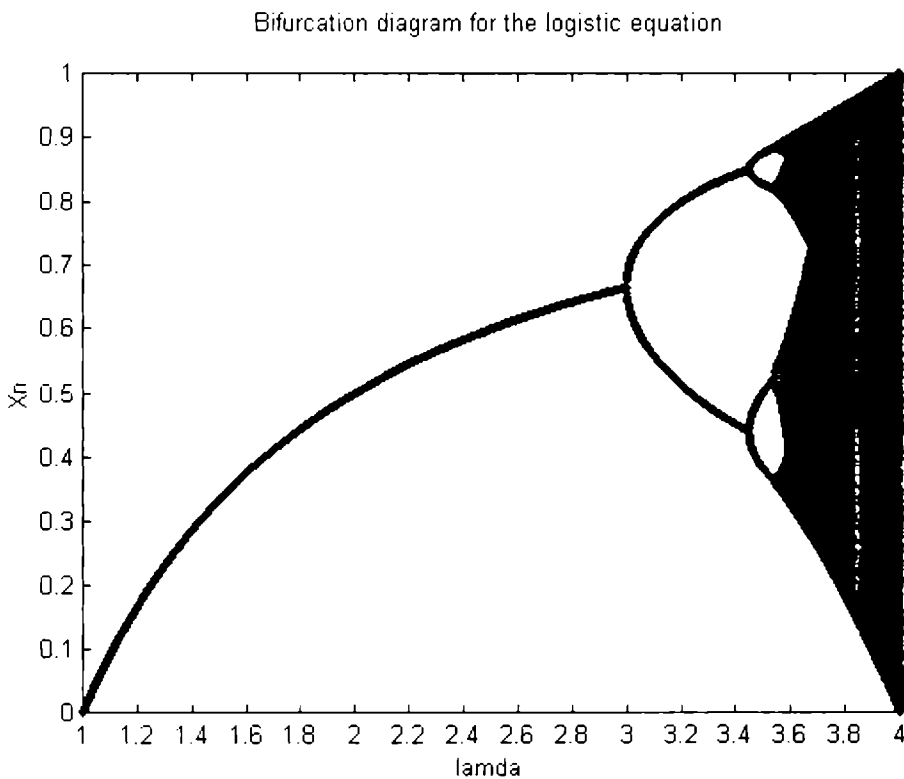


Fig 1.1
Bifurcation diagram of the logistic equation

After n bifurcations the length of the period becomes 2^n i.e. as n the period becomes 2. Period doubling bifurcations have some universal feature. The successive thresholds (λ_n) get closer and closer, as n Feigenbam has quantified them in terms of two numbers α and δ representing certain ratios. If λ_n is the point where the period 2^n bifurcates, then

$$\delta_n = \frac{\lambda_n - \lambda_{n-1}}{\lambda_{n+1} - \lambda_n} \quad (1.5)$$

As $n \rightarrow \infty$ $\delta_n \rightarrow \delta = 4.66920$

The second universal feature is quantified as α

$$\alpha_n = -\varepsilon_n / \varepsilon_{n-1}$$

when ε_n represents the size of opening of fork at the n^{th} bifurcation.^[7]

1.1.5.2 QUASIPERIODIC ROUTE

This is also called Ruelle-Takens route to chaos. The basic mechanism in this case is the Hopf bifurcation^[8]. Hopf bifurcation occurs when a stable fixed point in the phase space of the system generates a limit cycle at the critical value of the control parameter. Hopf bifurcation introduces a new fundamental frequency into the system. Consider a dynamical system in a steady state such as a laminar flow of a viscous fluid. In this case the control number is the Reynolds number defined as $Re = v\varphi/\nu$, where φ is the diameter of the cylinder through which the

fluid is flowing, v is the velocity of fluid flow and, ν is the viscosity of the fluid. As the Reynolds number is increased the laminar flow loses its stability and begins to oscillate with frequency f_1 (Hopf bifurcation). If the same process is repeated for two more times producing two new fundamental frequencies f_2 and f_3 , then according to Ruelle-Takens theory the time dependent behaviour no longer remains quasiperiodic with three frequencies but distinctly chaotic.

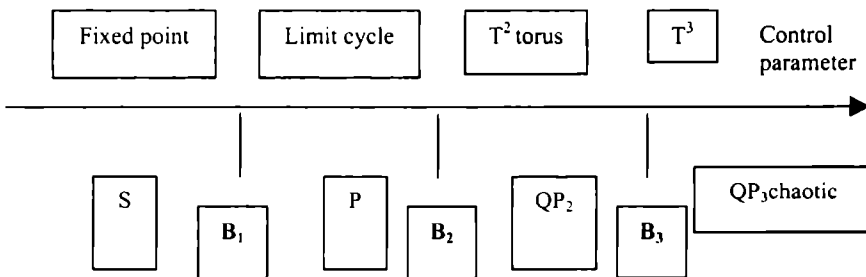


Fig 1.2

The schematic representation of the successive bifurcations

B_1 , B_2 and B_3 are the successive bifurcations: S = steady state; P = periodic state
 QP_2 = quasiperiodic regime with two frequencies; QP_3 = quasiperiodic regime with three frequencies; SA = strange attractor.

1.1.5.3 INTERMITTENCY

This is also called Pomeau-Manneville route to chaos. The intermittent motion of a dynamical system is characterised by alternation of bursts of apparently

chaotic behaviour and intervals of almost periodic oscillations. This phenomenon can be briefly explained as follows: for a value r of a control parameter less than a critical value r_i , the dynamical system oscillates in a regular fashion and is stable against small perturbations. When r increases above the intermittency threshold value r_i , the time signal of the dynamical system consists of oscillations which appear regular and resemble the stable oscillatory behaviour for $r < r_i$ but are interrupted from time to time by abnormal fluctuations whose amplitude and directions are approximately the same from one fluctuation to another with little dependence on r . The stable oscillations for $r < r_i$ correspond to a stable fixed point in the Poincaré map which becomes unstable for $r > r_i$. There are three types of transition through intermittency, each with its own characteristics^[8,9].

1.1.6 QUANTITATIVE MEASURES OF CHAOS

Chaotic behaviour of a system can be quantitatively characterised by several means. Brief description of some of them is provided in this section. The most important and commonly used measures include Lyapunov exponent, Correlation function and Attractor dimensions.

1.1.6.1 LYAPUNOV EXPONENT

Lyapunov exponent is defined as a measure of the exponential divergence of two initially close trajectories in the phase space of a system. The Lyapunov

exponent, named after A.M. Lyapunov, a Russian mathematician, is a measure of the sensitive dependence of the dynamics on the initial conditions^[4]. This exponent λ , may be readily computed for a one-dimensional map such as the logistic map. If a system is allowed to evolve from two slightly differing initial states, x and $x+\varepsilon$, their divergence after n iterations may be characterised approximately as

$$\varepsilon(n) \approx \varepsilon e^{n\lambda} \quad (1.6)$$

where the Lyapunov exponent λ gives the average rate of divergence per iteration..

1.1.6.2 CORRELATION FUNCTION

Correlation function is a measure of the extent to which iterates which are ‘m’ steps apart are correlated in their evolution. For a unimodular map $x_{n+1} = f(x_n)$, the correlation function^[10] can be expressed as

$$C(m) = \lim_{N \rightarrow \infty} \frac{1}{N} \sum_{n=0}^N (x_n x_{n+m} - \bar{x})^2 \quad (1.12)$$

$$\text{where } \bar{x} = \lim_{N \rightarrow \infty} \frac{1}{N} \sum_{n=0}^N x_n \text{ is the mean value of } x(n). \quad (1.13)$$

Decaying correlation is a characteristic feature of chaotic evolution.

1.1.6.4 ATTRACTOR DIMENSION

Dissipative dynamical systems are characterised by attraction of all trajectories passing through a certain domain of phase space towards a geometric object in the phase space. This object is called an attractor. The set of initial points $\{x_0\}$ each of which gives rise to a trajectory that approaches a particular attractor is called its basin of attraction. Systems in both chaotic and non-chaotic regimes will have attractors in their phase space. Attractors of periodic motions will be simple geometric objects such as fixed points or limits cycles, whereas those of chaotic motions will have complicated structure. The characteristic difference in the attractors of periodic motions and those of chaotic motions is in their attractor dimensions. Consider a set of points in a 'p' - dimensional space. To cover this set by hypercubes of linear dimension ϵ , a unit cube will contain $N(\epsilon) = \epsilon^{-3}$ cubes, a unit square will contain $N(\epsilon) = \epsilon^{-2}$ squares of side ϵ and, a unit line segment will contain $N(\epsilon) = \epsilon^{-1}$ segments of length ϵ . In general, the dimension d can be expressed as ⁽¹¹⁾

$$d_c = \left[\lim_{\epsilon \rightarrow 0} \frac{\ln N(\epsilon)}{\ln(1/\epsilon)} \right] \quad (1.14)$$

This is known as capacity dimension⁽¹¹⁾. For an attractor, if d_c is an integer then it is called a regular attractor. On the other hand if d_c is a fractional number then the attractor is called a fractal or a strange attractor. In addition to the capacity dimension d_c , one can define a sequence of generalised dimension d_q to measure the distribution of points on the attractor.

1.2 LASERS

One of the important impacts of the spectacular developments in optical technology is the large scale replacement of several electronic devices by optical devices. This exactly is an area where lasers can play pivotal roles in several respects. The emphasis is on semiconductor lasers emitting visible light which have application in optical data storage, optical telecommunication, bar code scanners, laser pointers, patient positioning devices such as CT/ MRI scanners and, many more. Study of laser chaos assumes great importance due to the multifarious applications it commands in various scientific and technological fields.

Since semiconductor lasers are nonlinear dynamical systems and chaos is one of the manifestations of the inherent nonlinearity of any dynamical systems, chaotic dynamics of such systems can play very significant role in their operations. The only practical method for studying the chaotic dynamics of any system is by simulating their determining equations numerically. Thus, understanding and taming of chaos together make study of laser chaos an interdisciplinary subject comprising of laser physics, nonlinear mathematics and engineering.

Laser is a very special source of light. The attractive property of this source of light is its coherence property. This coherence is due to the stimulated emission. In ordinary incoherent sources of light each photon is emitted from its atom or molecule independently of each other while in a laser, a photon which interacts

with an excited atom can cause the atom to emit a similar photon which can again cause the emission of another similar photon from another atom and this process can go on repeating. This phenomenon is called stimulated emission. This co-operative behaviour leads to the characteristic properties of lasers such as monochromaticity, directionality and spatial and temporal coherence. One of the essential conditions for the operation of a laser is the population inversion, i.e. creation of more number of atoms in a higher energy state than that in a lower energy state under thermal equilibrium. A medium with population inversion can act as a light amplifier only if it can act as an oscillator, i.e. a part of its output is to be fed back into the system so that the light oscillates inside the medium for a considerable amount of time before going out of the system, which is achieved by placing the medium between a pair of mirrors. If the population inversion is maintained with the help of an external energy source and, if a light quantum entering the system can cause stimulated emission of more than one quantum before being absorbed by the mirrors or in the sample, then the system will operate as a laser.

The first laser to be operated was a ruby laser fabricated by Maiman in 1960. The first gas laser became operational in 1961 using He-Ne gas mixture as the active medium. Stimulated emission in semiconductors became the focal theme of research of several groups during late 1950s and, finally in 1962, led to the fabrication of a semiconductor laser that consisted of a forward biased Gallium arsenide GaAs p - n junction (homostructure lasers). In a homostructure p - n junction, since there are more number of electrons in the conduction band of the

n type material than in the conduction band of the p type material, electrons tend to diffuse from n to p region and holes diffuse from p to n type region. Thus the two sides of the junction become electrically charged with n being positively and p negatively charged. This produces an electric field, which oppose further diffusion of charge carriers. Thus an energy level barrier of height eV_0 is produced, where V_0 is the diffusion potential. If a forward bias is now applied to the junction, i.e. positive terminal to p region and negative terminal to n type region, the junction barrier level height gets reduced to $e(V_0 - V)$, where V is the forward bias potential. This makes it easier for the carriers to surmount the junction potential barrier. Thus a large current will flow from p to n region. In a narrow region near the junction, called the depletion region, both electrons and holes are present simultaneously and they become minority carriers in excess of normal concentration. At this point they recombine either radiatively or non-radiatively. When an electron-hole undergoes a radiative recombination, it falls back from the conduction band to the valence band thus emitting a photon of energy $h\nu = E_g$, where E_g is the energy difference between the conduction band and valence band and is called the band gap energy

$$\text{i.e. } E_g = (E_c - E_v) = hc/\lambda \quad (1.15)$$

where E_c and E_v are the energies of conduction and valence bands respectively, h is the Planck's constant = 6.6256×10^{-34} J-s and c is the velocity of light = 2.99792×10^8 m/s

However these photons can also get absorbed through a reverse process inside the cavity itself. This can produce an electron-hole pair. When the externally applied current exceeds a critical value known as the threshold current, I_{th} , a condition similar to the population inversion condition in other types of lasers is satisfied. Then the rate of photon emission is greater than the rate of photon absorption. Now the p-n junction is able to amplify the electromagnetic radiation and is said to exhibit optical gain. Not all semiconductor materials are efficient in undergoing radiative recombination. Si and Ge are inefficient emitters. Semiconductor materials such as Ga-As and GaAsP are better emitters. Such doping introduces new energy levels within the energy band either below the conduction band or above the valence band. Transitions take place via these levels. The end faces perpendicular to the junction are polished to provide optical feedback so that active medium itself acts as the resonator. The output wavelength was around $0.8\mu\text{m}$ and the output power was below 50mw. These earlier models could not provide continuous operations at room temperatures because of their large values of threshold current densities. For homostructure semiconductors, thickness of the active region where the gain is high is very small ($0.01\mu\text{m}$), since carriers could not be confined to the active region. To improve the performance of semiconductor lasers, one approach is to sandwich a semiconductor material between two cladding layers of another semiconductor material that has a relatively wider band gap. These types of devices were referred to as heterostructure and double heterostructure devices depending on whether the active region where the lasing occurs is surrounded on one or both sides by a cladding layer of higher band gap. Now electrons and

holes can move freely to the active region under forward bias but cannot cross over to the other side of the potential barrier because of the higher band gap of the cladding material. This provides carrier confinement to the active region where they can recombine to produce optical gain. Double heterostructure semiconductor lasers now in use are made of various combinations of GaAs, AlGaAs, InGaAs, and InGaAsP. Presently with the availability of ultra low loss dispersion free fibers at 1.3 and 1.55 μm wavelength respectively, InGaAsP lasers operating in the vicinity of 1.3-1.6 μm have become very important.

1.2.1 CHAOS IN LASERS

The semiclassical model of a single mode laser known as Maxwell Bloch equation describes time dependence of electrical field E , mean polarization of the atoms P and the population inversion D and is expressed as ^[4]

$$\begin{aligned}\frac{dE}{dt} &= -\kappa E + \kappa P, \\ \frac{dP}{dt} &= \gamma_1 ED - \gamma_1 P, \\ \frac{dD}{dt} &= \gamma_2(\gamma + 1) - \gamma_2 D - \gamma_2 \lambda EP\end{aligned}\tag{1.16}$$

In 1975 Herman Haken^[16] investigated the dynamics of the above equations and reported an analogy between the instabilities shown by these equations and the Lorenz equations^[11] for fluid dynamics. This similarity kindled the search in theoretical and experimental fields to find evidence of chaotic behaviour in laser systems. In 1982 Arecchi^[17] et al found out experimental evidence of

period doubling in a Q-switched CO₂ laser. Gioggia and Abraham^[18] in 1983 observed period doubling, two frequency and intermittency route to chaos in a single mode inhomogenously broadened Xenon laser. In 1984, Klische *et. al.*^[19] described chaos in solid state lasers with modulated pump beam. Jarroja *et. al.*^[1] in 1986 compared the results of theoretical and experimental works in a sin.^[20]gle mode inhomogenously broadened ring laser and found that the output was chaotic. In the same year Dupertuis^[21] *et. al.* listed six conditions that should be fulfilled by continuous wave optically pumped far-infrared lasers to display Lorenz chaos. It was later discovered that multimode lasers also exhibited chaotic behaviour when there is nonlinear coupling between the different modes.

Semiconductor lasers can be made chaotic either by modulating the injection current^[22] or by giving an external feedback^[23]. Tang *et. al.*^[24] and Winful *et. al.*^[25] in 1986 studied the chaotic dynamics of semiconductor laser and its dependence on modulation depth and modulation frequency. The dependence of chaotic output on the modulation depth and modulation frequency was numerically investigated by Tang *et. al.*^[24] and it was observed that the chaotic region was limited to a small range of parameter values. Winful *et. al.*^[25] experimentally observed quasiperiodicity route to chaos in a modulated self-pulsing laser. Kao *et. al.*^[26] in 1993 investigated the period doubling phenomenon in modulated semiconductor laser and proved that period doubling event had a virtual Hopf precursor, which was enhanced by Langevin noise. In practical semiconductor laser systems there is always a small power dependent

reduction in the mode gain, represented as ϵ_{NL} , that is due to nonlinear phenomenon such as spectral hole burning. The dynamic response of a semiconductor laser is strongly affected by the nonlinear gain and therefore this factor should be included in the rate equations that models semiconductor lasers^[27]. The normal value of ϵ_{NL} for InGaAsP laser lies in the range $3-6 \times 10^{-17} \text{ cm}^3$. It was shown that chaos occurred at modulation frequency around 1GHz^[24]. This frequency range is of importance in optical communication systems and directly modulated semiconductor lasers are widely used in these systems.

Chaotic behaviour of laser systems can play both constructive and destructive roles. For most of the experimental works, a stable periodic laser output is needed. Therefore in such fields chaotic behaviour can become undesirable and should be controlled for producing reliable outputs. However, when it comes to applications such as optical communication, especially secure communication, chaos becomes a blessing. In this case it acts as a carrier and bodyguard for the message signal that is to be transmitted. In such applications synchronisation of lasers need much attention. In optical amplifiers and designing of high power optical sources, both control of chaos and synchronisation become equally important. Semiconductor optoelectronic devices like laser diodes find application in almost all realms of technology. Their output frequency range that falls in the visible region and their low cost make them very much inevitable in fiber optic communication systems and high power optical sources. In both cases synchronisation of such lasers is very crucial. It is with

this background in mind that we aimed our study on synchronisation and control of chaos in semiconductor lasers.

We present a general discussion of synchronisation and control of chaos in chapter 2. Synchronisation of lasers, especially semiconductor lasers, is also described in this chapter. The laser model used for our studies and its dynamical properties are discussed in chapter 3. Chapter 4 deals with the two types of coupling; (i) a uni-directional coupling (ii) a bi-directional coupling. Synchronisation and control of chaos and their dependence on the type of coupling and coupling strengths are discussed in detail. Chapter 5 discusses synchronisation of two semiconductor lasers using a variable feed back method in a drive response scenario. In chapter 6, is presented the use of a uni-directional coupling scheme, variable feedback scheme and a proportional integral coupling scheme for secure communication. Both digital and analog messages could be transmitted and successfully recovered only with the proportional integral scheme. Chapter 7 discusses synchronisation of chaos in an array of chaotic semiconductor lasers in which the number of elements is varied from three to ten. Effects of different types of coupling schemes on synchronisation of the array elements are also studied. It is observed that there is dependence of synchronisation and other dynamical properties of the individual laser systems on the number of elements that are present in a particular array and the coupling strengths. With chapter 8 we conclude our work with a note on the utility of the newly introduced schemes and possibilities of its improvements and possible applications.

SYNCHRONISATION AND CONTROL OF CHAOS

Different methods and types of synchronisation in chaotic systems form the subject matter of this chapter. Classification schemes relevant to our numerical studies are discussed in detail. Different methods adopted for synchronisation of chaotic lasers, especially semiconductor lasers, have been discussed. Details on control of chaos in dynamical systems with reference to laser systems also are presented.

2.1 SYNCHRONISATION OF CHAOTIC SYSTEMS

Synchronisation of two processes literally means '*to make one process work at the same time or at the same rate as the other process*' indicating the occurrence of two or more events in unison. A perfect example is synchronised swimming where the arm and leg movements are coordinated to take place in time in unison. Similarly in a march past, the arms and legs of the participating individuals swing in perfect co-ordination and unison, which is another example of synchronised movements. In the world of dynamical systems the concept of synchronisation implies the co-ordination of the temporal evolution of the dynamical systems. The above examples involve orderly systems where synchronisation immediately makes a sense of coordination. Synchronisation of chaotic systems may sound too embarrassing because of the very definition of chaos, which implies the exponential divergence or decorrelation of initially nearby trajectories. However, it is possible to make two or more chaotic systems to evolve in synchrony, i.e. even though two initially nearby trajectories of each of the systems diverge exponentially with time, the divergence will be similar in both the systems. When two chaotic systems get synchronised with each other, they exhibit identical chaotic behaviour. Each of the systems will wander erratically over their individual attractors but at any given point of time, the points at which the two systems are on their attractors will be the same. Synchronisation of chaotic systems has been defined variously such as, 'the exact equivalence of state variables' or 'the existence of a proportionality of the state variables' etc. From a dynamical system point of

view, synchronisation of two m -dimensional chaotic systems can be defined in a quantitative perspective as existence of identical solutions; i.e. if we have two systems x and y , each of which is m -dimensional and independently chaotic, this can be represented as follows

$$\begin{aligned}\dot{x}_k &= f_k^x(x_1, x_2, \dots, x_m) \\ \dot{y}_k &= f_k^y(y_1, y_2, \dots, y_m)\end{aligned}\tag{2.1}$$

where $k = 1, 2, 3, \dots, m$: i.e. x_k 's are vectors of variables of the driving system in the phase space 'D' and y_k 's are vectors of variables of response system in the phase space 'R'. If the trajectories of the drive and response systems are $x(t)$ and $y(t)$, then the two systems are said to be synchronised if there exists a transformation \mathfrak{T} from the trajectories of attractor in 'D' space to trajectories in 'R' space ^[28]

$$y(t) = \mathfrak{T}x(t)\tag{2.2}$$

Various methods have been studied for synchronisation of chaos suited for different applications. Pecorra and Carroll ^[29,32] initiated numerous studies for synchronisation of chaotic systems and developed efficient methods for the same, which have been found useful for different applications. Synchronisation has been effectively made use of for estimating unknown parameters of a system from a single variable time series. ^[33]

2.1.1. METHODS OF SYNCHRONISATION

In order to achieve synchronisation between two chaotic systems, there should be some type of coupling between them. The type and form of coupling are to be decided depending on the particular system and the application for which synchronisation is sought for. Numerous methods have been tried by various scientists for inducing synchronisation in almost all types of dynamical systems, e.g. global coupling^[34], output feedback control^[35], using sliding differentiators^[36] and variants of the above.^[31-33,35,37-40] In general, these can be divided into two types viz. drive response scheme and coupling scheme.

2.1.1.1 DRIVE-RESPONSE SCHEME

This system consists of a driving system that is chaotic, and a response system, a sub system of the driving system^[29,30]. The drive and response systems are coupled uni-directionally i.e. the variables of the response system are dependent on the drive system, but the variables of the drive system are *not* dependent on those of the response system. Fig 2. represents the above system.

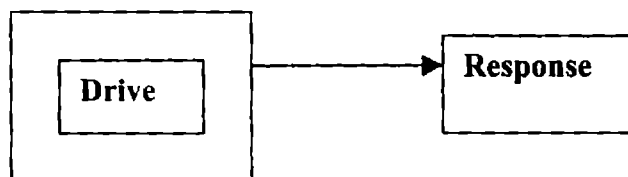


Fig 2.1

Drive-Response scheme

2.1.1.2 COUPLING SCHEME

The second type of coupling scheme includes two identical chaotic systems with a provision for slight differences in the initial conditions^[41, 42]. Coupling between the two systems can be unidirectional or bi-directional which can be chosen appropriately. In this coupling scheme, the direction and form of coupling have to be chosen by trial and error and adjusted suitably. Fig 2.2 is a schematic representation of the general coupling scheme.

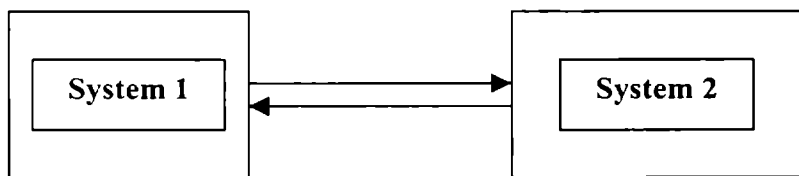


Fig 2.2
General coupling scheme

➤ *Occasional coupling*

Occasional coupling is a subclass of the drive-response scheme mentioned above. As the name implies the system consists of a drive and a response system but the coupling is given only occasionally. The response will be influenced by the drive only for a specific interval of time called the synchronisation phase during which the two systems get synchronised. For the next time interval called the autonomous phase there is no coupling between the drive and the response systems. Appropriate coupling parameter that is to be

fed into the response system during the synchronisation phase is to be decided according to the system and its specific application. Appropriate choice of duration of synchronisation and autonomous phases can provide an exponential decay of synchronisation error⁴³. This method can find application in the field of chaotic encryption where the message masked by the chaotic carrier can be transmitted in the autonomous phase.

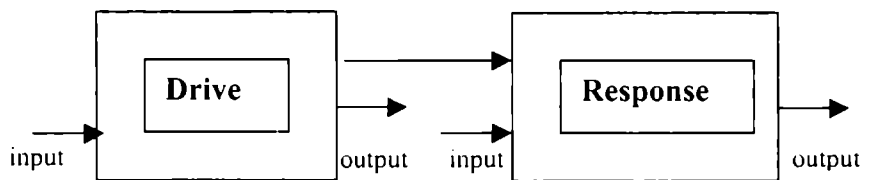


Fig 2.3
Synchronisation phase

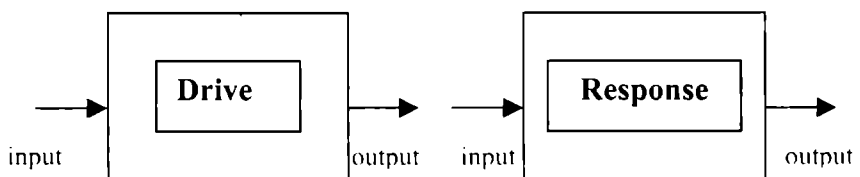


Fig 2.4
Autonomous phase

➤ *Variable feedback*

In the variable feedback scheme^[44], among the systems that are to be synchronised one acts as the master and the other acts as its slave. A fraction of the difference between the outputs of the master and the slave is fed back to the input of the slave system. The form of feedback function and the threshold value of the feedback fraction that can effectively synchronise the particular system are to be *chosen* appropriately. This is a modification of the method introduced by Pyragas^[45]. This scheme can prove to be useful when the master and the slave are at two distant sites like communications systems where the transmitter can act as the master and the receiver can act as the slave.

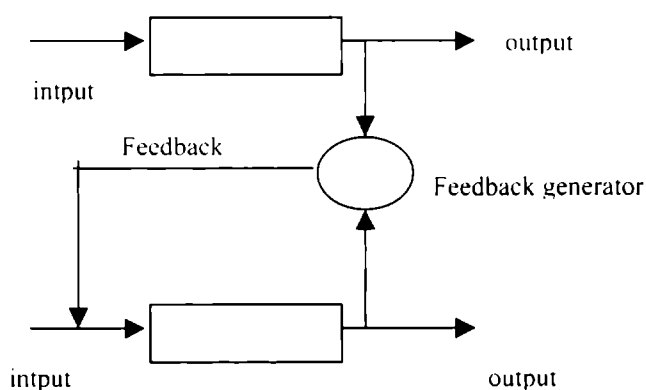


Fig 2.5

Variable feedback scheme

➤ ***Linear feedback control***

This is a conventional engineering technique and is based on the concept of stabilisation of unstable periodic orbits of the chaotic systems. The designing of appropriate feedback functions demands the knowledge of the full state of the systems. This is also called model predictive control^[46].

Apart from the above mentioned schemes, there are other methods such as phase controlling^[37], parameter controlling^[38] and, driving two systems having identical chaotic signals with an external source^[39,40] being used contemporarily.

2.1.2. TYPES OF SYNCHRONISATION

Synchronisation of any two dynamical systems is dependent on the state variables and the degree of correlation among them. Depending on the degree of correlation between the state variables of the systems, several types of synchronisations have been identified.

2.1.2.1 GENERALISED SYNCHRONISATION

In the equation

$$y(t) = \mathfrak{F} [x(t)] \quad (2.4)$$

when the form of \mathfrak{S} becomes more complicated, the parameter space plot will not show a straight line. It will appear, instead, a more complicated object. This kind of synchronisation is called generalised synchronisation^[28]. In this case parameter space plot will not serve the purpose. Therefore other methods such as mutual false nearest neighbours or calculation of synchronisation index have to be adopted.

2.1.2.2 PHASE SYNCHRONISATION

Two chaotic systems are phase synchronised when suitably defined phases of two systems get locked to each other, i.e.

$$n\phi_1 - m\phi_2 = \kappa, \text{ a constant} \quad (2.5)$$

while their amplitudes remain uncorrelated and sustain independent irregular motions^[47].

2.1.2.3 LAG SYNCHRONISATION

Two chaotic systems are lag synchronised when their corresponding state variables coincide when shifted in time^[48]. Lag synchronisation can be defined as another form of generalised synchronisation with the form of \mathfrak{S} defined in terms of temporal displacement of the interacting systems, i.e.

$$x_i(t+\tau) = y_i(t) \quad (2.6)$$

2.1.2.4 EXACT SYNCHRONISATION

To study this type of synchronisation a quantitative measure called synchronisation error is used. Synchronisation error can be defined as the difference between the corresponding state variables of the two systems i.e. $E = x_i(t) - y_i(t)$. If the synchronisation error exponentially converges to the origin, then the two systems are said to be exactly synchronised^[49], i.e. at a finite time $x_i(t) = y_i(t)$

2.1.2.5 PRACTICAL SYNCHRONISATION

Two chaotic systems are said to be practically synchronised, if the difference between synchronisation error converges to a neighbourhood around the origin^[49], i.e. for all time, $t > t^*$,

$$x_i(t) \approx y_i(t) \quad (2.7)$$

2.1.2.6 COMPLETE SYNCHRONISATION

Two chaotic systems can be considered as completely synchronised if, and only if, all states of both the systems are practically or exactly synchronised^[49]. e.g. consider two, three dimensional chaotic systems

$$X(x_1, x_2, x_3) \quad (2.8)$$

$$Y(y_1, y_2, y_3) \quad (2.9)$$

where the state variables of the first system are x_1, x_2, x_3 and the state variables of the second system are y_1, y_2, y_3 . The synchronisation errors, $'E_i$, can be defined as

$$'E_1 = x_1(t) - y_1(t); \quad (2.10)$$

$$'E_2 = x_2(t) - y_2(t); \quad (2.11)$$

$$'E_3 = x_3(t) - y_3(t) \quad (2.12)$$

The two systems are said to be completely synchronised after a finite time ' t ', if all the three errors exponentially decay to 0 or to at least nearly zero values.

2.1.2.7 PARTIAL SYNCHRONISATION

Consider the above dynamical system itself where x_1, x_2, x_3 and y_1, y_2, y_3 are the state variables and $'E_1, 'E_2,$ and $'E_3$ are synchronisation errors. Partial synchronisation is defined as a condition where at least one of the states is either practically or exactly synchronised and at least one is neither practically nor exactly synchronised^[49], i.e. at least one of the three synchronisation errors should exponentially converge to zero at finite time and at least one should not.

2.1.2.8 ALMOST SYNCHRONISATION

This is similar to the phase synchronisation mentioned earlier. Almost synchronisation can be defined as two systems having their phase oscillations

correlated and amplitudes uncorrelated^[49]. The phase can be suitably defined depending on the system and its particular application.

2.2 SYNCHRONISATION OF CHAOTIC LASER SYSTEMS

Laser systems provide an excellent example of high dimensional real chaotic systems. Important applications of high dimensional real chaotic systems are in the field of high-speed optical communication and design of high power optical sources. Most of the modern communication devices are opto-electronic or, all optic.

Winful *et.al.*^[50] first predicted the possibility of synchronisation of chaos in semiconductor lasers in 1990. This was followed by an experimental verification of synchronisation in a bi-directionally coupled system of two Nd:YAG lasers by Roy *et.al.*^[51] in 1994. It was in the same year that Sugawara *et.al.*^[52] demonstrated experimentally that two chaotic CO₂ lasers could be synchronised by modulating the saturable absorber in the cavity of one of the lasers with the output of the other. Their works signalled a breakthrough in the field of synchronisation of chaotic lasers, since these were the first experimental evidence of synchronisation of chaotic lasers. It was in these works that the simple method of a bi-directional coupling was first proposed for the purpose of synchronisation of chaotic laser systems. The coupling was given by an overlap of the intracavity laser fields. Study of synchronisation of semiconductor lasers was also independently considered by Mirasso *et.al.*^[53] in 1996. The following

years witnessed various developments in similar works aiming at applications in various technological areas. Important among them are those of Lodi *et.al.*^[54], Hohl *et.al.*^[55], Goedgbuer *et.al.*^[56], Van Wiggeren *et.al.*^[57, 58], and Sivaprakasam *et.al.*^[59] in 2000. Last few years, have witnessed tremendous progress in this area of research where chaotic semiconductor lasers made greater impact in scientific and technological innovations.

2.3 CONTROL OF CHAOTIC SYSTEMS

Until the discovery of deterministic chaos, chaotic behaviour of non-linear dynamical systems was mostly described as noise and hence was not given much attention. Now that the study of chaos has become a part of general science, scientists have started accepting its presence and they expect their systems to show this nature sometimes somewhere in their evolutionary process. Under such circumstances the question that evolves is that, when such uncontrolled erratic behaviours gets into the system trajectories how can we control it and take the system back to our desired working zone or, in other words, how can we control chaos? There are a handful of situations where chaos is undesirable such as arrhythmias of the heart, the most devastating of its kind to fallacious decisions of artificial intelligence systems.

The first attempt to control chaos was made by Pettini^[60] in 1988 by introducing some suitable time dependent variations into certain parameters so as to control chaos. Later in 1990, Ott, Grebogi and York^[61] developed a more

general method based on their observation that a chaotic attractor is composed of an extremely dense set of unstable periodic orbits. Thus, controlling a chaotic system becomes a process of stabilising any of these orbits by continuously applying small time dependent perturbations to a variable system parameter. The method employed is that after extracting the Poincaré section, the desired unstable periodic orbit that is to be stabilised, is selected. Now the system is allowed to run freely on the chaotic attractor until it approaches the desired unstable periodic orbit. At this point the driving parameter of the system is suitably perturbed so that the system never leaves that orbit. Another approach devised by Hunt^[62] in a diode resonator circuit in 1991 did not demand the knowledge of Poincaré section. In this method the difference of the chaotic output from a predefined reference value is calculated and is used to perturb the driving parameter of the system. A novel method that was devised by Murali and Lakshmanan^[63] in 1993, employs introduction of a second periodic signal generator in series with the original so that a quasiperiodic driving occurs which effectively suppresses chaos. Variations of the above methods then came in quick succession ^[64-68].

Control of chaos in laser systems has also attracted much attention because laser systems can serve as models of high dimensional chaotic systems where chaos can be undesirable and can play havoc. Roy *et. al.*^[69] used occasional proportional feedback for controlling chaos in Nd- YAG lasers. In 1994 a simple feed direct feedback was used successfully by Liu *et. al.*^[70].

LASER MODEL AND ITS DYNAMICAL PROPERTIES

The laser model used in our studies and its general dynamical properties are described in brief. The rate equations governing the dynamics of directly modulated semiconductor lasers, the route taken by the system to enter the chaotic regime as also the reverse period doubling route to enter the stable regime are described.

3.1 LASER MODEL

The laser model used for our numerical studies and its dynamical properties are discussed in this chapter. The laser model is a semiconductor laser with directly modulated injection current. A semiconductor laser is a forward biased heavily doped p-n junction fabricated from direct-gap semiconductor material. The injected current is sufficiently large to provide optical gain. The optical feedback is provided by mirrors, which are usually obtained by cleaving the material along its crystal planes. The sharp refractive index difference between the crystal and its surrounding air causes the cleaved surface to act as reflectors^[13]. Semiconductor lasers are the smallest among all the conventional lasers, their size being <1mm. Semiconductor lasers emitting long wavelengths in the range 1.1 - 1.6 μm are of considerable interest in optical fiber communication. The most perfect material having the above characteristics has been identified as InGaAsP-InP combination because of its nearly perfect lattice match^[25]. Its active layer is composed of $\text{In}_{1-x}\text{Ga}_x\text{As}_y\text{P}_{1-y}$ quaternary alloy. By varying the mole fractions x and y , almost any wavelength in the range 1.1-1.6 μm can be selected. The practical semiconductor laser systems of the present era are heterostructure lasers in which the active region is surrounded either on one or both sides by a material of higher band gap and lower refractive index. This layer is known as the cladding layer. The cladding layer in the InGaAsP laser consists of either InP or InGaAsP itself with a different mole fraction. The higher band gap helps to confine electrons to the active region where they can successfully undergo radiative recombination to produce photons. The

difference in refractive index confines the optical mode close to the active region thus acting as a wave guide and helping to reduce internal losses. This in turn reduces the threshold current density. Fig 3.1 shows the double heterostructure laser model^[13].

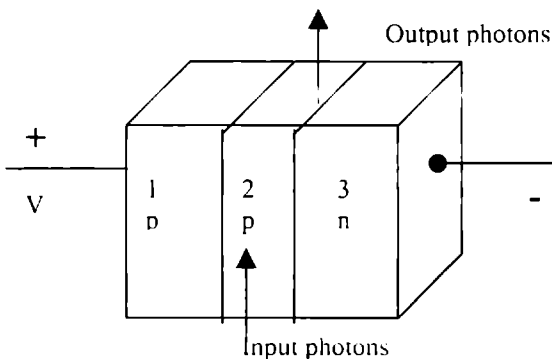


Fig.3.1

Double heterostructure semiconductor laser

Layer 1- p -type with refractive index n_1 and energy gap E_{g1} , Layer 2- p -type with refractive index n_2 and energy gap E_{g2} , Layer 3- n -type with refractive index n_3 and energy gap E_{g3}

In a double heterostructure laser the optical mode is confined perpendicular to the junction plane because the cladding layers have a lower refractive index. For this materials are selected in such a way that E_{g1} and $E_{g3} > E_{g2}$, n_1 and $n_3 < n_2$. The usefulness of a specific structure depends on its performance characteristics and how well they match the requirements for a particular application. InGaAsP lasers operating in the wavelength 1.3 -1.6 μm are used mainly as light source in fiber communication systems.

The laser model used in our studies is a single mode semiconductor laser, with directly modulated injection current. The injection current is subjected to sinusoidal modulation. The single mode rate equations^[27] for photon density S and carrier density n can be represented as

$$\frac{dn}{dt} = \frac{I}{qV} - \frac{n}{\tau_e} - A(n - n_0)S \quad (3.1)$$

$$\frac{dS}{dt} = \Gamma A(n - n_0)S - \frac{S}{\tau_p} + \Gamma \beta \frac{n}{\tau_e} \quad (3.2)$$

where n is the carrier density, S is the photon density, I is the injection current, q is the electron charge, V is the active volume, τ_e and τ_p are the electron lifetime and the photon lifetime respectively, A is the gain constant, n_0 is the carrier density required for transparency, β is the spontaneous emission factor and Γ is the confinement factor.

In the above equations, a small power dependent reduction in the mode gain is to be accommodated so as to model the dynamics perfectly. This reduction in the mode gain occurs due to nonlinear phenomena like spectral hole burning. Thus the rate equations^[27] becomes

$$\frac{dn}{dt} = \frac{I}{qV} - \frac{n}{\tau_e} - A(n - n_0)S \quad (3.3)$$

$$\frac{dS}{dt} = \Gamma A(n - n_0)(1 - \varepsilon_{NL}S)S - \frac{S}{\tau_p} + \Gamma \beta \frac{n}{\tau_e} \quad (3.4)$$

where ε_{NL} is the nonlinear gain reduction factor.

These equations can be normalised and made dimensionless by defining the normalised carrier density N and normalised power P .

$$N = \frac{n}{n_{th}} \quad \text{and} \quad P = \frac{S}{S_0}$$

where $S_0 = \Gamma \left(\frac{\tau_p}{\tau_c} \right) n_{th}$ and $n_{th} = n_0 + (\Gamma A \tau_p)^{-1}$ is the threshold carrier density.

Thus equations 3.3 - 3.4 take the form^[27]

$$\frac{dN}{dt} = \left(\frac{1}{\tau_e} \right) \left[\left(\frac{I}{I_{th}} \right) - N - \left\{ \frac{(N - \delta)}{(1 - \delta)} \right\} P \right] \quad (3.5)$$

$$\frac{dP}{dt} = \left(\frac{1}{\tau_p} \right) \left[\left\{ \frac{(N - 1)}{(1 - \delta)} \right\} (1 - \varepsilon P) P - P + \beta N \right] \quad (3.6)$$

for the sinusoidal modulation of the injection current

$$I(t) = I_b + I_m \sin(2\pi f_m t) \quad (3.7)$$

where $I_{th} = qVn_{th}/\tau_e$ is the threshold current, $\delta = n_0/n_{th}$, $\varepsilon = \varepsilon_{nl}S_0$, I_b is the bias current, I_m is the modulation current and f_m is the modulation frequency.

Numerical studies of these equations show that output of such lasers can show chaotic behaviour with increase in the modulation index $m=I_m/I_{th}$. The route taken by the system for reaching the chaotic state is found to be the period doubling route. The phase diagrams at each stage of period doubling of the

output are shown in Fig 3.2 a-d, for $f_m = 0.8\text{GHz}$. However, higher value of ϵ induces suppression of chaos. The reverse period doubling route to stability is shown in Fig 3.3 a-d. It has been proved that the practical value of ϵ_{NL} for InGaAsP laser are higher than the critical value of 0.01 that is sufficient to suppress chaos at modulation frequencies around 1 GHz [27]. Modulation frequency has little effect on the output dynamics.

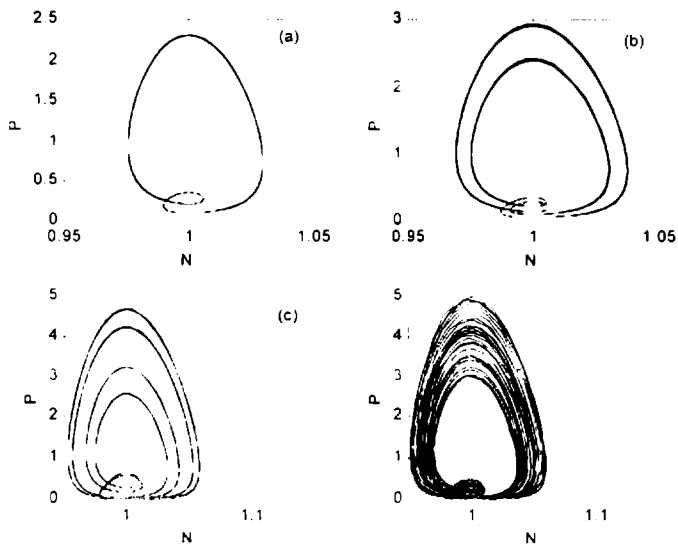


Fig 3.2

Period doubling route to chaos with respect to modulation index m .

a) $m = 0.4$ b) $m = 0.45$ c) $m = 0.49$ d) $m = 0.55$

N - Normalised carrier density; P – Normalised output power

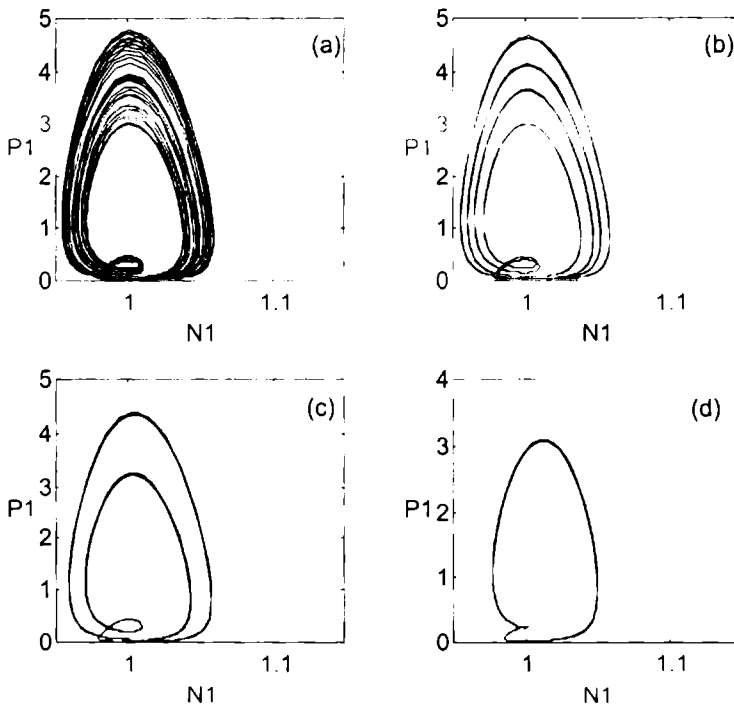


Fig 3.3

Reverse period doubling route to stability with respect to nonlinear gain reduction factor ϵ

a) $\epsilon = 0.001$ b) $\epsilon = 0.0017$ c) $\epsilon = 0.003$ d) $\epsilon = 0.013$

N - Normalised carrier density; P - Normalised output power

The appropriate parameter values for typical semiconductor laser in the chaotic range are shown in Table 3.1. Lyapunov exponents have been calculated^[71] for this system in their chaotic range as $+1.928 \times 10^{-4}$.

Table 3.1

Parameter values for semiconductor laser in chaotic regime

Parameter	Value
τ_e , electron lifetime	3ns
τ_p , photon lifetime	6ps
δ	0.692
f_m	0.8GHz
I_{th}	26mA
I_b	$1.5I_{th}$
I_m	$0.3 I_{th}$
β	$5 \cdot 10^{-5}$
E	0.0001

The above study indicates that strong modulation of injection current and low values of nonlinear gain reduction can induce chaos in the outputs of semiconductor lasers. Thus, by reducing the nonlinear gain suppression factor of InGaAsP lasers chaos can be induced in the output of such lasers, which can be harnessed for suitable application such as chaotic encryption, designing of high power coherent semiconductor arrays etc.

EFFECT OF UNI-DIRECTIONAL AND BI-DIRECTIONAL COUPLINGS ON SYNCHRONISATION OF TWO DIRECTLY MODULATED SEMICONDUCTOR LASERS

The results obtained in our studies on synchronisation of two directly modulated semiconductor lasers using uni-directional and bi-directional coupling schemes are presented. The major finding in our investigation is that bi-directional coupling scheme could provide exact synchronisation between the two lasers and also could control chaos. Uni-directional coupling could induce only practical synchronisation.

4.1 INTRODUCTION

Application of an external force has been found to drive a system to the desired states^[72-74]. Providing a coupling between any two similar systems can effectively induce synchronisation between them. From the preliminary studies of dynamic evolution such as the study of two pendulums hanging from the same rod, synchronised oscillations after an interval of time has been well established. During the past few years several scientific groups have concentrated their studies on the different aspects of synchronisation^[75-79]. Coupling in one direction (uni-directional) is found to be capable of inducing synchronisation^[78]. The effect of such a type of coupling has also been studied in laser systems^[52,81]. Coupling in both directions (bi-directional) has been found to be effective both in synchronisation^[51,55, 82] as well as in the control of chaos^[83,84].

In this chapter we discuss the effects of these two types of couplings on synchronisation of two directly modulated semiconductor lasers. In the uni-directional coupling scheme, a current proportional to a small fraction of the output of the first laser is fed to the input of the second, and the synchronisation properties of the systems with respect to the coupling strength are studied. In the bi-directional scheme^[85], a coupling current proportional to a small fraction of the output of the first laser is given to the input of the second laser in addition to its injection current and similarly a current proportional to a fraction of the second laser is fed to the input of the first laser. Both lasers have their

individual driving currents in addition to these feedback inputs. The fraction that is fed to both the inputs is kept the same during one case study. By changing this value, synchronisation and other dynamical properties are studied.

4.2 UNI-DIRECTIONAL COUPLING SCHEME

Uni-directional scheme can be considered as subclass of the drive-response scheme with no particular modification made to the feedback input. But here the drive and response lasers are almost identical systems. The questions addressed are: i) whether a simple feedback can induce any significant changes in the dynamical behaviour of such systems? ii) what is the minimum requirement for achieving synchronisation between such lasers? iii) what are the types of synchronisation that could be achieved?

4.2.1 COUPLING SCHEME

The model system consists of two identical semiconductor lasers operating in their chaotic regimes with starting from slightly different initial conditions. The injection currents are sinusoidally modulated. One of the two systems runs totally independent of the other. However the second system receives a milliamperic current proportional to a fraction of the output of the former. The schematic representation of the system is presented in Fig. 4.1.

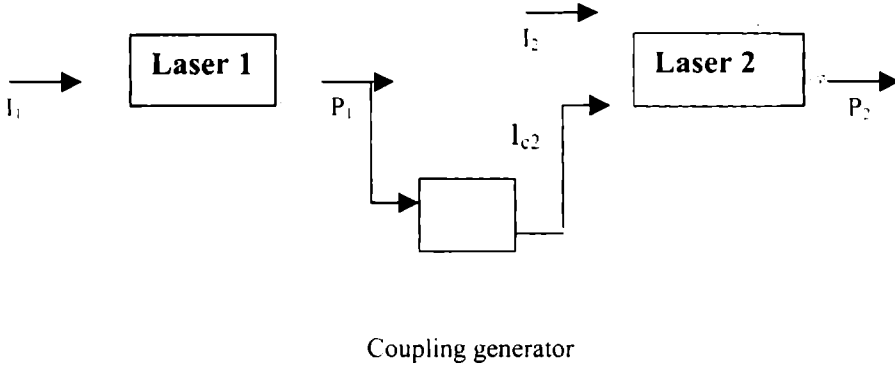


Fig 4.1

Uni-directional coupling scheme

I_1 – Input current of laser 1 ; I_2 – Input current of laser 2 ;
 P_1 – Output power of laser 1 P_2 – Output power of laser 2 ;
 I_{c2} – Coupling current

The rate equations representing the dynamics of the above discussed coupled lasers can be written as

$$\frac{dN_1}{dt} = \left(\frac{1}{\tau_c} \right) \left[\left(\frac{I_1}{I_{th}} \right) - N_1 - \left\{ \frac{(N_1 - \delta)}{(1 - \delta)} \right\} P_1 \right] \quad (4.1)$$

$$\frac{dP_1}{dt} = \left(\frac{1}{\tau_p} \right) \left[\left\{ \frac{(N_1 - 1)}{(1 - \delta)} (1 - \epsilon P_1) P_1 - P_1 + \beta N_1 \right\} \right] \quad (4.2)$$

$$I_1(t) = I_b + I_m \sin(2\pi f_m t) \quad (4.3)$$

$$\frac{dN_2}{dt} = \left(\frac{1}{\tau_e} \right) \left[\left(\frac{I_2}{I_m} \right) - N_2 - \left\{ \frac{(N_2 - \delta)}{(1 - \delta)} \right\} P_2 \right] \quad (4.4)$$

$$\frac{dP_2}{dt} = \left(\frac{1}{\tau_p} \right) \left[\left\{ \frac{(N_2 - 1)}{(1 - \delta)} (1 - \epsilon P_2) P_2 - P_2 + \beta N_2 \right\} \right] \quad (4.5)$$

$$I_2(t) = I_b + I_m \sin(2\pi f_m t) + G \times I_{C2} \quad (4.6)$$

$$G = (C \times P_1) \times 10^{-3} \quad (4.7)$$

where C is the coupling strength, N_1 , N_2 , are the carrier densities of laser 1 and laser 2. P_1 , P_2 are the normalised power of lasers 1 and 2 and, I_{C2} is the coupling current given to laser 2. The relevant parameter values are given in Table 3.1.

4.2.2 NUMERICAL ANALYSIS AND RESULTS

The above equations are numerically simulated with the step size in the picosecond range. Parameter space plots and synchronisation error plots are

used for studying the synchronisation properties. Parameter space plots are drawn with the output powers P_1 and P_2 along the two axes. Synchronisation error is defined as $E = \text{abs}(P_1 - P_2)$. A plot of time evolution of E is referred to as the synchronisation error plots. For the study of output dynamics, the phase diagrams with N and P are plotted along the two axes, are used.

The two outputs show no observable synchronisation till the coupling value reaches 7. Fig 4.2a shows the parameter space plots for $C < 7$ and 4.2b shows the parameter space plots for $C > 7$. As the coupling value reaches 7, even though the outputs remain chaotic, there is practical synchronisation with synchronisation error decaying to a region near the origin. Fig 4.3a shows the synchronisation error plot for $C < 7$ and Fig 4.3b shows the synchronisation error plot for $C > 7$. With further increase in coupling strength the output of the second laser gets amplified and the quality of synchronisation decreases. When coupling strength increases above 10 the systems lose synchronisation. In the range $C = 7-10$, the type of synchronisation remains practical. There is no pronounced effect of coupling on the output dynamics of individual lasers except for the amplification of the output power of second laser. The phase space plots of the two lasers show that they remain chaotic throughout the range of coupling strengths. Fig 4.4a shows phase plots of laser 1 and 2 for $C = 2$ and Fig 4.4b shows phase plots of laser 1 and 2 for $C = 20$. The absence of a closed loop indicates that the outputs are chaotic^[27]. This study reveals that uni-directional coupling between two chaotic semiconductor lasers can induce only practical synchronisation for a small range of coupling strength.

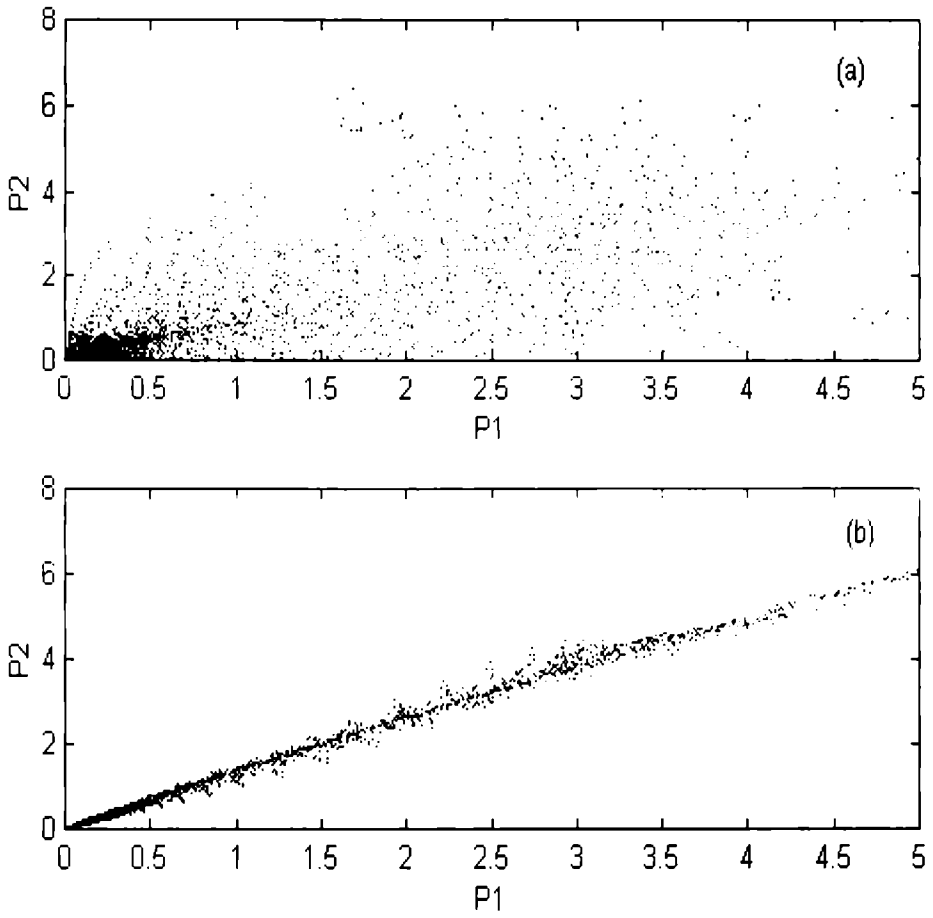


Fig 4.2

Parameter space plot for uni-directional coupling for

(a) $C < 7$ (b) $C > 7$

P_1 = Output power of laser1 ; P_2 = Output power of laser2

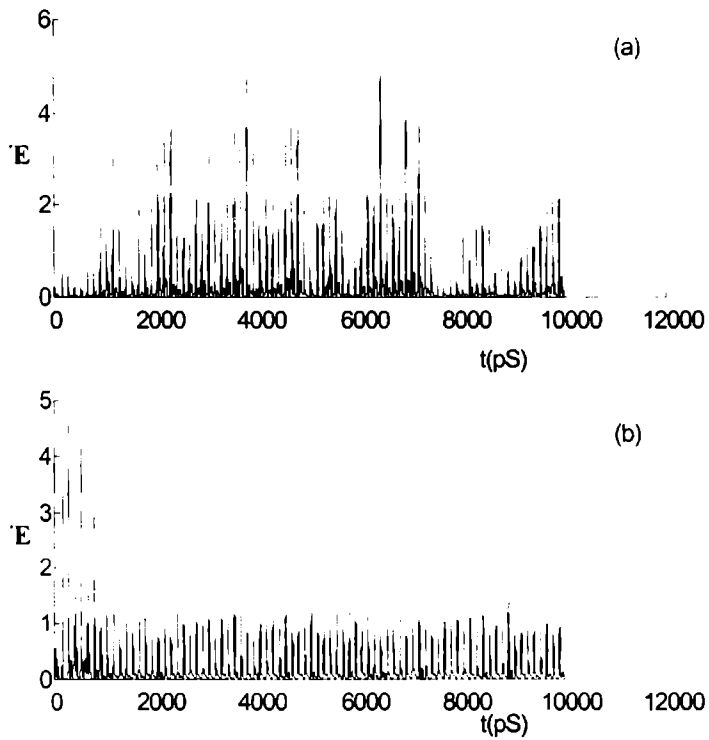


Fig 4.3

Synchronisation error plots for uni-directional coupling for

(a) $C < 7$ (b) $C > 7$

'E – Synchronisation error ; t - time in picosecond

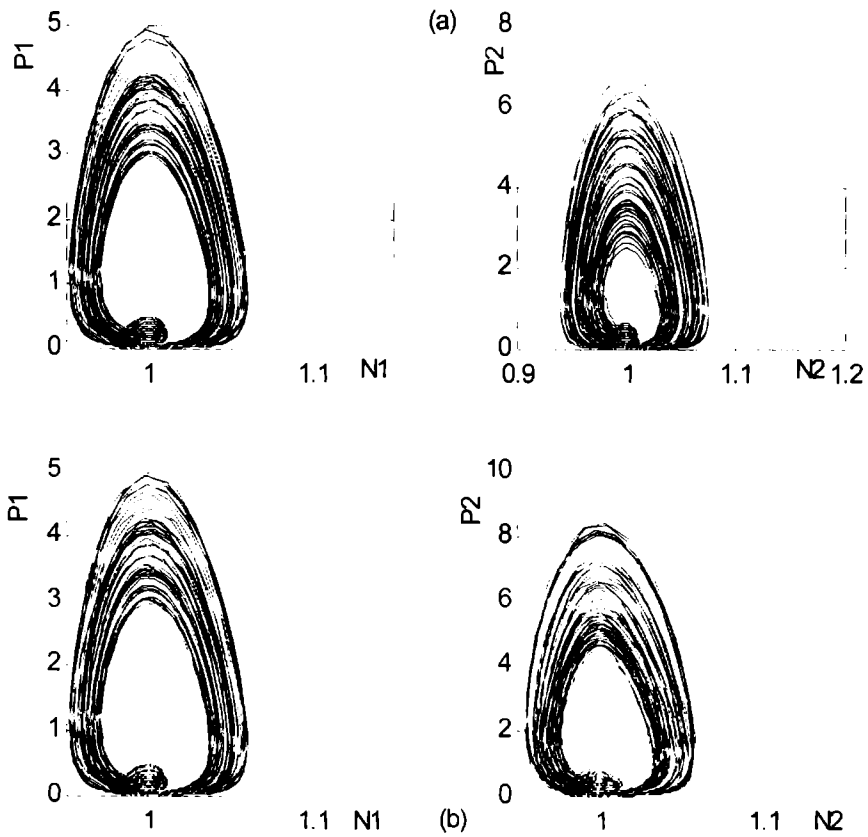


Fig 4.4

Phase space plots for of lasers 1 and 2

(a) $C = 2$

(b) $C = 20$

N_1 – Carrier density of laser 1 : N_2 – Carrier density of laser 2 : P_1 – Output power of laser 1

P_2 – Output power of laser 2

4.3 BI-DIRECTIONAL COUPLING

A method of bi-directional coupling has been recently employed to stabilise or control the chaotic outputs of directly modulated semiconductor lasers ^[83,84]. This scheme is used in our studies for synchronising the outputs of two such lasers with different initial conditions^[86]. Coupling is given by providing a small current proportional to the output of the first laser to the input of the second laser and similarly from the output of the second to the input of the first. The effect of the coupling strength on synchronisation and other dynamical properties of the two systems is studied using parameter space plots, synchronisation error plots and phase diagrams.

4.3.1 COUPLING SCHEME

The model system used for our numerical study consists of two identical semiconductor lasers operating in their chaotic regimes starting from slightly different initial conditions. The injection currents are sinusoidally modulated. A coupling current proportional to a small fraction of the output of the first laser is fed to the input of the second laser and similarly a current proportional to the output of the second laser is fed to the input of the first. Thus the output power of laser 1 will influence the dynamics of laser 2 and similarly the output power of laser 2 will influence the dynamics of laser 1. The schematic representation of the bi-directionally coupled directly modulated semiconductor laser system is presented in Fig. 4.5.

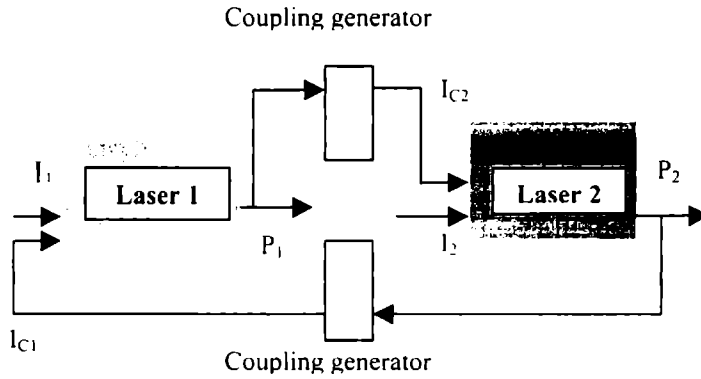


Fig. 4.5

Bi-directional coupling scheme

I_1 – Input current of laser 1 ; I_2 – Input current of laser 2 ; P_1 – Output power of laser 1 ;
 P_2 – Output power of laser 2; I_{c1} – Coupling current given to laser1 ; I_{c2} – Coupling current
 given to laser2

The rate equations governing the processes are as follows

$$\frac{dN_1}{dt} = \left(\frac{1}{\tau_e} \right) \left[\left(\frac{I_1}{I_{th}} \right) - N_1 - \left\{ \frac{(N_1 - \delta)}{(1 - \delta)} \right\} P_1 \right] \quad (4.8)$$

$$\frac{dP_1}{dt} = \left(\frac{1}{\tau_p} \right) \left[\left\{ \frac{(N_1 - 1)}{(1 - \delta)} \right\} (1 - \epsilon P_1) P_1 - P_1 + \beta N_1 \right] \quad (4.9)$$

$$I_1(t) = I_b + I_m \sin(2\pi f_m t) + G_1 \times I_{c1} \quad (4.10)$$

$$\frac{dN_2}{dt} = \left(\frac{1}{\tau_c} \right) \left[\left(\frac{I_2}{I_{th}} \right) - N_2 - \left\{ \frac{(N_2 - \delta)}{(1 - \delta)} \right\} P_2 \right] \quad (4.11)$$

$$\frac{dP_2}{dt} = \left(\frac{1}{\tau_p} \right) \left[\left\{ \frac{(N_2 - 1)}{(1 - \delta)} \right\} (1 - \epsilon P_2) P_2 - P_2 + \beta N_2 \right] \quad (4.12)$$

$$I_2(t) = I_h + I_m \sin(2\pi f_m t) + G_2 \times I_{c_2} \quad (4.13)$$

$$G_1 = (C \times P_2) \times 10^{-3} \quad (4.14)$$

$$G_2 = (C \times P_1) \times 10^{-3} \quad (4.15)$$

4.3.2 NUMERICAL ANALYSIS AND RESULTS

The rate equations are solved numerically using the fourth order Runge-Kutta method with parameter values as in Table 3.1 and step size in the picosecond range. The parameter space plots with the output power P_1 and P_2 along the two axes and synchronisation error plot showing the time evolution of the synchronisation error $E = \text{abs}(P_1 - P_2)$ are drawn for each value of the coupling strength C for checking synchronisation. For low values of C the initial error increases to very high values and remains high even in the long run. This indicates a lack of synchronisation between P_1 and P_2 . Above the value 2 of the coupling strength, the outputs start getting practically synchronised, i.e. as C increases the error, even though initially grows to slightly high values, soon decays off to near zero values within a few nanoseconds. At $C = 2.6$ the type of synchronisation becomes exact with error decaying to zero. Fig 4.6a, b and c represent the parameter space plots for $C < 2$, $2 < C < 2.6$, $C = 2.6$ and Fig 4.7a, b and c represent the synchronisation error plots for $C < 2$, $2 < C < 2.6$, $C = 2.6$

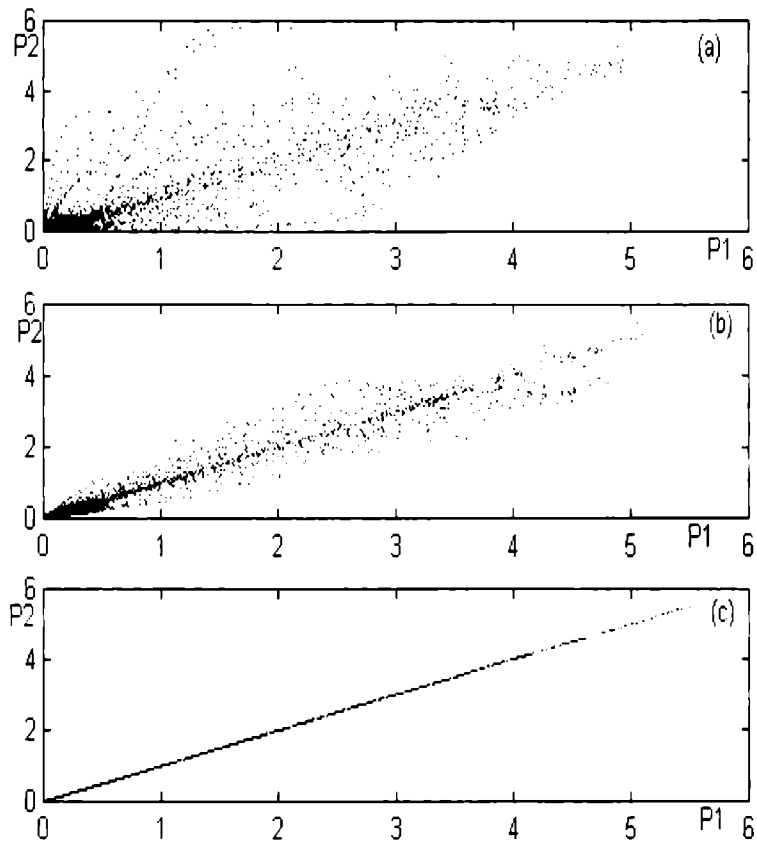


Fig.4.6

Parameter space plots for bi-directional coupling

(a) $C < 2$ (b) $2 < C < 2.6$ (c) $C = 2.6$

P_1 – Output power of laser 1 ; P_2 – Output power of laser 2

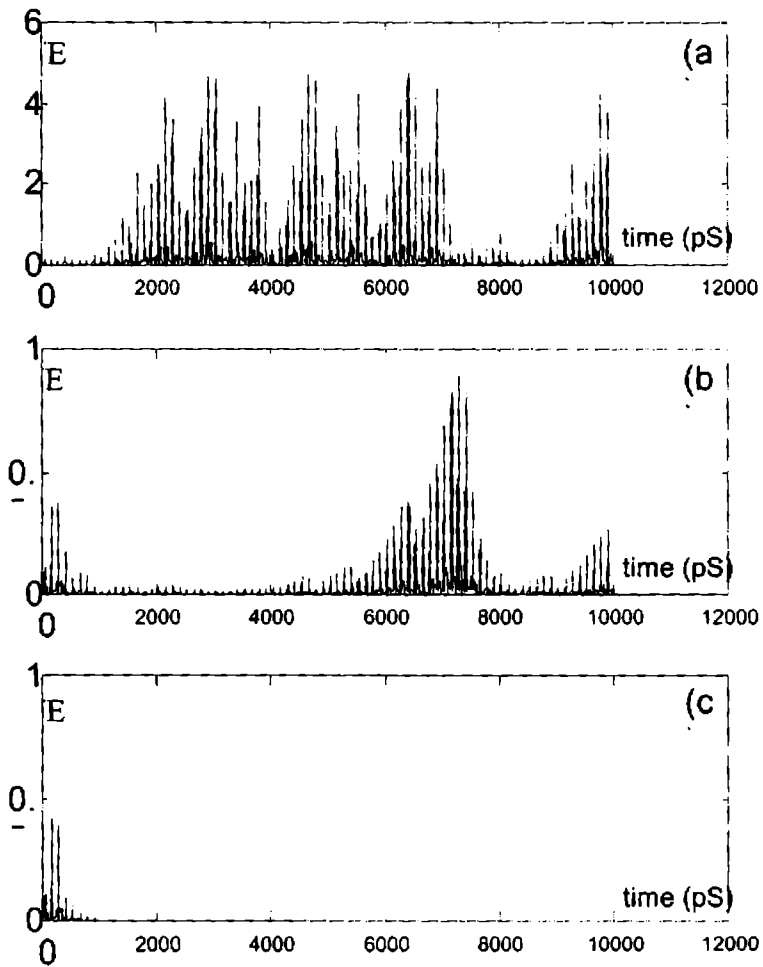


Fig 4.7

Synchronisation error plot for

(a) $C < 2$ (b) $2 < C < 2.6$ (c) $C = 2.6$ E – Synchronisation error

As C is increased further above 2.6 the output dynamics of the two lasers changes. The phase diagrams in Fig. 4.8a-d indicate that the systems undergo a reverse period doubling with a period four cycle at $C=6$; a period two cycle at $C=9$; and a period one cycle at $C=17$.

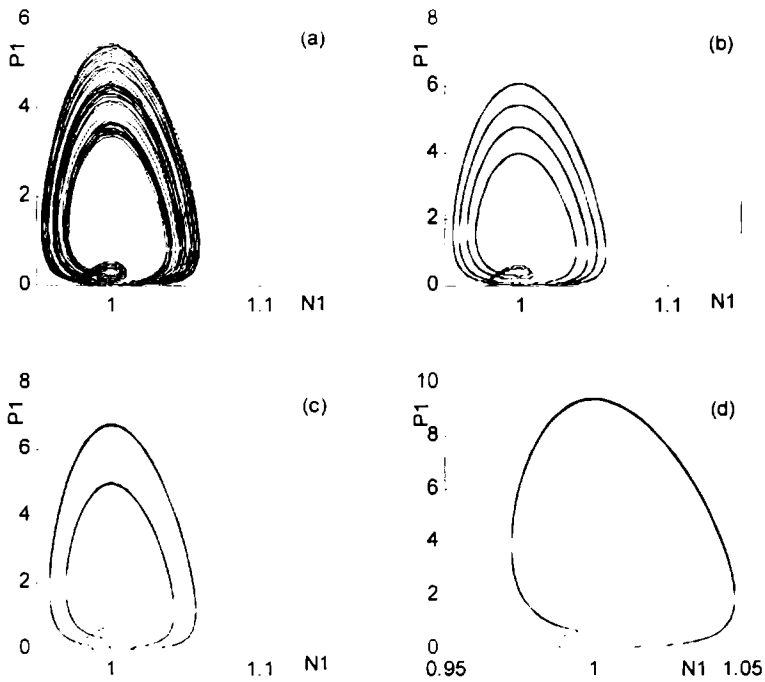


Fig 4.8

Phase plots of lasers for coupling strength

(a) $C = 2.6$ (b) $C = 6$ (c) $C = 9$ (d) $C = 17$

N_1 – Carrier density of laser1 ; N_2 – Carrier density of laser2 ; P_1 – Output power of laser 1
 P_2 – Output power of laser 2

For coupling values 1 to 17, the time series of P_1 and P_2 shows a double peak structure, which is a manifestation of relaxation oscillation. For C values above 18 this second peak inside a single modulation period almost disappear, simultaneously with an increase in the output power. The time series of the outputs P_1 and P_2 for $C = 2$ and $C = 20$ are shown in Fig 4.9a and b. The time series of output P_2 at $C = 20$ shows the increase in the output power.

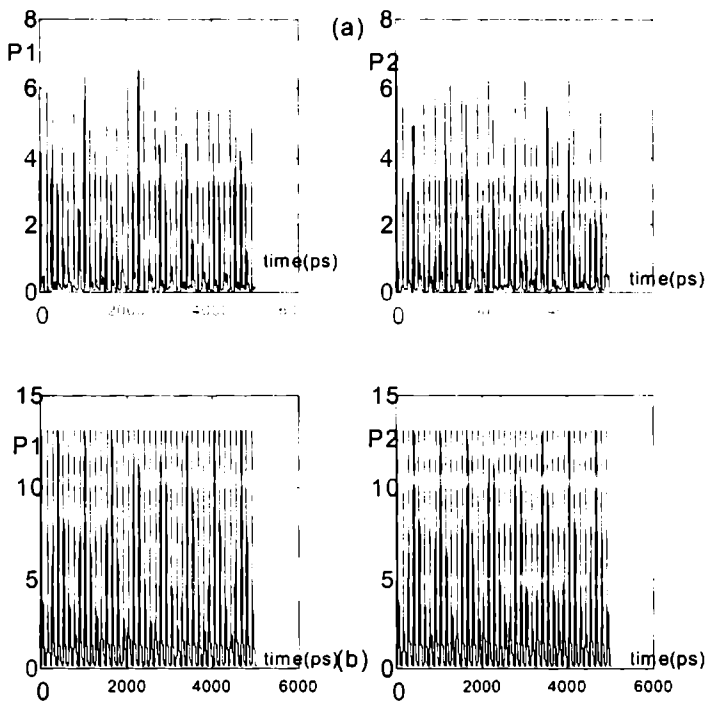


Fig 4.9

Time series of output powers of lasers 1 and 2 for

(a) $C = 2$ (b) $C = 20$

P_1 – Output power of laser 1 ; P_2 – Output power of laser 2

For $C = 18$ to 25 the suppression of double peak that is evident from the deformation of the phase plot becomes more pronounced and when $C = 26$, the phase diagrams become a single closed curve without the notch that was present for low values of C (Fig 4.10). This confirms the suppression of the double peak structure.

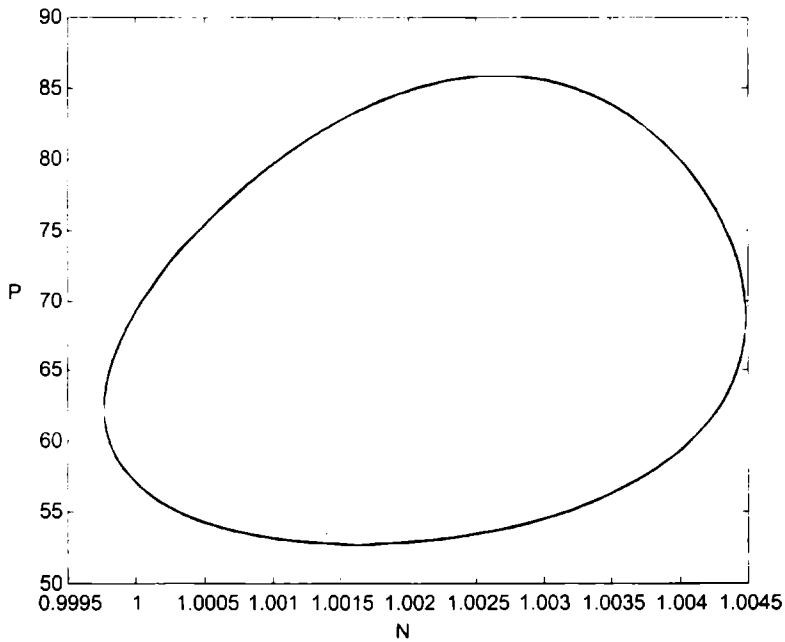


Fig 4.10

Phase space plots of laser 1 and laser 2 for coupling strength $C = 26$

N – Carrier density of the lasers P – Output power of the lasers

A reverse period doubling route to stability, suppression of the double peak, and high increase in the output power are apparent here. Above all, there is synchronisation between the two outputs at all these stages of the system dynamics. With the introduction of the CP_2 in the above equations for making the coupling bi-directional we achieve synchronisation, reverse period doubling and suppression of the second peak together with an amplification of the output power

The double peak within a single modulation period has been explained as a manifestation of relaxation oscillation, which gets damped by an increase in ϵ , the term governing nonlinear gain reduction^[27]. In this situation the double peak structure and period doubling are suppressed by an increase in ϵ , but at the cost of the output power. However, our method, based on the results obtained, shows a definite advantage as it provides an alternate method for suppressing the chaotic nature and the second peak together with an increase in the output power^[86].

To check the stability of the synchronised state, we perturb the system after it achieves synchronisation. When the error becomes low such that the system can be considered in synchronisation, P_1 and P_2 are in such a way that the synchronisation error is made as large as it was in the beginning. This is done for each value of coupling strength and the corresponding error plots are taken. For values of C less than 2, since the system never achieves synchronisation, artificial perturbation is not applied. Above the threshold a perturbation is

applied when the two outputs are in synchronisation. The corresponding error plots are shown in Fig 4.11a and b. For low values of C , where the system outputs are chaotic, the perturbation grows to slightly high values but eventually decays to almost zero within an interval of about 20 nanoseconds. For higher values of C , this interval gets reduced to around one or two nanoseconds. This shows that the stability of the synchronised states increase with increasing values of C . Thus by choosing appropriate coupling values, we can choose among chaotic synchronisation, suppression of chaos, or high gain outputs. All these results are summarised in Table 4.1 showing the different coupling values and the corresponding dynamics of the systems.

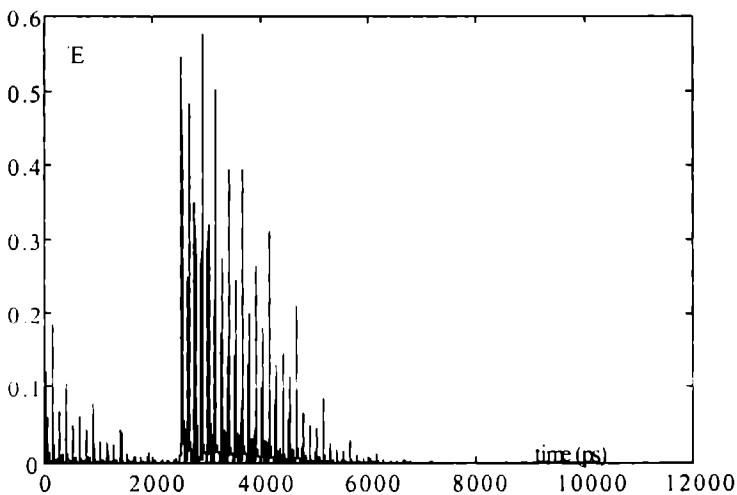


Fig 4.11 a

Error vs corresponding time with perturbation for coupling strength
for $C = 6$

'E -Synchronisation error

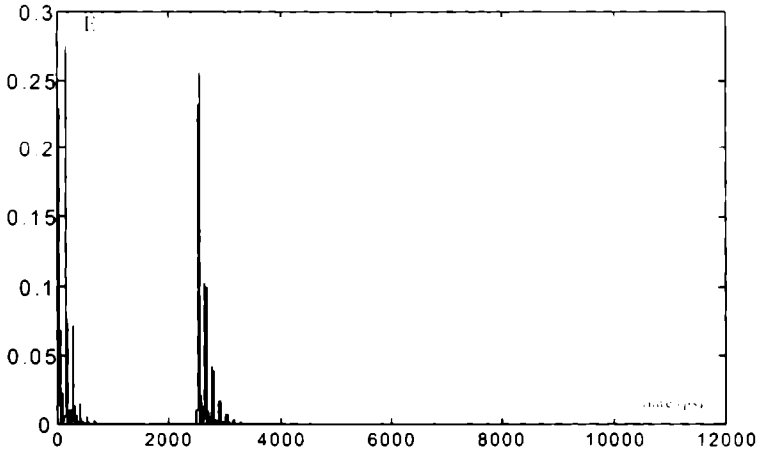


Fig 4.11b

Error vs corresponding time with perturbation for coupling strength
for $C = 20$

E -Synchronisation error

The above study shows that bi-directional coupling is more effective in inducing synchronisation between two directly modulated semiconductor lasers. Bi-directional coupling can synchronise the two outputs for lower values of coupling strength than the uni-directional coupling scheme. Uni-directional coupling can result only in practical synchronisation whereas bi-directional scheme can provide exact synchronisation between the two outputs. In addition bi-directional scheme can control the chaotic outputs and bring them to stability for strong coupling strengths together with suppression of double peaks in the outputs and output amplification.

Table 4.1
Coupling strength and the corresponding dynamics

Coupling strength C	Dynamics	Synchronisation
1,2	Chaotic	No
3 to 5	Chaotic	Yes
6	Four cycle	Yes
7,8	Four cycle	Yes
9 to 16	Two cycle	Yes
17 to 25	One cycle	Yes
26	One cycle	Yes

VARIABLE FEEDBACK METHOD FOR SYNCHRONISATION OF TWO DIRECTLY MODULATED SEMICONDUCTOR LASERS

The results of our studies on synchronisation of two directly modulated semiconductor lasers using the variable feedback method are presented in this chapter. The results indicate that there is a critical value feedback fraction that can induce synchronisation between the two lasers. The type of synchronisation that could be achieved is exact.

5.1 INTRODUCTION

A very important characteristic of semiconductor lasers is its unique output wavelength that matches with the optimal performance of the optical fibers and that is one of the reasons why it remains a subject for active discussion and intense research. Feedback methods are widely used for the control and synchronisation of two or more chaotic systems. Some of the methods currently in use are the following

- 1) Giving a proportional feedback from another system^[87]
- 2) Occasional proportional feedback from another system^[88]
- 3) Self- feedback for intensity noise control^[89]
- 4) Varying self feed back^[45, 74].

A variation of the method 4 mentioned above^[45], introduced by Ali for synchronisation of two logistic maps^[90] is the variable feedback method. This method was later studied in detail by Morgul^[44]. This is the method adopted in our study^[91] for synchronisation of two chaotic semiconductor lasers.

5.2 VARIABLE FEED BACK SCHEME

We employed a drive response scheme where one of the two lasers is taken as the drive laser and the other as the response laser. The drive and response lasers are identical semiconductor lasers. Both these systems operate in their

chaotic regime, but start from slightly different initial conditions. Outputs of the drive laser and response laser are fed to a feedback generator where a fraction of the difference between these two outputs (i.e. the synchronisation error) is generated. A feedback current proportional to a small fraction of this value is fed to the input of the response laser in addition to its input current. This scheme is numerically implemented and studied. The feedback function defined at each step will be different since the outputs are chaotic and different from each other. The schematic representation is shown in Fig 5.1

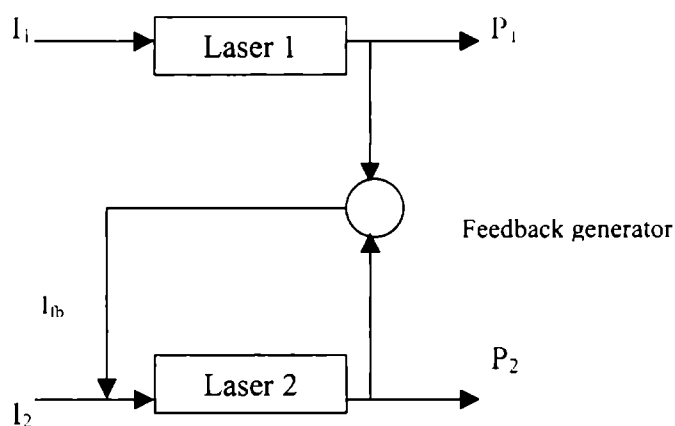


Fig 5.1

Variable feed back scheme

I_1 and I_2 are the input currents of lasers 1 and 2 ; P_1 and P_2 are the outputs of lasers 1 and 2 ; I_{fb} is feedback current

The rate equations governing the dynamics of the system represented in Fig 5.1 can be written as

$$\frac{dN_1}{dt} = \left(\frac{1}{\tau_e} \right) \left[\left(\frac{I_1}{I_{th}} \right) - N_1 - \left\{ \frac{(N_1 - \delta)}{(1 - \delta)} \right\} P_1 \right] \quad (5.1)$$

$$\frac{dP_1}{dt} = \left(\frac{1}{\tau_p} \right) \left[\left\{ \frac{(N_1 - 1)}{(1 - \delta)} \right\} (1 - \alpha P_1) P_1 - P_1 + \beta N_1 \right] \quad (5.2)$$

$$I_1(t) = I_b + I_m \text{Sin}(2\pi f_m t) \quad (5.3)$$

$$\frac{dN_2}{dt} = \left(\frac{1}{\tau_e} \right) \left[\left(\frac{I_2}{I_{th}} \right) - N_2 - \left\{ \frac{(N_2 - \delta)}{(1 - \delta)} \right\} P_2 \right] \quad (5.4)$$

$$\frac{dP_2}{dt} = \left(\frac{1}{\tau_p} \right) \left[\left\{ \frac{(N_2 - 1)}{(1 - \delta)} \right\} (1 - \alpha P_2) P_2 - P_2 + \beta N_2 \right] \quad (5.5)$$

$$I_2(t) = I_b + I_m \text{Sin}(2\pi f_m t) + G \times I_{th} \quad (5.6)$$

where G is the feedback function defined as

$$G = r (P_1 - P_2) \times 10^{-3} \quad (5.7)$$

5.2.1 NUMERICAL ANALYSIS AND RESULTS

The above rate equations are solved numerically using fourth order Runge-Kutta method. The time step used in the calculations is in the picosecond range. The appropriate value of feedback fraction 'r' that can effectively induce

synchronisation between the two systems is to be decided by trial and error method. The relevant parameters are given in Table 3.1.

The value of 'r' is slowly increased from 0 and synchronisation is checked at each value. For checking the synchronisation between the two systems, parameter space plot and the synchronisation error plot are used. The parameter space plot contains P_1 along the x axis and P_2 along the y axis. The synchronisation error is defined as the difference between the two outputs, i.e. $E = \text{abs}(P_1 - P_2)$. Synchronisation error is plotted against the corresponding time in the synchronisation error plot. Synchronisation error plots reveal the time evolution of the synchronisation error.

Results of our study indicate that there is a critical value of the feedback fraction above which the two systems synchronise with each other. Below this value the two outputs remain uncorrelated with each other. This critical value of the feedback fraction 'r' is found to be 7. Fig 5.2a, b shows the parameter space plots for 'r' below and above this critical value. The two systems achieve synchronisation above the critical value, the synchronisation type being the 'exact'. For low values of 'r', the synchronisation error initially grows to higher values and never decays off. But as 'r' becomes 7 the synchronisation error, even though initially grows to some higher values, soon decays off to zero. Fig 5.3 a, b shows the synchronisation error plots before and after achieving synchronisation.

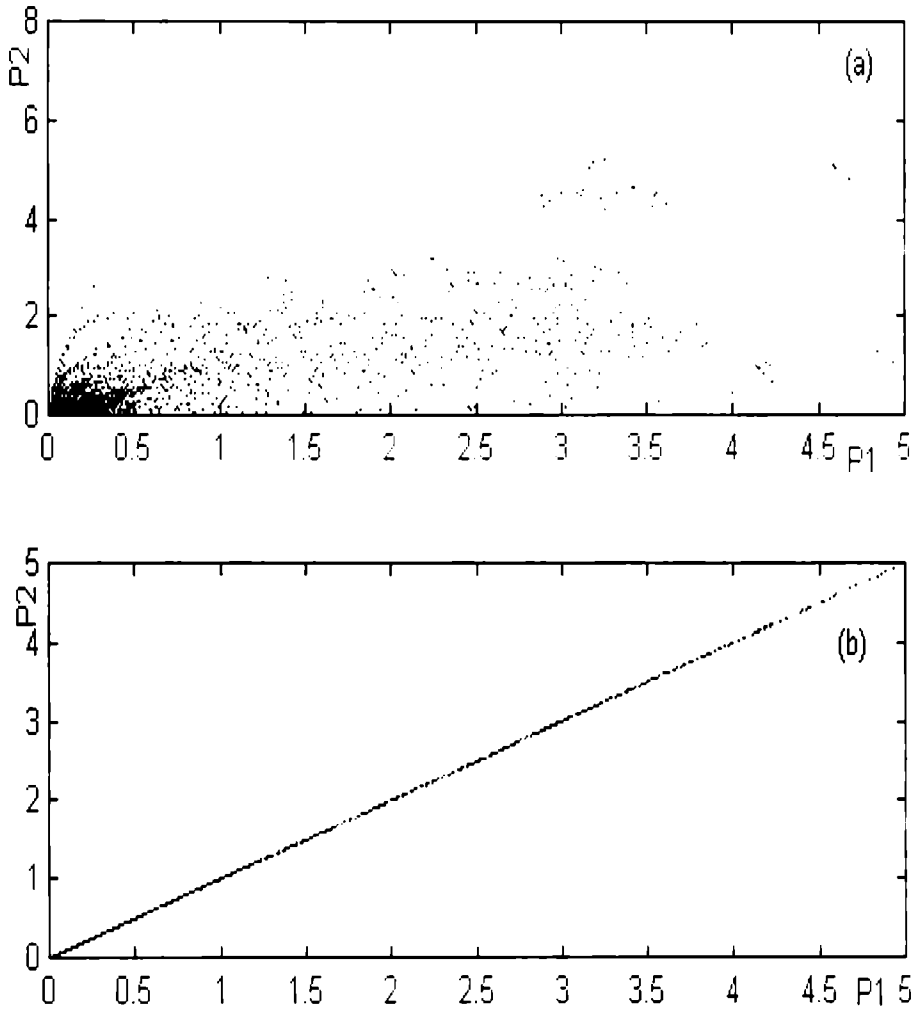


Fig 5.2

Parameter space plot of laser 1 and 2 for

a) $r < 7$ b) $r = 7$ P_1 -output power of laser 1 ; P_2 -output power of laser 2

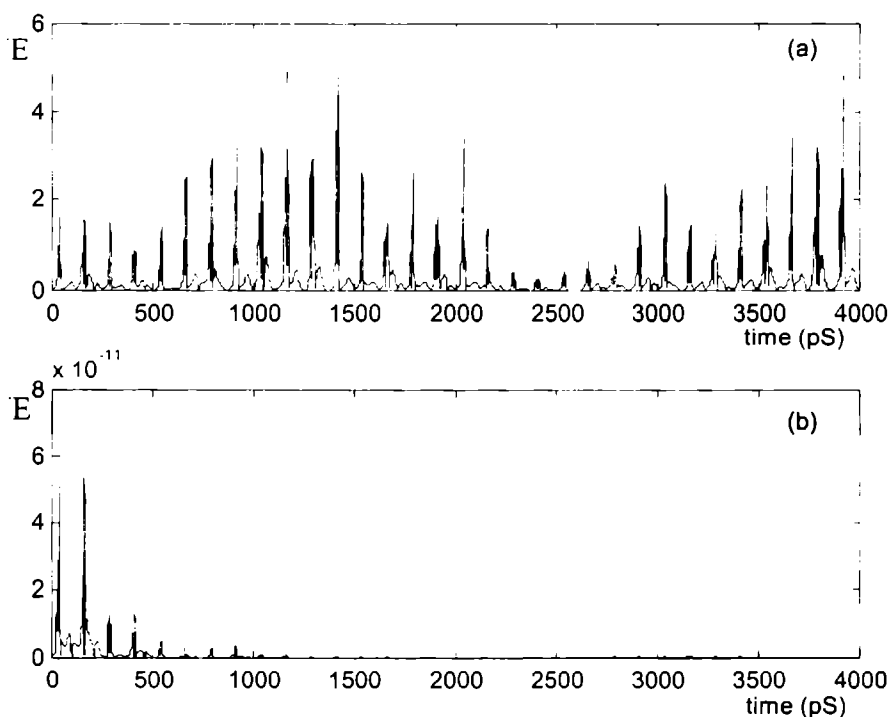


Fig 5.3

Synchronisation error plots for

a) $r < 7$ b) $r = 7$

'E - synchronisation error

These results indicate that for synchronising similar semiconductor lasers with slightly different initial conditions the variable feedback method is more effective than the uni-directional method. However, compared to the bi-directional coupling scheme, which can suppress the chaotic fluctuation of the laser output the variable feedback method is not effective in controlling chaos.

The usefulness of a method, anyhow, depends on the effectiveness of that method for the particular application for which it is used. On this basis it is reasonable to assume that the variable feedback scheme will be appropriate for applications in the field of chaotic communication systems, where the drive response scheme is the most suitable one.

CHAOTIC ENCRYPTION USING LONG WAVELENGTH DIRECTLY MODULATED SEMICONDUCTOR LASERS

A new feedback function called the Proportional-Integral (**P-I**) feedback is introduced for synchronising two chaotic direct current modulated long wavelength semiconductor lasers and is applied to the secure communication system. Encoding of the message is achieved by direct amplitude modulation at the output of the transmitter. The message is decoded at the receiving end by synchronising it with the transmitter employing the (**P-I**) function optimised for the semiconductor lasers.

6.1 INTRODUCTION

The communication system has undergone revolutionary changes from the days of Graham Bell and today is almost considered synonymous with a measure of human progress and civilization. Every form of life on earth has its own mode of communication. Human beings communicate with each other through the medium of language as well as gestures. With the territorial development of the world, the need for distant communication became inevitable and in the present world scenario the need for secret communication is increasing. A conventional communication system consists of a transmitter, a receiver, and a transmission channel. The transmitter should have a message generator and a carrier wave generator. The receiver should contain a decoder for the process of decoding the messages from the received composite signal. Encryption is the process by which a message, either electronic or optical signal, is transmitted *confidentially* to a receiver. To accomplish this the carrier signal should play the role a masking signal.

6.2 CHAOTIC ENCRYPTION

The distinctive features of a secure communication system are

- i) ability of the carrier signal to shield the message from eavesdroppers.
- ii) easy separation of the masking signal at a distant site (receiver end) without any loss of the information.

Messages can be encoded and decoded by various methods. Encoding is the process of mixing the carrier and message signals and decoding refers to the filtering of the carrier from the message. In the conventional methods that use noise signals for masking, the messages can be easily decoded by using suitable noise filters thus making the message amenable for tapping or jamming. In this context it becomes very essential to develop a method of communication, particularly in matters connected with national security, safe conveyance of secure scientific data etc. that is tamper proof and can maintain its confidentiality until it reaches the intended hands. Chaos can play significant role in this respect. The necessary characteristics of a message carrier are matched in full by the unpredictability and possibility of synchronisation of a chaotic system, which makes it an ideal choice to act as a carrier for message encryption. When the carrier/ masking signal is chaotic the use of conventional filters for decoding will not be fruitful since these are signals generated by some deterministically evolving dynamical systems.

When the carrier signal is chaotic, the nonlinear interactions between the carrier and message generators will result at times in characteristics of the transmitted signal which bear no resemblance at all with the combining frequencies. This would result in difficulties in retrieving the original message frequency. At the receiver end the filtering unit should identify and replicate the chaotic signal for proper unmasking of the encoded message. For this purpose the receiver should get perfectly synchronised with the transmitter and therefore chaotic synchronisation assumes much importance^[92-101]. Several methods have been

proposed for achieving chaotic encryption such as chaotic masking^[102,103], chaos shift keying^[54, 93,104, 105] and chaotic modulation^[106-108].

Semiconductor lasers and Erbium doped fiber lasers are the most efficient optical sources in the present day communication systems. Secure communication wherein the message is hidden and transmitted has been achieved with various types of such lasers^[56,57,59,109,110]. Semiconductor lasers emitting radiation in the long wavelength region (1.3 -1.5 μm) are very useful in optical communication systems since they can provide large bandwidth for transmission in contrast to electronic systems. Minimum loss and dispersion of radiation in this wavelength window is a characteristic feature of optical fibers. They also allow a higher bandwidth compared to their electronic counterparts. Hence a combination of semiconductor lasers and optical fibers can serve as a very effective tool in long distance communication. In this chapter we are discussing the synchronisation of chaotic long wavelength directly modulated semiconductor lasers and their application in secure communication^[111].

6.3 MESSAGE ENCODING AND DECODING

Encoding and decoding of the message is shown in Fig. 6.1. The transmitter end is equipped with a message generator, carrier chaos generator (drive) and a modulator that adds the message on to the chaotic carrier waveform. A semiconductor laser is used as the chaos generator, which also acts as the drive for the response at the receiver end.

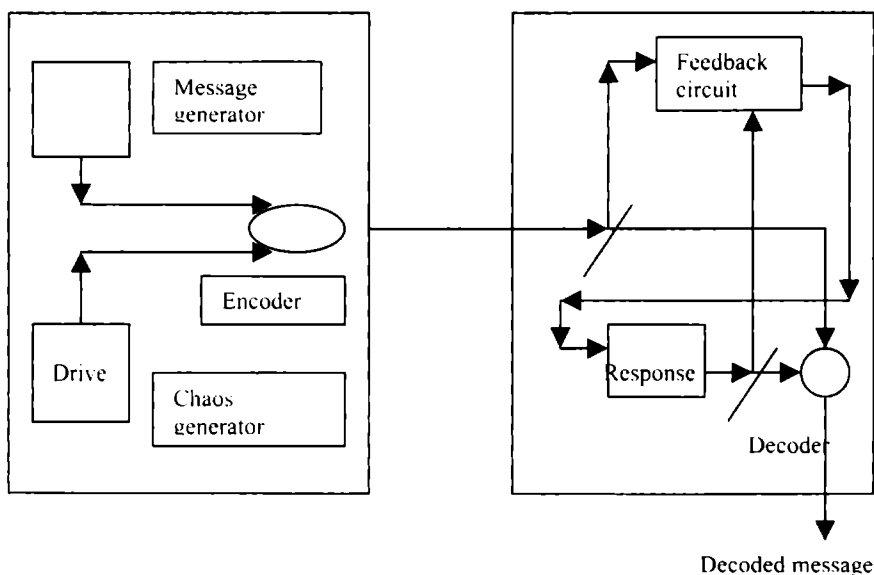


Fig 6.1

Encoding and decoding scheme

The message encoding is done by a simple amplitude modulation at the transmitter output. The message is added to the chaotic carrier wave, i.e. $P_{\text{tm}} = P_{\text{tr}} + P_{\text{m}}$, where P_{tm} is the transmitted signal, P_{tr} is the transmitter laser output and P_{m} is the message signal amplitude. The chaos generator at the receiver end, which is a semiconductor laser, is similar to the one at the transmitter end. The function of this diode laser is to act as the response system, which will try to generate chaotic waveform similar to the carrier wave. Also, there is a feedback function generator. A part of the received signal is fed to the input of the feedback generator together with a fraction of the chaotic output of the response laser diode. A feedback current is generated here, which is fed to the input of the response laser diode as a feedback current I_{fb} in addition to its drive current. This

controls the receiver dynamics and tries to synchronise it with the dynamics of the drive at the transmitter. After the two systems are synchronised, a simple difference between the amplitude of the received signal and the output of the receiver will provide the decoded message. This shows that the receiver gets synchronised only with the chaotic part of the received modulated signal. Decoding of the message is successful only when perfect synchronisation is achieved.

The transmitter and the receiver are two identical semiconductor lasers operating in their chaotic regime starting from slightly different initial conditions. Synchronisation of such lasers has been achieved, as discussed in the previous chapters, using uni-directional coupling, bi-directional coupling and variable feedback, of which uni-directional coupling and variable feedback can be used for the purpose of chaotic encryption. In the present study a simple addition of the message to the carrier is employed for masking the signal^[111]. This method has been successfully employed^[54,59,110] for chaotic encryption, where a fraction of the received modulated signal is fed into the input of the receiver for synchronising the response laser in the receiver with the drive in the transmitter i.e. the feedback fraction is proportional to the received signal amplitude. This scheme is similar to the uni-directional coupling scheme.

The transmitter and receiver are two similar semiconductor lasers with a feedback given to the input of the one that is chosen as the receiver. The

rate equations modeling the transmitter and receiver system can be represented as follows

$$\frac{dN_{tr}}{dt} = \left(\frac{1}{\tau_c} \right) \left[\left(\frac{I_{tr}}{I_{th}} \right) - N_{tr} - \left\{ \frac{(N_{tr} - \delta)}{(1 - \delta)} \right\} P_{tr} \right] \quad (6.1)$$

$$\frac{dP_{tr}}{dt} = \left(\frac{1}{\tau_p} \right) \left[\left\{ \frac{(N_{tr} - 1)}{(1 - \delta)} (1 - \epsilon P_{tr}) P_{tr} - P_{tr} + \beta N_{tr} \right\} \right] \quad (6.2)$$

$$I_{tr}(t) = I_{btr} + I_{mtr} \text{Sin}(2\pi f_{mtr} t) \quad (6.3)$$

$$\frac{dN_{rc}}{dt} = \left(\frac{1}{\tau_c} \right) \left[\left(\frac{I_{rc}}{I_{th}} \right) - N_{rc} - \left\{ \frac{(N_{rc} - \delta)}{(1 - \delta)} \right\} P_{rc} \right] \quad (6.4)$$

$$\frac{dP_{rc}}{dt} = \left(\frac{1}{\tau_p} \right) \left[\left\{ \frac{(N_{rc} - 1)}{(1 - \delta)} (1 - \epsilon P_{rc}) P_{rc} - P_{rc} + \beta N_{rc} \right\} \right] \quad (6.5)$$

$$I_{rc}(t) = I_{brc} + I_{mrc} \text{Sin}(2\pi f_{mrc} t) + G \times I_{fb} \quad (6.6)$$

where I_{fb} is a milliamper current given to the receiver as an additional input, G is a control function which modifies the feedback current I_{fb} , N_{tr}, N_{rc} are the carrier densities, P_{tr}, P_{rc} are output powers of the transmitter and receiver, I_{tr}, I_{rc} are driving currents I_{btr}, I_{brc} are the bias currents, I_{mtr}, I_{mrc} are the modulation currents and f_{mtr}, f_{mrc} are the modulation frequencies of the transmitter and receiver lasers respectively. The parameter values are so adjusted that the above equations represent InGaAsP lasers in the chaotic region. The values are given in Table 3. 1.

The form of the control function that can synchronise a particular system is to be suitably chosen by trial and error.

The uni-directional and variable feedback methods are tried for achieving synchronisation between the transmitter and the receiver using the received composite signal. The synchronisation is checked with the parameter space plot with P_{tr} along X-axis and P_{rc} along Y-axis.

It is found that the uni-directional coupling scheme is not efficient enough for achieving synchronisation between the transmitter and receiver. Even though the variable feedback scheme could provide exact synchronisation between the transmitter and the receiver, for improvement of the quality of the recovered signal the synchronisation technique is modified by optimising the feedback function so that perfect synchronisation is achieved. This new scheme incorporates a feedback, which consists of a fraction of the synchronisation error (the difference in amplitudes of the received signal and the receiver output) and an integral function of it. This scheme is hereafter referred to as **P-I** (i.e. Proportional-Integral) scheme. This function, due to its characteristic nature, would induce faster convergence of the synchronisation error to zero.

The appropriate form of this feedback function for the present system is found as

$$G = R + f(R) \quad (6.7)$$

$$\text{where } R = r(P_{tr} - P_{rc}) \quad (6.8)$$

$$f(R) = \frac{2}{\sqrt{\pi}} \int_0^R e^{-t^2} dt \quad (6.9)$$

The upper limit of $f(R)$ is R , which in turn is a function of the normalised powers P_{tr} and P_{rc} .

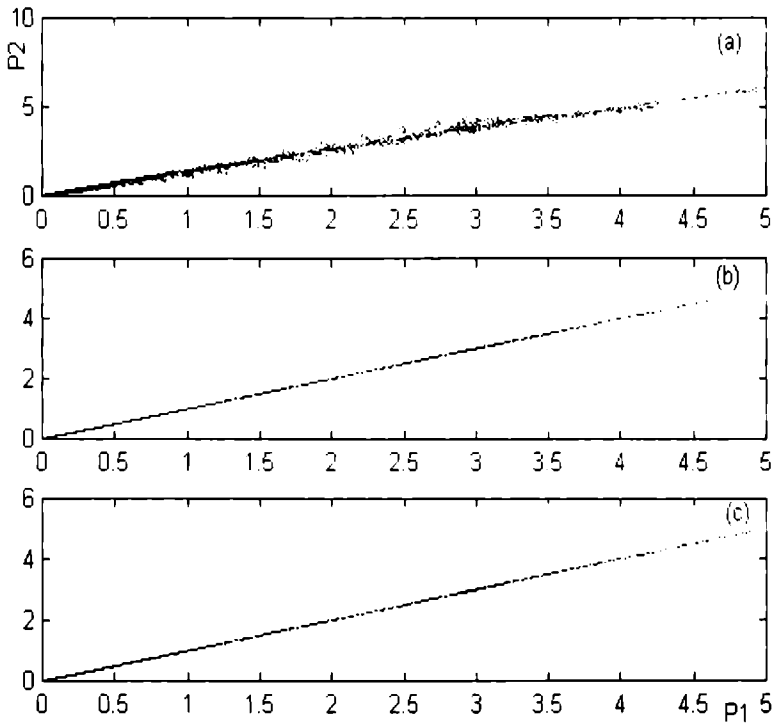


Fig 6.2

Parameter space plot for

a) $G = r \times P_{tr}$

b) $G = r \times (P_{tr} - P_{rc})$

c) $G = f(P_{tr}, P_{rc})$

Fig 6.2 a, b, c shows the parameter space plot for $G = r \times P_{tr}$, $G = r \times (P_{tr} - P_{rc})$, and $G = f(P_{tr}, P_{rc})$ (P-I scheme). Fig 6.3 a, b, c shows the synchronisation error plots for the above three feedback schemes.

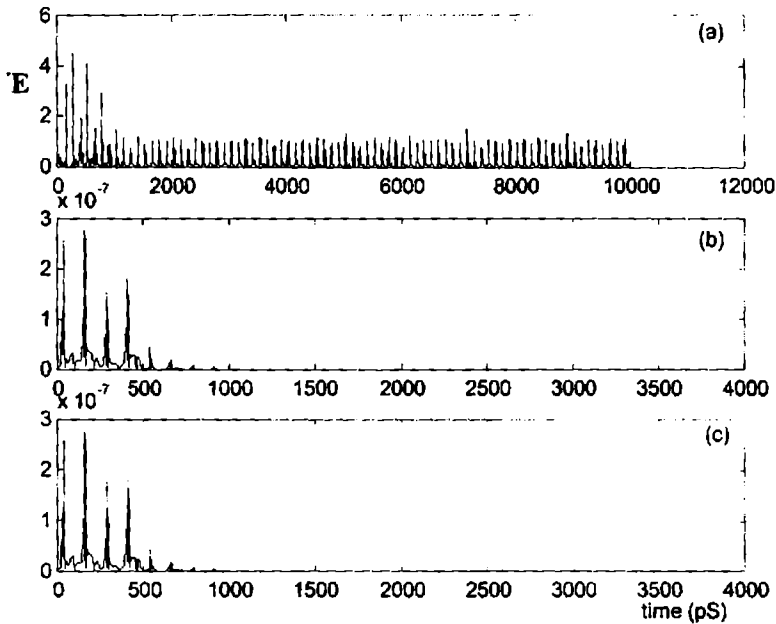


Fig 6.3

Synchronisation error plot

a) $G = r \times P_{tr}$

b) $G = r \times (P_{tr} - P_{rc})$

c) $G = f(P_{tr}, P_{rc})$

Fig 6.4a shows the original message generated at the transmitter end and Fig 6.4b, c and d show the recovered message at the receiver end for uni-directional coupling, variable feedback and P-I schemes respectively. It

is evident that a good recovery of the message is possible by employing the P-I scheme.

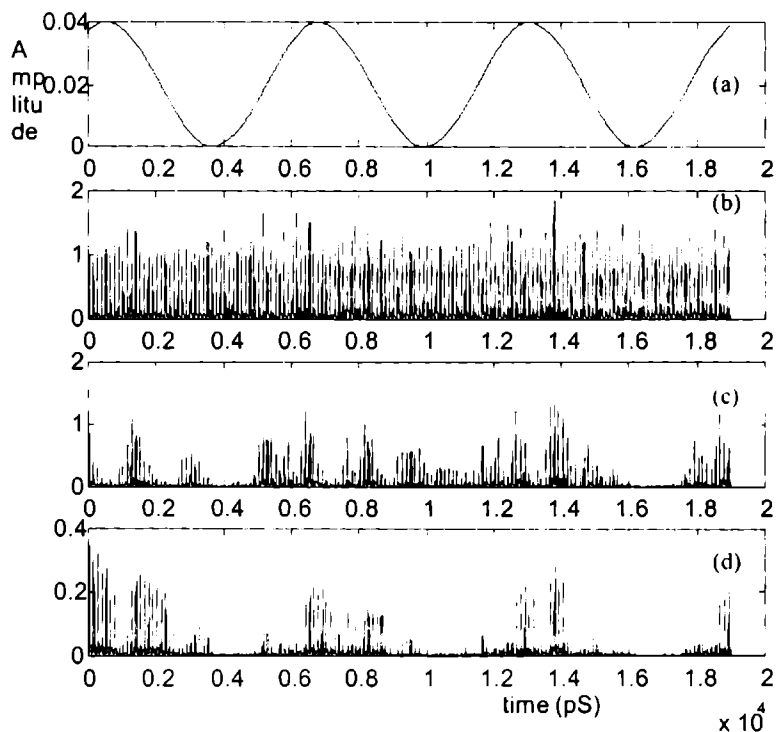


Fig 6.4

Original and recovered analog messages

a) Original message

Message recovered using b) $G = r \times P_{ir}$ c) $G = r \times (P_{ir} - P_{rc})$ d) $G = f(P_{ir}, P_{rc})$

Similarly Fig 6. 5 a shows the original square wave message and Fig 6.5 b, c and d show the corresponding recovered messages for uni-directional

coupling, variable feedback and **P-I** scheme respectively. It is obvious that the **P-I** feedback scheme provides better recovery of the encrypted message.

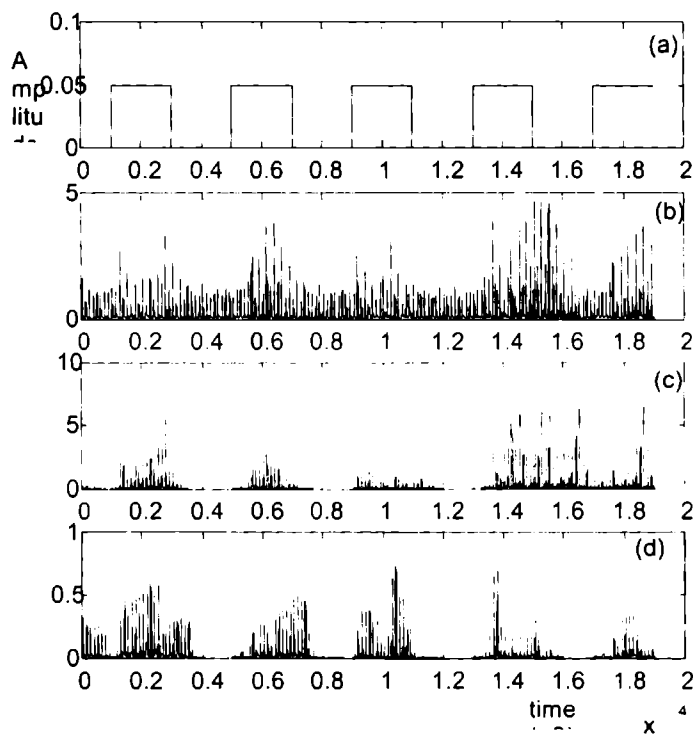


Fig 6.5

Original and recovered digital messages

b) Original message

Recovered using

b) $G = r \times P_{tr}$

c) $G = r \times (P_{tr} - P_{rc})$

d) $G = f(P_{tr}, P_{rc})$

Proper filtering of this message can provide perfect reproduction of the original message. Fig 6.6 shows the filtered recovered message using P-I scheme.

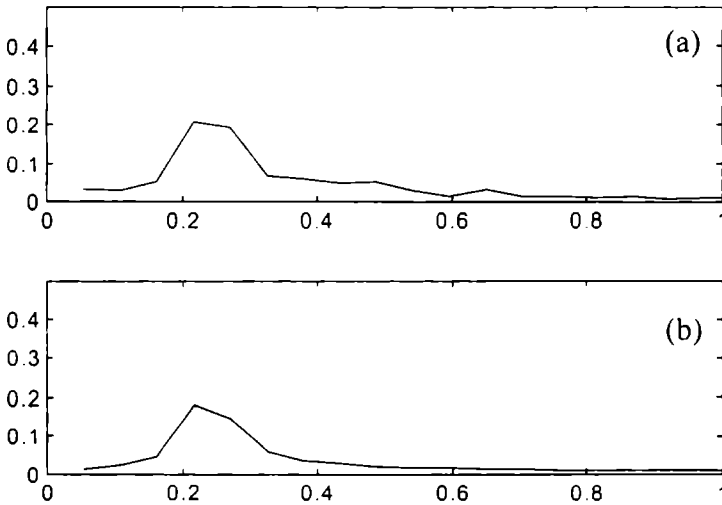


Fig 6.6
Frequency spectra of
(a) filtered message (b) original message

Proper masking of the message is a critical need for the application of this method in secure communication. The amplitude and frequencies of the message signal have to be chosen appropriately so that the chaotic carrier properly masks them. For ensuring proper masking of the message in the chaos of the carrier, the message amplitude is restricted to $< 12\%$ of the maximum of the transmitter output amplitude. For the same reason the

modulation index, $m = f_{\text{message}}/f_{\text{mtr}}$ (ratio of frequency of message to modulation frequency of the transmitter) should also be <1 . However while using the present scheme the transmitted signal does not show any kind of periodic behaviour. Fig 6.7a shows the transmitter output without any message and Fig 6.7b and c show the transmitted signal with analog and digital messages respectively. It is clear from these figures that the transmitted signal does not reveal the fact that it contains any sort of periodic signal in it. This ensures that simply any intruder cannot distinguish it from an ordinary chaotic signal. Only by properly synchronising the receiver with the transmitter the message can be decoded. For this purpose the system parameters should match. If this is achieved secure communication will be possible using another transmission scheme. For this, a key can be assigned to a predefined set of receivers that are eligible for reception. The key can be given in the form of initial conditions and as the system parameters of the transmitter. This can facilitate better synchronisation of the receiver. Work in this direction will be useful to decide whether providing a key to predefined receivers can induce better recovery of messages.

These results show that proper recovery of the received message demands perfect synchronisation and, for the achievement of a perfect synchronisation the feedback function is a very important factor. It is not only the feedback function but also the parameter values of the transmitter

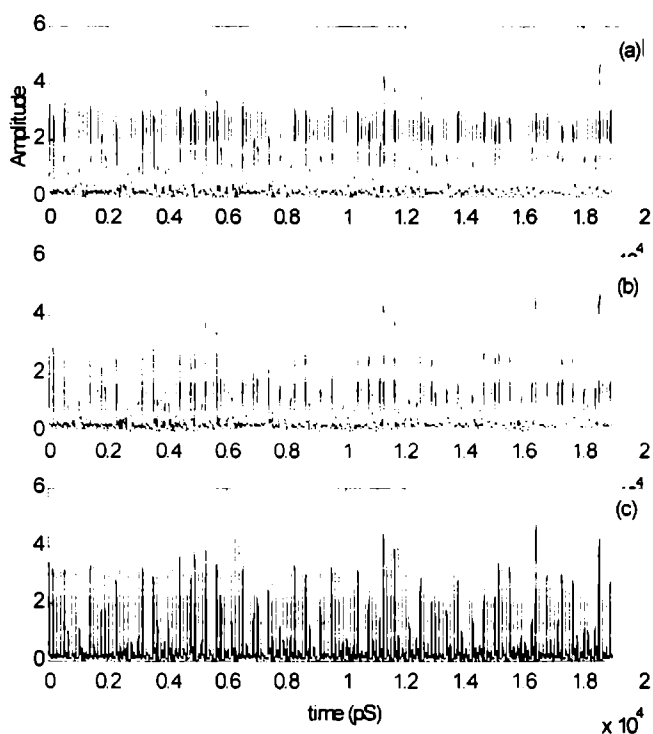


Fig 6.7

Time series of

- a) Transmitter output without message ; b) Transmitted signal with analog message ; c) Transmitted signal with digital message

and the receiver systems that are very crucial in this respect. The parameter values of the transmitter and receiver systems should match for the purpose of proper recovery. These can save the message from intruders. This would ensure that any outsider who simply gets into the

transmission channel would not be able to decode the message. The level of security that can be provided by this method is to be investigated more thoroughly. However, it is proved that the method is useful for long wavelength directly modulated semiconductor lasers, which are the commonly used sources in the optical communication systems. Since optical fibers render minimum loss and dispersion to these radiations, this can definitely prove to be useful for secure long distance communication through optical fibers. The level of security that can be offered by this scheme and the effect of a time delay in the synchronisation of the receiver with the transmitter need further investigation.

SYNCHRONISATION AND CONTROL OF CHAOS IN ONE-DIMENSIONAL AND TWO-DIMENSIONAL ARRAYS OF DIRECTLY MODULATED SEMICONDUCTOR LASERS

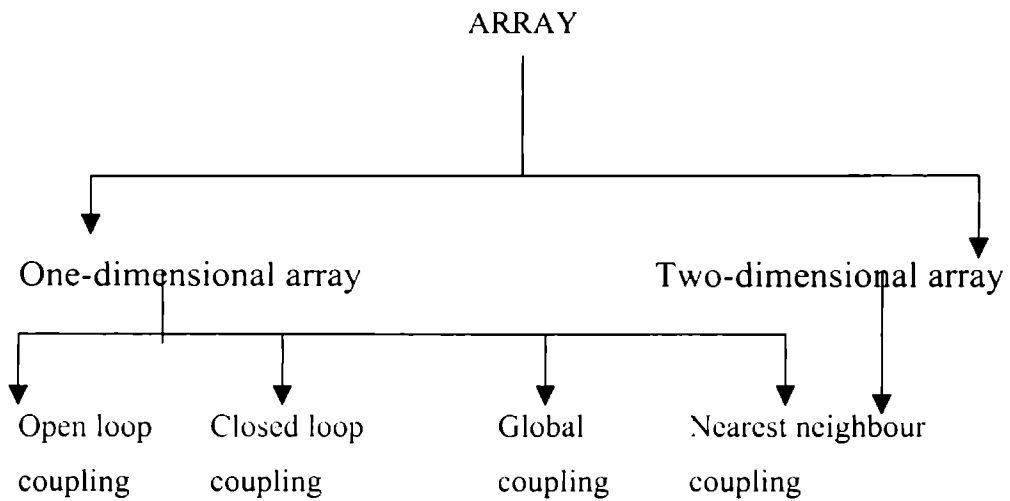
In this chapter we present the results of the numerical study of synchronisation of one-dimensional and two-dimensional arrays of chaotic semiconductor lasers. Eight different arrays are simulated numerically with the number of elements in the array varying from three to ten. Results of the numerical study on open loop coupling, closed loop coupling, global coupling and, nearest neighbour coupling indicate that the synchronisation and output dynamics of the array elements are strongly dependent on the number of elements in the array and also on the type of coupling used.

7.1 INTRODUCTION

Array of coupled systems has generated considerable interest because of the wide variety of phenomena this can exhibit such as spatiotemporal chaos, autowaves, spiral waves, synchronisation and, formation of synchronised clusters. These have proved the importance of such systems for various applications such as image processing modelling population dynamics and, production of synchronised stochastic dynamics^[112-114]. Coupled arrays of semiconductor lasers are modelled according to this principle and is one of the accepted methods for the production of high power outputs. The outputs of the elements of the array are to be synchronised to achieve high power coherent lasers. Dynamics of an array of lasers, especially semiconductor lasers, have been studied extensively^[115-119]. Until now there were only limited studies on coupled arrays of chaotic lasers^[51, 120-124]. Winful *et.al.*^[50] have done numerical simulation of an array of three chaotic semiconductor lasers, and Terry, *et.al.*^[122] have experimentally investigated three chaotic Nd:YAG lasers. Both these investigations were based on a linear array with nearest neighbour coupling whereas Ojalvo^[124] *et. al.* investigated on an array based on global coupling with the help of an external mirror.

Our studies were concerned with the synchronisation of one-dimensional and two-dimensional array of semiconductor lasers. The array elements numbering three to ten are studied individually with respect to different types of coupling schemes each for a range of coupling strengths in the one-dimensional arrays.

The general schematics of different coupling schemes considered in this chapter is given as a chart below. For each coupling schemes we have added the numerical results. In the two-dimensional array four elements are incorporated with nearest neighbour coupling.



7.2 ONE-DIMENSIONAL ARRAY

This array is designed in such a way that the number of elements, type of coupling and the coupling strength can be varied. In this set up we have tried the open loop coupling, closed loop coupling, global coupling and nearest neighbour coupling. To study the effect of these coupling schemes, each of

these models are simulated for a range of coupling strengths for arrays with different number of elements ranging from three to ten.

7.1.1 OPEN LOOP COUPLING SCHEME

We consider an array of semiconductor laser whose elements are coupled uni-directionally such that each element is influenced by the output of the previous element. The array elements are numbered from 1 to 10 continuously. The coupling fraction is kept a constant for all the array elements. The schematic representation of open loop coupling scheme is shown in Fig 7.1.

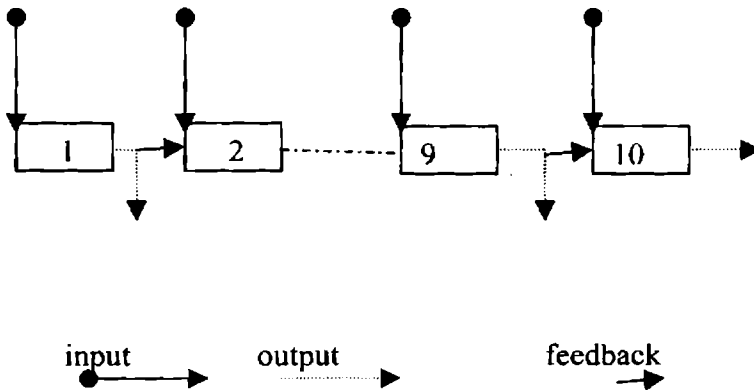


Fig 7.1

Open loop coupling scheme

The coupling is given in the form of a coupling current proportional to a fraction of the output of laser 1 to the input of laser 2. Similarly from the output of laser 2 to the input of laser 3 and so on until the last element, which receives a coupling current proportional to the output of its previous element. Thus the last element in the array will be influenced by the dynamics of all the preceding elements indirectly.

The rate equations governing the dynamics of the above system can be represented as

$$\frac{dN_1}{dt} = \left(\frac{1}{\tau_c} \right) \left[\left(\frac{I_1}{I_{th}} \right) - N_1 - \left\{ \frac{(N_1 - \delta)}{(1 - \delta)} \right\} P_1 \right] \quad (7.1)$$

$$\frac{dP_1}{dt} = \left(\frac{1}{\tau_p} \right) \left[\left\{ \frac{(N_1 - 1)}{(1 - \delta)} \right\} (1 - \epsilon P_1) P_1 - P_1 + \beta N_1 \right] \quad (7.2)$$

$$I_1(t) = I_b + I_m \sin(2\pi f_m t) \quad (7.3)$$

$$\frac{dN_2}{dt} = \left(\frac{1}{\tau_c} \right) \left[\left(\frac{I_2}{I_{th}} \right) - N_2 - \left\{ \frac{(N_2 - \delta)}{(1 - \delta)} \right\} P_2 \right] \quad (7.4)$$

$$\frac{dP_2}{dt} = \left(\frac{1}{\tau_p} \right) \left[\left\{ \frac{(N_2 - 1)}{(1 - \delta)} \right\} (1 - \epsilon P_2) P_2 - P_2 + \beta N_2 \right] \quad (7.5)$$

$$I_2(t) = I_b + I_m \sin(2\pi f_m t) + G_2 I_{c_2} \quad (7.6)$$

$$\frac{dN_n}{dt} = \left(\frac{1}{\tau_e} \right) \left[\left(\frac{I_n}{I_{th}} \right) - N_n - \left\{ \frac{(N_n - \delta)}{(1 - \delta)} \right\} P_n \right] \quad (7.7)$$

$$\frac{dP_n}{dt} = \left(\frac{1}{\tau_p} \right) \left[\left\{ \frac{(N_n - 1)}{(1 - \delta)} (1 - \epsilon P_n) P_n - P_n + \beta N_n \right\} \right] \quad (7.8)$$

$$I_n(t) = I_b + I_m \sin(2\pi f_m t) + G_n I_{c_n} \quad (7.9)$$

$$G_n = (C \times P_{n-1}) \times 10^{-3}$$

where C is the coupling strength and n is the number of elements.

The parameter values are so fixed that in the uncoupled case the individual lasers operate in their chaotic regimes. The parameter values are those given in Table 3.1.

7.1.1.1 NUMERICAL ANALYSIS AND RESULTS

The above sets of equations are solved numerically by fourth order Runge-Kutta method. Eight different arrays with number of elements varying from 3 to 10 are studied where the coupling strength is increased in steps of 1 for each array. Synchronisation is checked using parameter space plots and synchronisation error plots. The results of the above study reveal that synchronisation and other dynamical properties of the array elements are

dependent on the number of elements present in an array and also on the coupling strength.

As the coupling strength is increased, the systems show a rise in the amplitudes of the laser outputs till the coupling value of 7 is reached for all the elements except the first. The output amplitude of the first laser remains unchanged throughout the range of coupling strengths. The increase in amplitude is more for the last laser in an array. All the elements in the array achieve synchronisation simultaneously at a coupling value of 8. The optimal synchronisation is achieved between the first and the second element in the array. Fig 7.2a shows the synchronisation error plots between all pairs of lasers in an array with four elements for $C = 8$ and, Fig 7.2b shows the parameter space plots between all pairs of lasers in an array with four elements for $C = 8$. The type of synchronisation is practical. This synchronisation is maintained for a small range of coupling strengths (7-11).

With further increase in coupling strength synchronisation is lost between the elements but the output amplitude increases gradually as C goes beyond 11. It can be said that there is no observable synchronisation for $C > 11$. The output amplitude steadily increases when the coupling strength increases from 7-11; however, the increase of amplitude occurs at a much slower rate than in the range of coupling strengths where there is no synchronisation between the outputs. Throughout the range of coupling strengths the outputs remain chaotic.

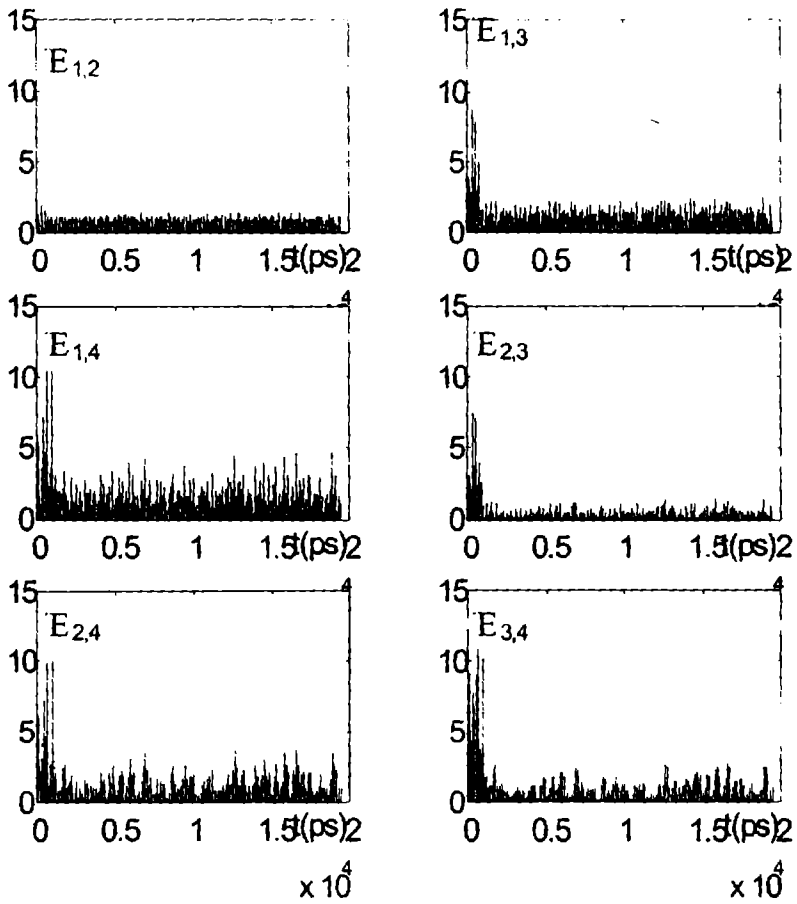


Fig 7.2a

Synchronisation error plots between all pairs of lasers
in an open loop coupled array with 4 elements for $C = 8$

$E_{x,y}$ – synchronisation error between lasers x and y , where x and y are positions of elements in an array.

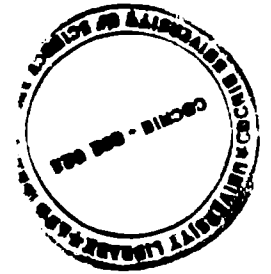
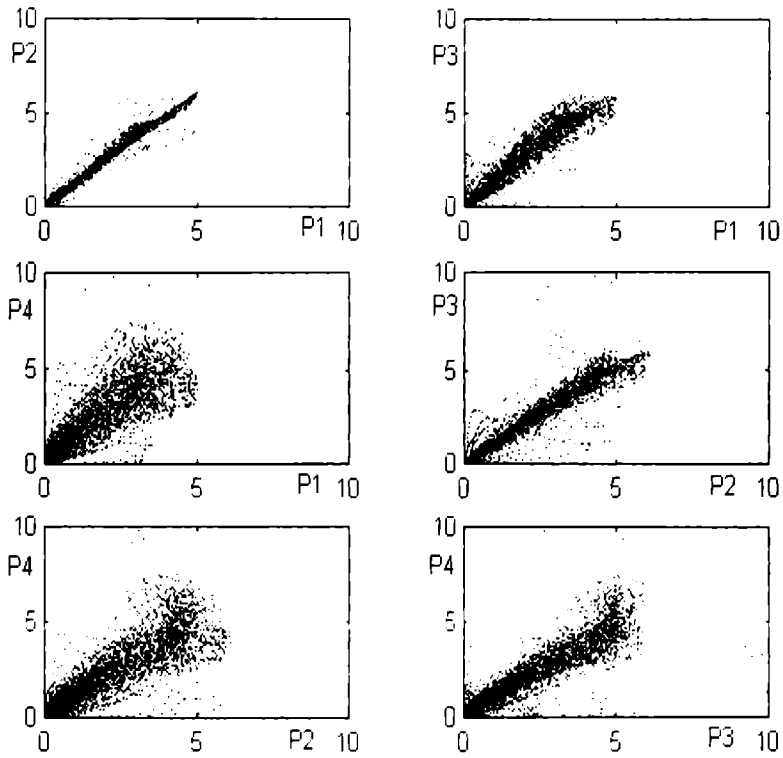


Fig 7.2b

Parameter space plots between all pairs of lasers in an open loop coupled array
with 4 elements for $C = 8$

P1, P2, P3, P4 – output powers of lasers 1,2,3,4

R
531.3:535.876
BIN
G8535

Table 7.1

Dynamical properties of open loop coupled array

c	n	3	4	5	6	7	8	9	10
1	↓	no sync chaotic	no sync chaotic	no sync chaotic	no sync chaotic	no sync chaotic	no sync chaotic	no sync chaotic	--
2	↓	no sync chaotic	no sync chaotic	no sync chaotic	no sync chaotic	no sync chaotic	no sync chaotic	no sync chaotic	
3		no sync chaotic	no sync chaotic	no sync chaotic	no sync chaotic	no sync chaotic	no sync chaotic	--	
4		no sync chaotic	no sync chaotic	no sync chaotic	no sync chaotic	no sync chaotic	--		
5		no sync chaotic	no sync chaotic	no sync chaotic	no sync chaotic	--			
6		no sync chaotic	no sync chaotic	no sync chaotic	no sync chaotic	--			
7		p- sync chaotic	p- sync chaotic	p- sync chaotic	p- sync chaotic				
8		p- sync chaotic	p- sync chaotic	p- sync chaotic	p- sync chaotic				
9		p- sync chaotic	p- sync chaotic	p- sync chaotic	p- sync chaotic				
10		p- sync chaotic	p- sync chaotic	p- sync chaotic	p- sync chaotic				
11		p- sync chaotic	no sync chaotic	no sync chaotic	no sync chaotic				
12		no sync chaotic	no sync chaotic	no sync chaotic	no sync chaotic				
13		no sync chaotic	no sync chaotic	no sync chaotic	no sync chaotic				

There is no significant dependence of synchronisation or other dynamical properties on the number of elements in an array. For $n=3$ to 7, the range of coupling strengths for which the array elements are synchronised and the type of synchronisation achieved between the array elements remains the same. When the number of elements in an array increases to more than 7 the numerical model loses stability to give a clear picture of the synchronisation and other dynamical behaviours. The above results are shown in Table.7.1

7.1.2 CLOSED LOOP COUPLING

A closed loop array of semiconductor lasers is designed in such a way that each element is influenced by the output of all the other elements present in the array. The array elements are numbered from 1 to 10 continuously. A closed loop coupling scheme differs from an open loop scheme only in one respect, i.e. the last element in the array is coupled back to the first element^[123]. The feedback fraction that is given to all the array elements is constant. This array is designed in such a way that a coupling current proportional to a fraction of the output of the first array element is fed to the input of the second element in addition to its conventional input. Similarly from the second element a current is fed to the input of the third element. This is continued till the last element in the array from which a current proportional to a fraction of its output is fed to the input of the first element. Thus all the elements in the array are influenced by all other elements indirectly. This is schematically shown in Fig.7.3.

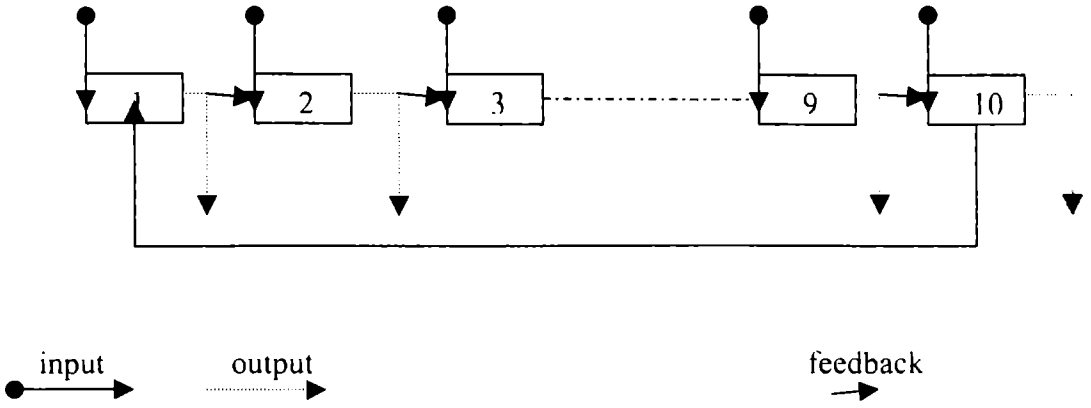


Fig.7.3.

Closed loop coupling scheme

The rate equations representing the whole system can be written as

$$\frac{dN_1}{dt} = \left(\frac{1}{\tau_e} \right) \left[\left(\frac{I_1}{I_{th}} \right) - N_1 - \left\{ \frac{(N_1 - \delta)}{(1 - \delta)} \right\} P_1 \right] \quad (7.10)$$

$$\frac{dP_1}{dt} = \left(\frac{1}{\tau_p} \right) \left[\left\{ \frac{(N_1 - 1)}{(1 - \delta)} \right\} (1 - \epsilon P_1) P_1 - P_1 + \beta N_1 \right] \quad (7.11)$$

$$I_1(t) = I_b + I_m \text{Sin}(2\pi f_m t) + G_1 I_c \quad (7.12)$$

$$\frac{dN_2}{dt} = \left(\frac{1}{\tau_e} \right) \left[\left(\frac{I_2}{I_{th}} \right) - N_2 - \left\{ \frac{(N_2 - \delta)}{(1 - \delta)} \right\} P_2 \right] \quad (7.13)$$

$$\frac{dP_2}{dt} = \left(\frac{1}{\tau_p} \right) \left[\left\{ \frac{(N_2 - 1)}{(1 - \delta)} \right\} (1 - \epsilon P_2) P_2 - P_2 + \beta N_2 \right] \quad (7.14)$$

$$I_2(t) = I_b + I_m \text{Sin}(2\pi f_m t) + G_2 I_c \quad (7.15)$$

$$\frac{dN_n}{dt} = \left(\frac{1}{\tau_c} \right) \left[\left(\frac{I_n}{I_h} \right) - N_n - \left\{ \frac{(N_n - \delta)}{(1 - \delta)} \right\} P_n \right] \quad (7.16)$$

$$\frac{dP_n}{dt} = \left(\frac{1}{\tau_p} \right) \left[\left\{ \frac{(N_n - 1)}{(1 - \delta)} (1 - \epsilon P_n) P_n - P_n + \beta N_n \right\} \right] \quad (7.17)$$

$$I_n(t) = I_b + I_m \sin(2\pi f_m t) + G_n I_c \quad (7.18)$$

$$G_n = (C \times P_{n-1}) \times 10^{-3}$$

where C is the coupling strength and n is the number of elements.

7.1.2.1 NUMERICAL ANALYSIS AND RESULTS

Numerical simulation of the above equations shows a strong dependence of synchronisation and other dynamical properties on the coupling strength and the number of elements present in an array. Accordingly, the results can be classified into two groups^[126]:

- i) Arrays with even number of elements ii) Arrays with odd number of elements.

➤ Arrays with even number of elements

Synchronisation properties and the dynamical behaviour are the same for all arrays with even number of elements, i.e. when $n = 2, 4, 6, 8$. Consider an array with four elements as a prototype of this class. Synchronisation and

other dynamical properties of the array elements change considerably with a change in the coupling strength. For coupling strengths 1 and 2 the first and third elements show synchronisation as well as the second and fourth elements show synchronisation between them. The type of synchronisation achieved by these two pairs of lasers is *exact*. These pairs are called *odd pairs* (1-3) and *even pairs* (2-4)

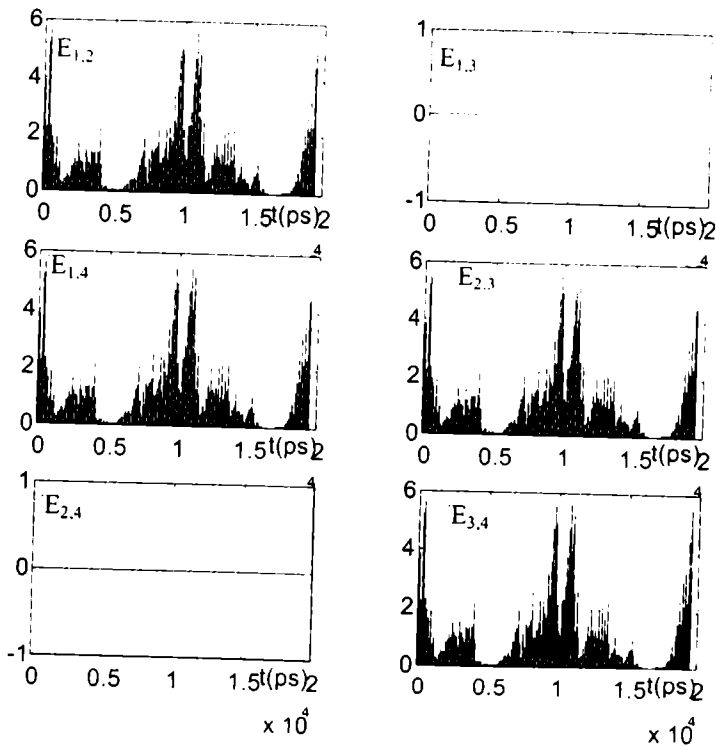


Fig 7.4a

Synchronisation error plots between all pairs of lasers in a closed loop coupled array with 4 elements for $C = 2$

$E_{x,y}$ – synchronisation error between lasers x and y ; where x and y are positions of elements in an array.

Fig. 7.4(a) shows the parameter space plots between output powers of all pairs for $C=2$ and (b) shows the synchronisation error plots for the same. However, there is no synchrony between any other laser pairs (first and second, first and fourth, second and third, third and fourth). These pairs will be called *odd-even* pairs. The output powers of all the lasers in the array show chaotic nature.

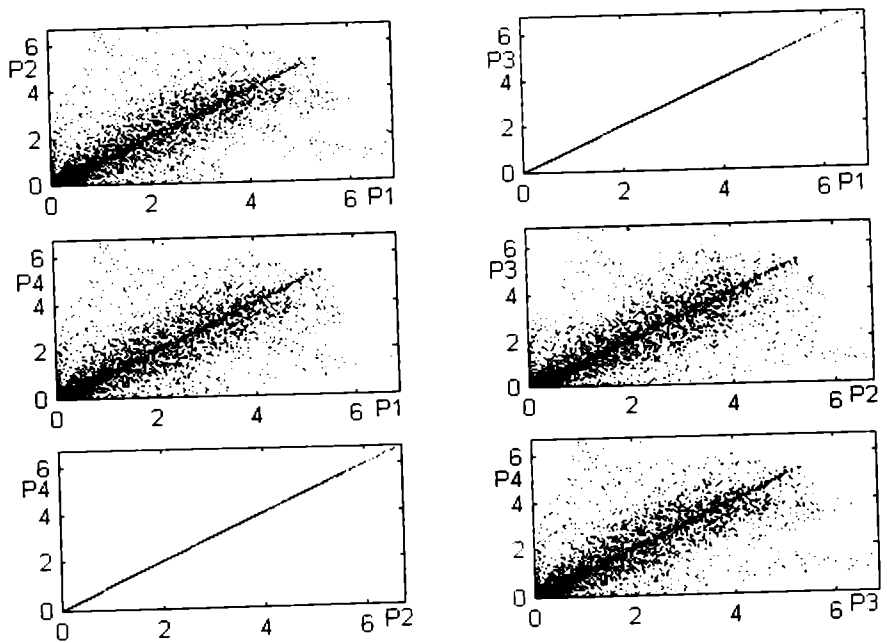
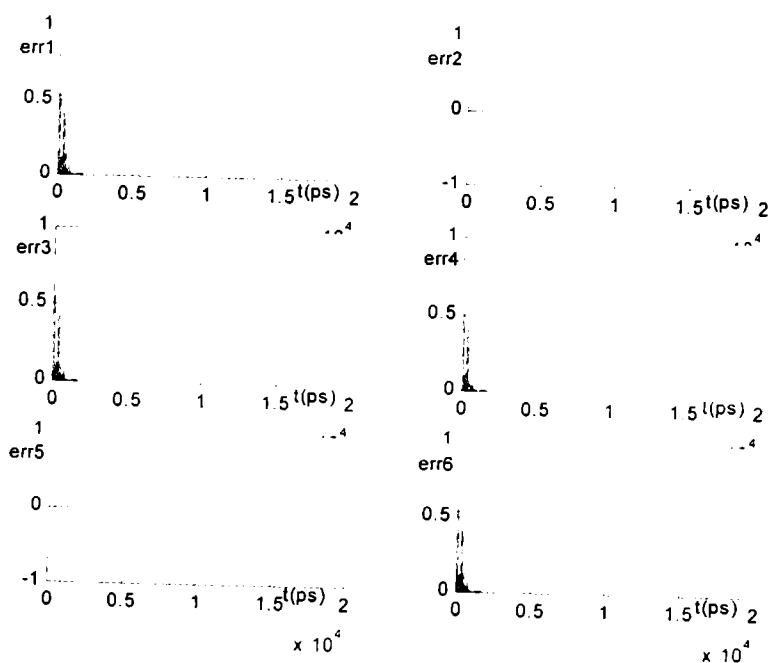


Fig 7.4a

Parameter space plots between all pairs of lasers in a closed loop coupled array with 4 elements for $C = 2$

P_1, P_2, P_3, P_4 – output powers of lasers 1,2,3,4

As the coupling strength increases to 3, all the lasers get synchronised with each other with the type of synchronisation being exact. The output amplitude value also steadily increases. Fig.7.5a shows the synchronisation error plots for output powers between all pairs of lasers at coupling strength of 3 and Fig 7.5b shows the parameter space plots between all pairs of lasers at coupling strength of 3. This synchronisation is maintained throughout the range of the coupling strength.



7.6a

Synchronisation error plots between all pairs of lasers in a closed loop coupled array with 4 elements for $C = 3$

$E_{x,y}$ – synchronisation error between lasers x and y ; where x and y are positions of elements in an array.

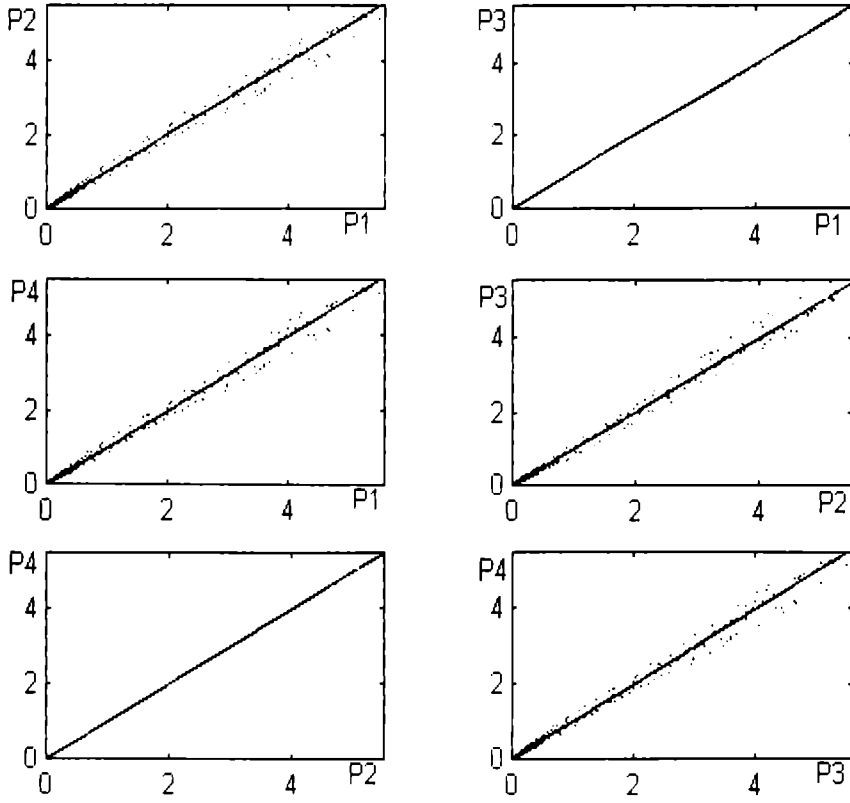


Fig 7.6b

Parameter space plots between all pairs of lasers in a closed loop coupled array with 4 elements for $C = 3$

P1, P2, P3, P4 – output powers of lasers 1,2,3,4

As the coupling strength increases to 6, the previously synchronised chaotic signals assume synchronised four cycle nature. With further increase in C , the dynamics undergoes a reverse period doubling i.e. at $C=9$, the outputs become two cycled and at $C=17$, it becomes a period one cycle. For higher values of coupling strength, the period one cycle output is maintained [127]. Fig. 7.6 shows the phase diagrams of the array elements undergoing reverse period doubling.

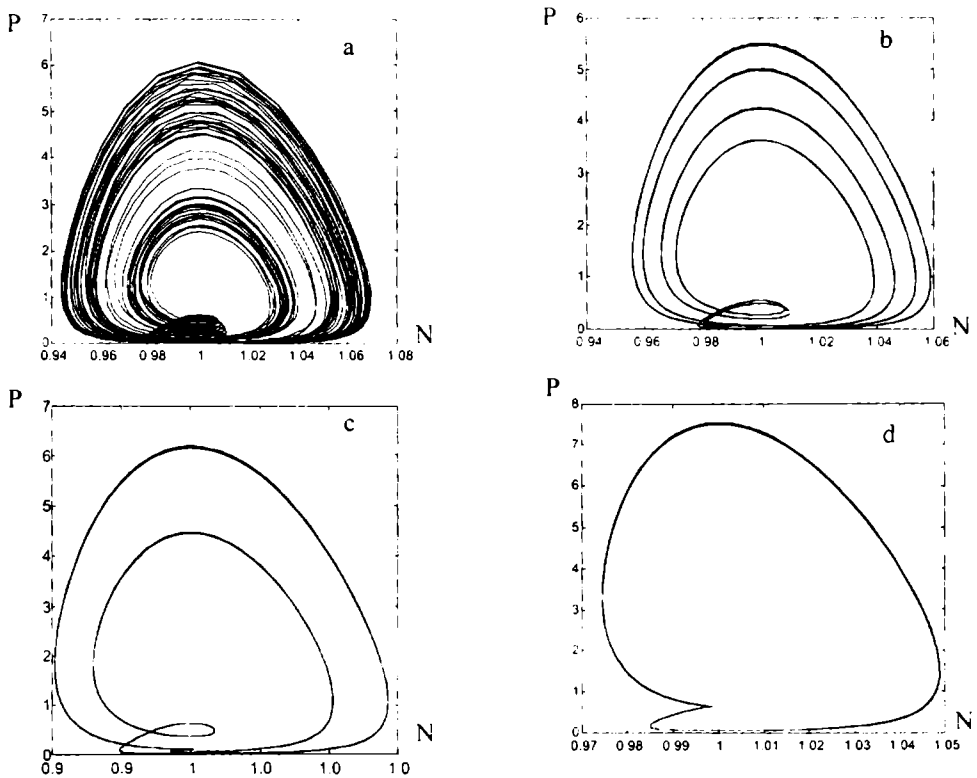


Fig 7.6

Reverse period doubling route lasers in a closed loop coupled array with 4 elements for
 (a) $C = 3$ (b) $C = 6$ (c) $C = 9$ (d) $C = 17$

This indicates that increased coupling strengths help to induce stability to the chaotic dynamics through a reverse period doubling route. Both synchronisation and control of chaos are the peculiarities of arrays with even number of elements. Together with these there is an amplification of the output power with increase in coupling strengths.

➤ *Arrays with odd number of elements*

In the case of arrays with odd number of elements synchronisation is not observed for any coupling strength. The outputs of all laser elements remain chaotic throughout the range of coupling strengths. In such cases the output power gets amplified drastically even for small increase in coupling strength thus differing from the arrays with even number of elements where also such changes do occur, but is not significant. Consider an array with three elements as a prototype of this class. Increasing the coupling strength does not show any effect on the synchronisation property. Even at a high enough value of $C=17$, there is no synchronisation between elements of any of the even pairs, odd pairs or odd-even pairs. Coupling strength does not induce stability in this case as it could in the case of arrays with even number of elements. The amplitude values of all the three elements are different even though they increase steadily with increase in the coupling strengths. When the number of elements in an array increases to more than 7 the numerical model loses stability to provide a clear picture of the synchronisation and other dynamical behaviours. Table 7.2 depicts the overall dynamics of closed loop coupled array.

Table 7.2

Dynamical properties of closed loop coupled one-dimensional array

n C	3	4	5	6	7	8	9	10
1	No syn chaotic	1-3,2-4 chaotic	No syn Chaotic	1-3,2-4 chaotic	No syn Chaotic	1-3,2-4 chaotic	No syn Chaotic	--
2	No syn Chaotic	1-3,2-4 chaotic	No syn Chaotic	1-3,2-4 chaotic	No syn Chaotic	1-3,2-4 chaotic	No syn Chaotic	
3	No syn Chaotic	All syn chaotic	No syn Chaotic	All syn chaotic	No syn Chaotic	All syn chaotic	No syn Chaotic	
4	No syn Chaotic	All syn chaotic	No syn Chaotic	All syn chaotic	No syn Chaotic	All syn chaotic	No syn Chaotic	
5	No syn chaotic	All syn chaotic	No syn Chaotic	All syn chaotic	No syn Chaotic	All syn chaotic	No syn Chaotic	
6	No syn Chaotic	All syn P=4	No syn Chaotic	All syn P=4	No syn Chaotic	All syn P=4	No syn Chaotic	
7	No syn Chaotic	All syn P=4	No syn Chaotic	All syn P=4	No syn Chaotic	All syn P=4	No syn Chaotic	
8	No syn Chaotic	All syn P=4	No syn Chaotic	All syn P=4	No syn Chaotic	All syn P=4	No syn Chaotic	
9	No syn Chaotic	All syn P=2	No syn Chaotic	All syn P=2	No syn Chaotic	All syn P=2	No syn Chaotic	
10	No syn chaotic	All syn P=2	No syn Chaotic	All syn P=2	No syn Chaotic	All syn P=2	No syn Chaotic	
11	No syn Chaotic	All syn P=2	No syn Chaotic	All syn P=2	No syn Chaotic	All syn P=2	No syn Chaotic	
12	No syn Chaotic	All syn P=2	No syn Chaotic	All syn P=2	No syn Chaotic	All syn P=2	No syn Chaotic	
13	No syn Chaotic	All syn P=2	No syn Chaotic	All syn P=2	No syn Chaotic	All syn P=2	No syn Chaotic	
14	No syn Chaotic	All syn P=2	No syn Chaotic	All syn P=2	No syn Chaotic	All syn P=2	No syn Chaotic	
15	No syn Chaotic	All syn P=2	No syn Chaotic	All syn P=2	No syn Chaotic	All syn P=2	No syn Chaotic	
16	No syn Chaotic	All syn P=2	No syn Chaotic	All syn P=2	No syn Chaotic	All syn P=2	No syn Chaotic	
17	No syn chaotic	All syn P=1	No syn Chaotic	All syn P=1	No syn chaotic	All syn P=1	No syn chaotic	

7.1.3 GLOBAL COUPLING SCHEME

This scheme is designed in such a way that all the elements in an array are directly influenced by the dynamics of all other elements. The system consists of the array elements and a feedback generator, which provides a current proportional to a fraction of the total output power of the array to the inputs of all the array elements simultaneously. The feedback current received by each of the elements in the array will be the same. The schematic representation of this system is depicted in Fig 7.7.

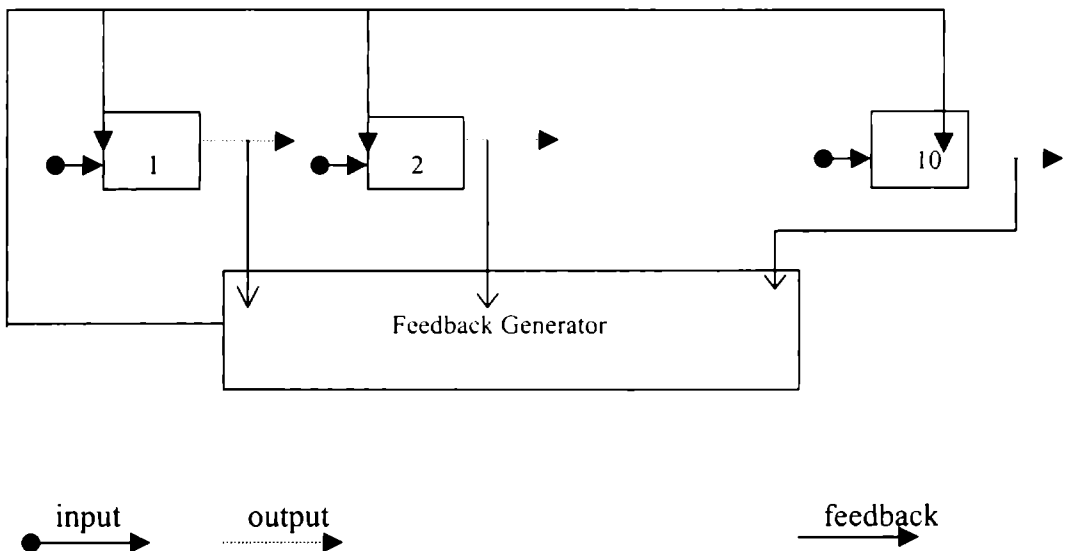


Fig 7.7

Schematic representation of global coupling scheme

The rate equation is represented as follows

$$\frac{dN_1}{dt} = \left(\frac{1}{\tau_e} \right) \left[\left(\frac{I_1}{I_{th}} \right) - N_1 - \left\{ \frac{(N_1 - \delta)}{(1 - \delta)} \right\} P_1 \right] \quad (7.19)$$

$$\frac{dP_1}{dt} = \left(\frac{1}{\tau_p} \right) \left[\left\{ \frac{(N_1 - 1)}{(1 - \delta)} \right\} (1 - \epsilon P_1) P_1 - P_1 + \beta N_1 \right] \quad (7.20)$$

$$I_1(t) = I_b + I_m \sin(2\pi f_m t) + G_1 I_c \quad (7.21)$$

$$\frac{dN_2}{dt} = \left(\frac{1}{\tau_e} \right) \left[\left(\frac{I_2}{I_{th}} \right) - N_2 - \left\{ \frac{(N_2 - \delta)}{(1 - \delta)} \right\} P_2 \right] \quad (7.22)$$

$$\frac{dP_2}{dt} = \left(\frac{1}{\tau_p} \right) \left[\left\{ \frac{(N_2 - 1)}{(1 - \delta)} \right\} (1 - \epsilon P_2) P_2 - P_2 + \beta N_2 \right] \quad (7.23)$$

$$I_2(t) = I_b + I_m \sin(2\pi f_m t) + G_2 I_c \quad (7.24)$$

$$\frac{dN_n}{dt} = \left(\frac{1}{\tau_e} \right) \left[\left(\frac{I_n}{I_{th}} \right) - N_n - \left\{ \frac{(N_n - \delta)}{(1 - \delta)} \right\} P_n \right] \quad (7.25)$$

$$\frac{dP_n}{dt} = \left(\frac{1}{\tau_p} \right) \left[\left\{ \frac{(N_n - 1)}{(1 - \delta)} \right\} (1 - \epsilon P_n) P_n - P_n + \beta N_n \right] \quad (7.26)$$

$$I_n(t) = I_b + I_m \sin(2\pi f_m t) + G_n I_c \quad (7.27)$$

$$G_n = C \times P_T \times 10^{-3}$$

where C is the coupling strength, P_T is the total output power of the array which can be represented as $P_T = (P_1 + P_2 + \dots + P_n)$, and n is the number of elements.

7.1.3.1 NUMERICAL ANALYSIS AND RESULTS

The above sets of equations were numerically simulated for different values of 'n' and C. Global coupling can induce exact synchronisation and control over the chaotic output for low coupling strengths. Synchronisation and control of the chaotic output are achieved in all arrays without preference to odd or even number of elements. As the number of elements increases, synchronisation is achieved for lower values of coupling strengths. Thus it becomes apparent that synchronisation is more dependent on the number of elements than on the coupling strengths. The amplitude of the output power is dependent on both the coupling strength and the number of elements.

For an array with four elements synchronisation between all pairs of array elements is achieved at a coupling strength of 1. Fig 7.8a show the synchronisation error plots between all pairs of lasers for an array with four elements for $C = 1$ and 7.8b show the parameter space plots between all pairs of lasers for an array with four elements for $C = 1$.

As the coupling strength increases the output powers, which are chaotic for low coupling strengths attain stability through a reverse period doubling route. The output powers which are chaotic at $C = 1$ become periodic with a periodicity of four at $C = 2$. With further increase in coupling strength at $C=3$ the periodicity becomes 2 which then becomes at a single period orbit at $C=6$. This is maintained at all higher coupling strengths

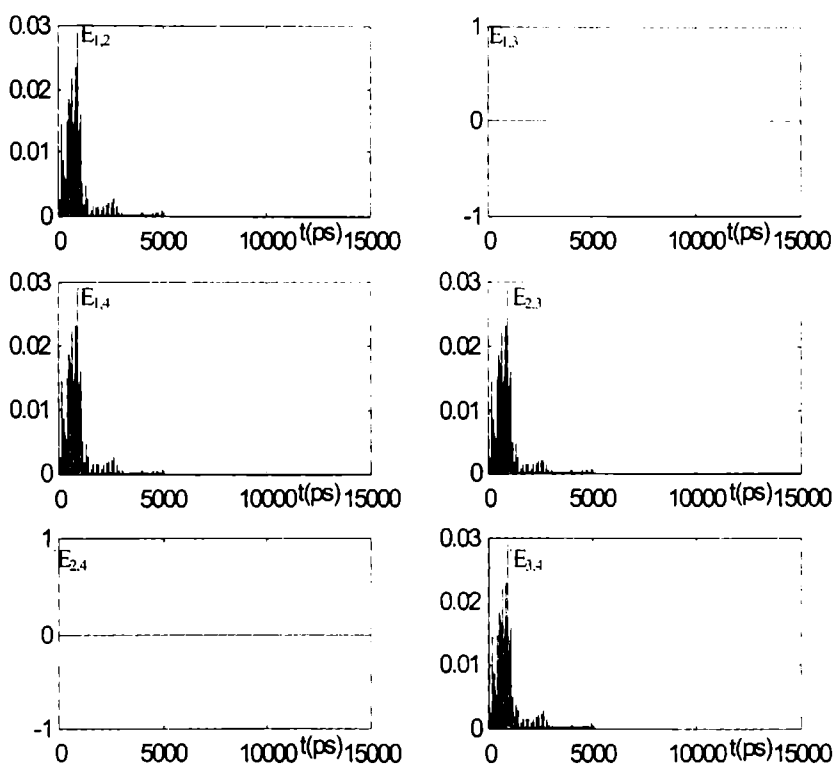


Fig 7.8a

Synchronisation error plots between all pairs of lasers in a
Globally coupled array with 4 elements for $C = 1$

$E_{x,y}$ – synchronisation error between lasers x and y ; where x and y are positions of elements in an array.

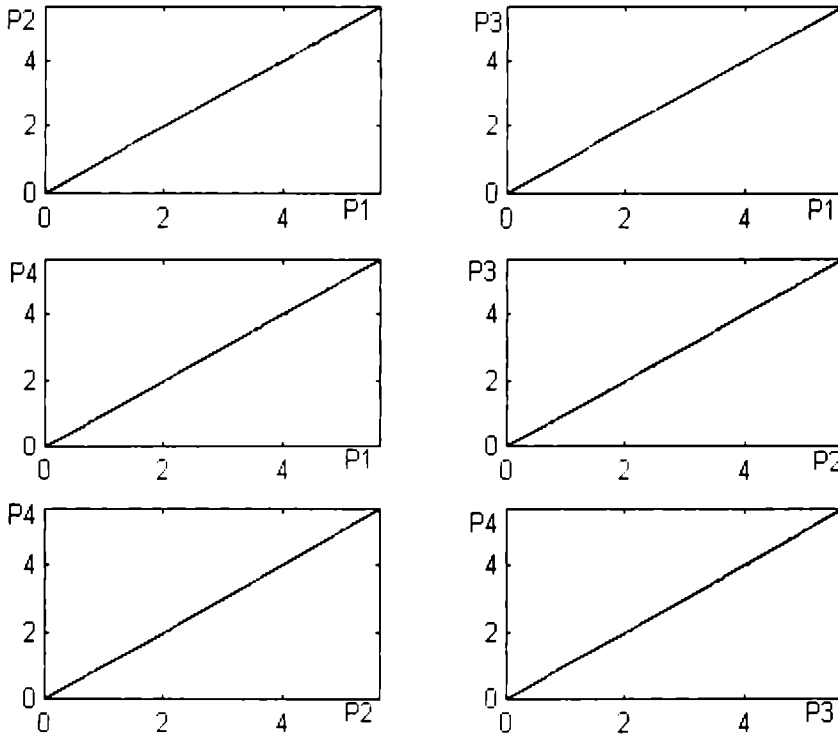


Fig 7.8b

Parameter space plots between all pairs of lasers in a
Globally coupled array with 4 elements for $C = 1$

P1, P2, P3, P4 – output powers of lasers 1,2,3,4

Table 7.3

Dynamical properties of globally coupled array

N C	3	4	5	6	7	8	9	10
1	(1-3)E Chaotic	All E Chaotic	All E Chaotic	All E P=4	All E P=4	All E P=4	All E P=2	1-3-5-7-9 E 2-4-6-8-10 E P=4
2	All E P=4	All E P=4	1-3-5 E P=4	All E P=2	All E P=2	All E P=2	All E P=1	All E P=1
3	All E P=2	All E P=2	All E P=2	All E P=1	All E P=1	All E P=1	--	--
4	All E P=2	All E P=2	All E P=1	All E P=1	--	--		
5	All E P=2	All E P=1	All E P=1	--				
6	All E P=1	All E P=1	--					
7	All E P=1	--						
8	All E P=1							
9	--							
10								

At $C=8$ the double peak nature of the synchronised output powers gets suppressed indicating damping of relaxation oscillations. As the number of elements in an array increases the coupling strength needed for inducing synchronisation and control progressively diminishes. The coupling strength at which stable one cycle output is obtained progressively decreases as the number of elements in an array increases and when $n=10$, reverse period doubling occurs between $C=0.5$ and 2. As the coupling strength increases, the output amplitudes undergo amplification. The stability of the numerical model is not affected by increase in the number of elements in an array, but is strongly affected by increase in the coupling strength for all the arrays. The overall results are shown in Table 7.3

7.1.4 NEAREST NEIGHBOUR COUPLING SCHEME

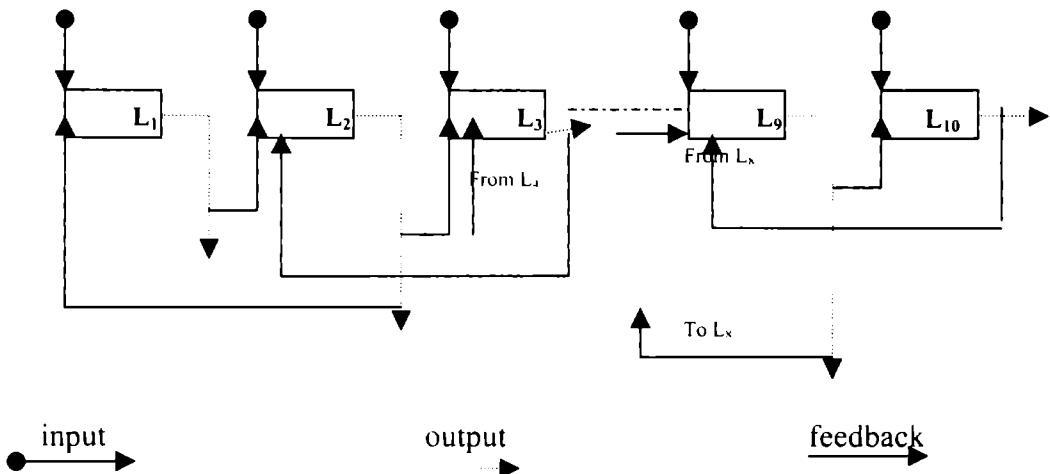


Fig 7.9

Nearest neighbour coupling scheme

The rate equations is summarized as follows

$$\frac{dN_1}{dt} = \left(\frac{1}{\tau_e} \right) \left[\left(\frac{I_1}{I_{th}} \right) - N_1 - \left\{ \frac{(N_1 - \delta)}{(1 - \delta)} \right\} P_1 \right] \quad (7.28)$$

$$\frac{dP_1}{dt} = \left(\frac{1}{\tau_p} \right) \left[\left\{ \frac{(N_1 - 1)}{(1 - \delta)} \right\} (1 - \epsilon P_1) P_1 - P_1 + \beta N_1 \right] \quad (7.29)$$

$$I_1(t) = I_b + I_m \text{Sin}(2\pi f_m t) + G_1 I_{c_1} \quad (7.30)$$

$$\frac{dN_2}{dt} = \left(\frac{1}{\tau_e} \right) \left[\left(\frac{I_2}{I_{th}} \right) - N_2 - \left\{ \frac{(N_2 - \delta)}{(1 - \delta)} \right\} P_2 \right] \quad (7.31)$$

$$\frac{dP_2}{dt} = \left(\frac{1}{\tau_p} \right) \left[\left\{ \frac{(N_2 - 1)}{(1 - \delta)} \right\} (1 - \epsilon P_2) P_2 - P_2 + \beta N_2 \right] \quad (7.32)$$

$$I_2(t) = I_b + I_m \text{Sin}(2\pi f_m t) + G_2 I_{c_2} \quad (7.33)$$

$$\frac{dN_n}{dt} = \left(\frac{1}{\tau_e} \right) \left[\left(\frac{I_n}{I_{th}} \right) - N_n - \left\{ \frac{(N_n - \delta)}{(1 - \delta)} \right\} P_n \right] \quad (7.34)$$

$$\frac{dP_n}{dt} = \left(\frac{1}{\tau_p} \right) \left[\left\{ \frac{(N_n - 1)}{(1 - \delta)} \right\} (1 - \epsilon P_n) P_n - P_n + \beta N_n \right] \quad (7.35)$$

$$I_n(t) = I_b + I_m \text{Sin}(2\pi f_m t) + G_n I_{c_n} \quad (7.36)$$

$$G_n = C \times (P_{n-1} + P_{n+1}) \times 10^{-3}$$

where C is the coupling strength, n is the position of an element in the array.

7.1.4.1 NUMERICAL ANALYSIS AND RESULTS

The above set of equations is numerically simulated for number of elements varying from 3 to 10 each for a range of coupling strengths. The results show that synchronisation and other dynamical properties are dependent on the number of elements.

As the coupling strength is increased the outer lasers get synchronised first and later, with further increase in the coupling strength, the inner lasers get synchronised with each other but there is no synchronisation between the outer pairs with the inner pairs. For example, in an array with 4 elements when $C = 5$, the first and the fourth elements in the array get synchronised with the type of synchronisation being exact. Similarly the second and the third lasers get synchronised exactly but there is no synchronisation between first (1-2), (1-3), (2-4) and (3-4) pairs. Fig.7.10a show the synchronisation error plots between all pairs of lasers for an array with four elements for $C = 5$ and 7.10b show the parameter space plots between all pairs of lasers for an array with four elements for $C = 5$.

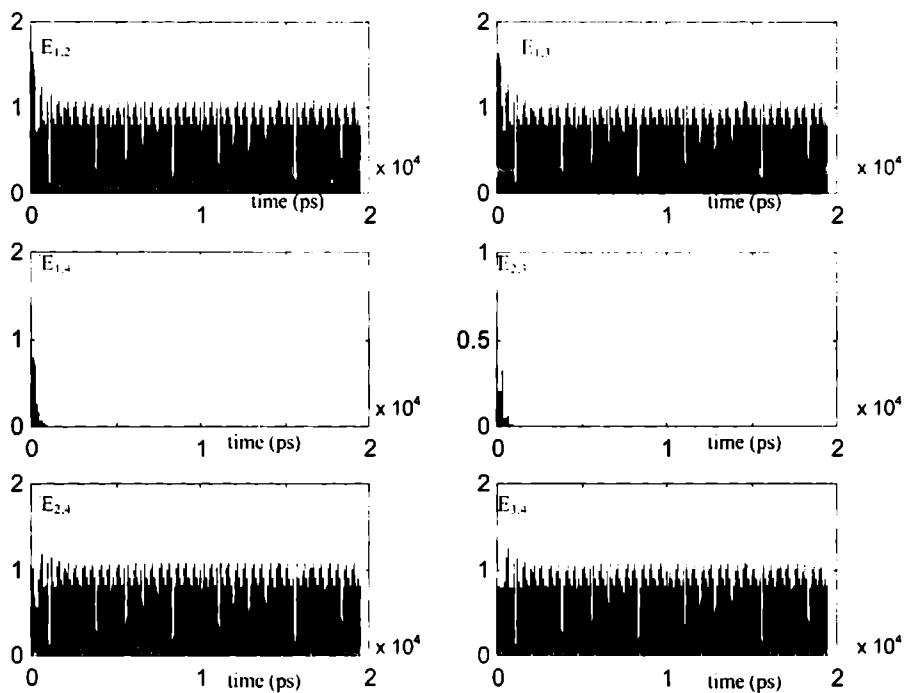


Fig. 7.10a

Synchronisation error plots between all pairs of lasers in a nearest neighbour coupled array with 4 elements for $C = 5$

$E_{x,y}$ – synchronisation error between lasers x and y ; where x and y are positions of elements in an array.

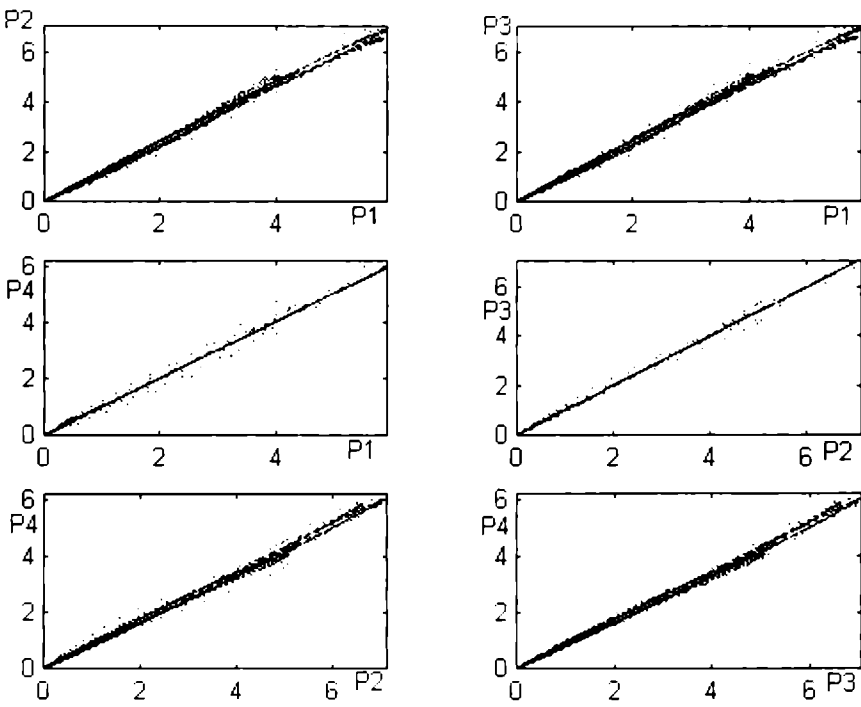


Fig 7.10b

Parameter space plots between all pairs of lasers in a
Nearest neighbour coupled array with 4 elements for $C = 5$

P1, P2, P3, P4 – output powers of lasers 1,2,3,4

The coupling value at which synchronisation occurs is lower when the number of elements in an array is odd. For example When $n = 5$, (1-5) and (2-4) pairs gets exactly synchronised at $C = 1$, however there is no synchronisation between any other pairs. The amplitude of the inner pairs shows a slightly more amplification of the outputs than for outer pairs. In arrays with odd numbers the central laser without a pair will show slightly greater amplitude than all the outer pairs. The results are in perfect agreement with those of Winful *et. al.*^[50] and Terry *et. al.*^[122].

As the coupling strength is increased, for $C < 3$ the outputs of all the lasers show chaotic nature. As C becomes 4 the output of the elements start undergoing a reverse period doubling route and attains stable one cycle nature at $C = 10$. This is true for arrays with odd or even number of elements. When the number of elements in an array is increased beyond 7, the numerical model loses stability for even numbers and for $n = 9$ only the 1-7 lasers show slight synchronisation and, no other pairs show any sort of synchronisation. The outputs of all the lasers undergo reverse period doubling and become stable one cycle at around $C = 10$ for both the arrays with even number of elements and odd number of elements. The overall results are shown in Table 7.5.

Table 7.5
Dynamical properties of nearest neighbour coupled one-dimensional array

C	3	4	5	6	7	8	9	10
1	1-3 E Chaotic	No Syn Chaotic	1-5, 2-4 E Chaotic	No Syn Chaotic	1-7,2-6,3-5 E Chaotic	--	No Sync Chaotic	--
2	1-3. E Chaotic	No Syn Chaotic	1-5, 2-4 E Chaotic	No Syn Chaotic	1-7,2-6,3-5e Chaotic		No Sync Chaotic	
3	1-3 E Chaotic	1-4,2-3 E Chaotic	1-5, 2-4 E P~4	No Syn Chaotic	1-7,2-6,3-5e Chaotic		No Sync Chaotic	
4	1-3. E P~4	1-4,2-3 E P=8	1-5,2-4 E P=4	No Syn P~4	1-7,2-6,3-5 E P=4		No Sync P~4	
5	1-3 E P=4	1-4,2-3 E P=4	1-5, 2-4 E P=2	1-6,2-5,3-4 E P=2	1-7,2-6,3-5 E P=2		No Sync P=2	
6	1-3. E P=2	1-4,2-3 E P=2	1-5, 2-4 E P=2	1-6,2-5,3-4 E P=2	1-7,2-6,3-5 E P=2		No Sync P=2	
7	1-3. E P=2	1-4,2-3 E P=2	1-5, 2-4 E P=2	1-6,2-5,3-4 E P=2	1-7,2-6,3-5 E P=2		No Sync P=2	
8	1-3. E P=2	1-4,2-3 E P=2	1-5, 2-4 E P=2	1-6,2-5,3-4 E P=2	1-7,2-6, 3-5 E P=2		No Sync P=2	
9	1-3. E P=2	1-4,2-3 E P=2	1-5, 2-4 E P=2	1-6,2-5,3-4 E P~1	1-7,2-6,3-5 E P=1		No Sync P=2	
10	1-3. E P=2	1-4,2-3 E P=1	1-5, 2-4 E P=1	1-6,2-5,3-4 E P=1	1-7,2-6,3-5 E P=1		No Sync P=1	

7.2 TWO-DIMENSIONAL ARRAY

This scheme refers to a set of four lasers arranged in two dimensions or in a matrix format with nearest neighbour coupling. This scheme can also be described as a bi-directionally coupled closed loop system. Coupling is given in milliamperes current which is proportional to a fraction of the total power generated by its two nearest neighbours. The schematic is given in Fig 7.11. The difference between this scheme and the above mentioned nearest neighbour coupling scheme is that in this scheme all the elements in the array will receive coupling from the nearest two neighbours as it is a closed system while in the other the outer two lasers will be coupled only to one nearest neighbour.

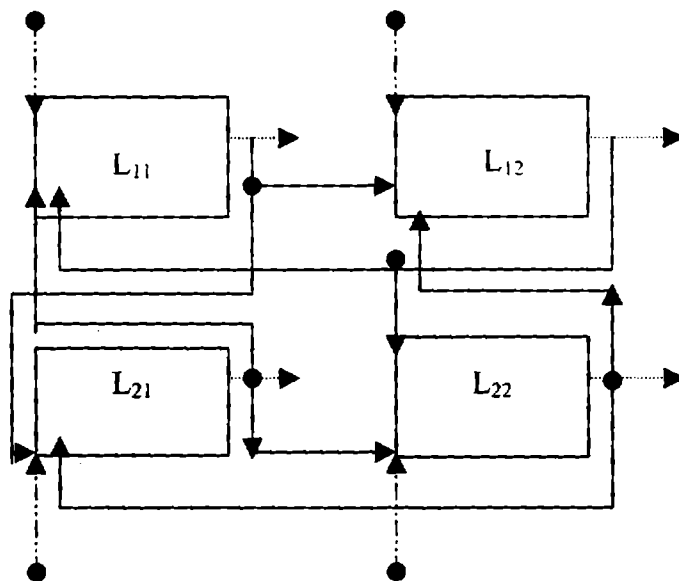


Fig 7.11

Two dimensional array with nearest neighbour coupling

The governing rate equation can be represented as follows,

$$\frac{dN_{11}}{dt} = \left(\frac{1}{\tau_e} \right) \left[\left(\frac{I_{11}}{I_{th}} \right) - N_{11} - \left\{ \frac{(N_{11} - \delta)}{(1 - \delta)} \right\} P_{11} \right] \quad (7.37)$$

$$\frac{dP_{11}}{dt} = \left(\frac{1}{\tau_p} \right) \left[\left\{ \frac{(N_{11} - 1)}{(1 - \delta)} (1 - \varepsilon P_{11}) P_{11} - P_{11} + \beta N_{11} \right\} \right] \quad (7.38)$$

$$I_{11}(t) = I_b + I_m \sin(2\pi f_m t) + G_{11} I_{c,1} \quad (7.39)$$

$$\frac{dN_{12}}{dt} = \left(\frac{1}{\tau_e} \right) \left[\left(\frac{I_{12}}{I_{th}} \right) - N_{12} - \left\{ \frac{(N_{12} - \delta)}{(1 - \delta)} \right\} P_{12} \right] \quad (7.40)$$

$$\frac{dP_{12}}{dt} = \left(\frac{1}{\tau_p} \right) \left[\left\{ \frac{(N_{12} - 1)}{(1 - \delta)} (1 - \varepsilon P_{12}) P_{12} - P_{12} + \beta N_{12} \right\} \right] \quad (7.41)$$

$$I_{12}(t) = I_b + I_m \sin(2\pi f_m t) + G_{12} I_{c,2} \quad (7.42)$$

$$\frac{dN_{21}}{dt} = \left(\frac{1}{\tau_e} \right) \left[\left(\frac{I_{21}}{I_{th}} \right) - N_{21} - \left\{ \frac{(N_{21} - \delta)}{(1 - \delta)} \right\} P_{21} \right] \quad (7.43)$$

$$\frac{dP_{21}}{dt} = \left(\frac{1}{\tau_p} \right) \left[\left\{ \frac{(N_{21} - 1)}{(1 - \delta)} (1 - \varepsilon P_{21}) P_{21} - P_{21} + \beta N_{21} \right\} \right] \quad (7.44)$$

$$I_{21}(t) = I_b + I_m \sin(2\pi f_m t) + G_{21} I_{c,1} \quad (7.45)$$

$$\frac{dN_{22}}{dt} = \left(\frac{1}{\tau_e} \right) \left[\left(\frac{I_{22}}{I_{th}} \right) - N_{22} - \left\{ \frac{(N_{22} - \delta)}{(1 - \delta)} \right\} P_{22} \right] \quad (7.46)$$

$$\frac{dP_{22}}{dt} = \left(\frac{1}{\tau_p} \right) \left[\left\{ \frac{(N_{22} - 1)}{(1 - \delta)} (1 - \varepsilon P_{22}) P_{22} - P_{22} + \beta N_{22} \right\} \right] \quad (7.47)$$

$$I_{22}(t) = I_b + I_m \sin(2\pi f_m t) + G_{22} I_{c,2} \quad (7.48)$$

$$G_{11} = C \times (P_{21} + P_{12}) \times 10^{-3}$$

$$G_{12} = C \times (P_{11} + P_{22}) \times 10^{-3}$$

$$G_{21} = C \times (P_{11} + P_{22}) \times 10^{-3}$$

$$G_{22} = C \times (P_{21} + P_{12}) \times 10^{-3}$$

where C is the coupling strength and P_{xy} , the output power of the array elements with x, y denoting the position of the elements in the array.

7.2.1 NUMERICAL ANALYSIS AND RESULTS

The above sets of equations are numerically simulated for different values of C . As the coupling strength is increased to 2 all the lasers get synchronised with each other. With further increase in C , the outputs undergo reverse period doubling and attains a stable one period output at $C = 9$. The exact synchronisation achieved at $C = 2$ is maintained for all coupling strengths. Fig 7.12a shows the synchronisation error plots between the array elements for $C > 2$ and Fig 7.12b shows the parameter space plots between the array elements for $C > 2$. The output amplitudes increase with increase in the coupling strengths. Dependence of the synchronisation and the dynamical properties are represented in Table 7.6.

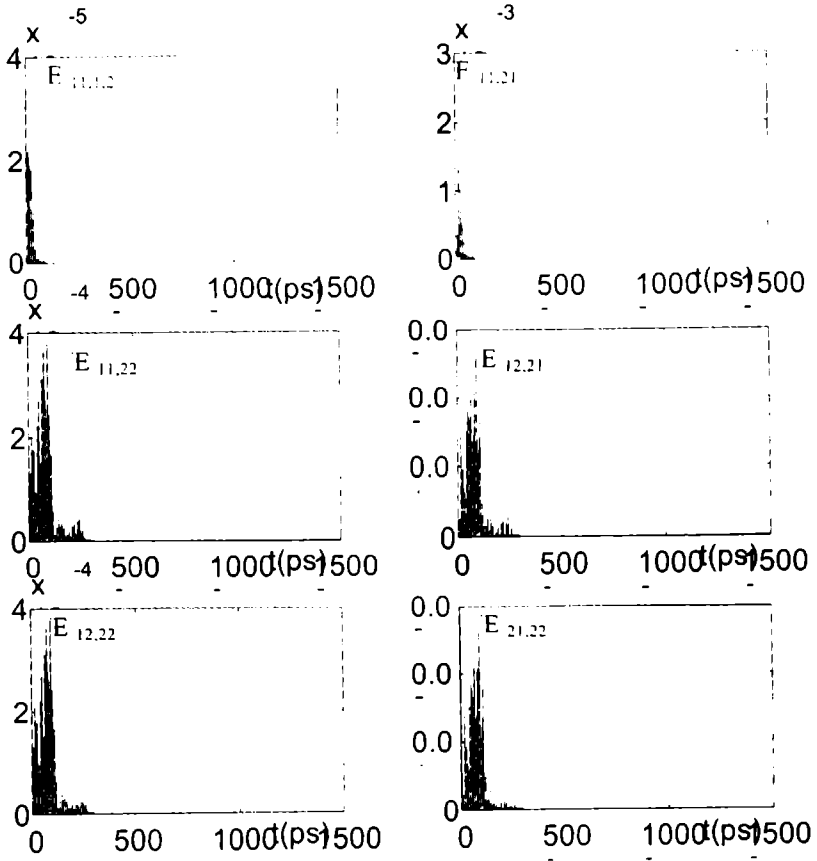


Fig 7.12a

Synchronisation error plots between all pairs of lasers in a two dimensional array with nearest neighbour coupling $C = 2$

$E_{xk, yl}$ – synchronisation error between lasers xk and yl ; where xk and yl are positions of elements in an array arranged in matrix format

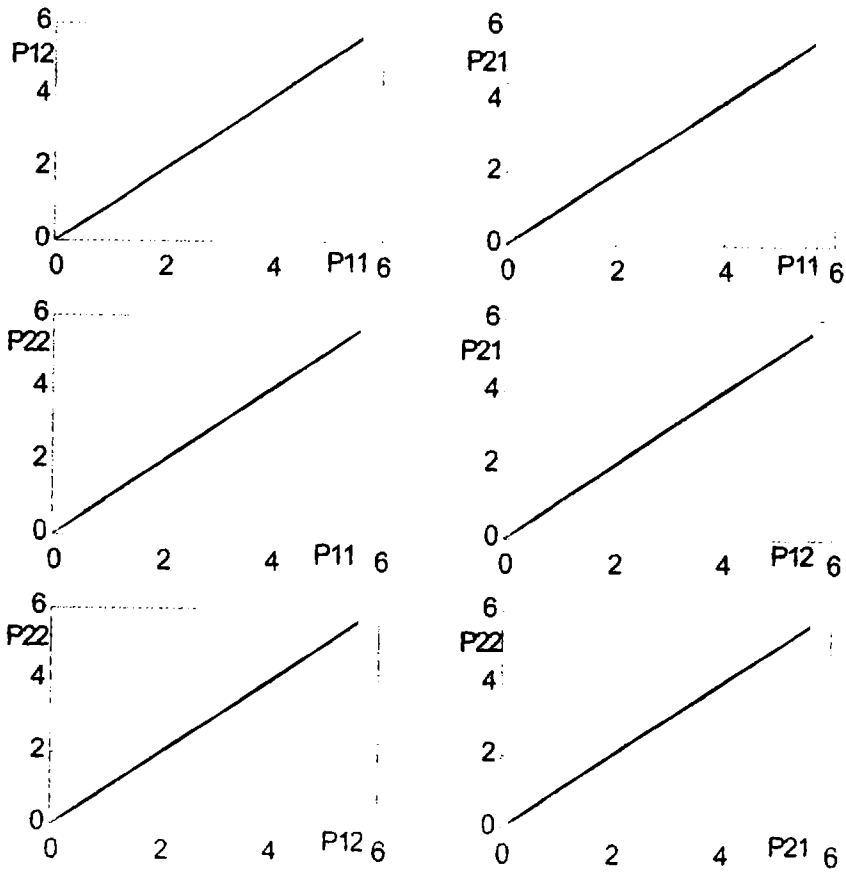


Fig 7.12b

Parameter space plots between all pairs of lasers in an
two dimensional array with nearest neighbour coupling $C = 2$

P_1, P_2, P_3, P_4 – output powers of lasers 1,2,3,4

Table 7.6

Dynamical properties of nearest neighbour coupled two-dimensional array

C	Synchronisation		Dynamical Property
1	No Syn		All Chaotic
2	All E Syn		All Chaotic
3	All E Syn		All P= 4
4	(11-12)-P	(12-22)-No	All P=4
	(11-21)-P	(21-22)-No	
	(11-22)-E		
	(12-21)-E		
5	(11-12)-E	(12-22)-No	All P = 4
	(11-21)-E	(21-22)-No	
	(11-22)-No		
	(12-21)-No		
6	All E Syn		All P = 2
7	All E Syn		All P = 2
8	All E Syn		All P = 1
9	All E Syn		All P = 1
10	All E Syn		All P = 1

SUMMARY AND CONCLUSION

This part of the thesis contains a summary of the work carried out, the results obtained and some suggestions regarding scope for continued research in the field of chaos in semiconductor lasers.

The overall focus of our work presented here is on the synchronisation and the control of chaos in directly modulated semiconductor lasers with respect to different coupling schemes.

The results of our studies on the use of uni-directional and bi-directional coupling schemes for synchronisation of two directly modulated chaotic semiconductor lasers reveal that both uni-directional coupling and bi-directional coupling can induce synchronisation. The uni-directional coupling scheme induces practical synchronisation between the output powers of the two lasers for a small range of coupling strengths. However, this practical synchronisation cannot be improved to exact synchronisation by increasing the coupling strength. Increase in coupling strength can only increase the output amplitudes of the second laser, which will desynchronise the two outputs.

Bi-directional coupling scheme, on the other hand, induces exact synchronisation between the two lasers for relatively low coupling strengths and stability of the synchronised laser outputs for higher coupling strengths. In addition, this method effectively amplifies the synchronised output powers and suppresses the double peak in the outputs, which is a manifestation of relaxation oscillations. These results indicate that bi-directional coupling can prove to have far reaching effects on the dynamical properties of chaotic semiconductor lasers. By varying the coupling strength we can suppress chaos and the double peak and achieve synchronisation between the two outputs together with a high increase in the output powers. The range of the coupling

strengths has to be chosen according to whichever application for which the semiconductor laser system is to be used.

The variable feedback method is used for synchronising two chaotic directly modulated semiconductor lasers in the drive-response scenario. Our results indicate that this method can give exact synchronisation for a wide range of coupling strengths and can prove to be more useful compared to the unidirectional coupling scheme, which also works in a drive-response scenario. This method can be more effective than the uni-directional coupling in areas communication systems where bi-directional coupling scheme cannot be used. where the receiver cannot be coupled back to the transmitter.

We then focussed our attention on the application of the variable feedback method in synchronising the semiconductor lasers used as the transmitter and receiver in a secure communication system. It was found that even though effective synchronisation could be achieved between the lasers without the message in the received signal, this was lost once the message was encoded on to the transmitted signal. Therefore, the feedback function is to be modified appropriately by introducing an integral part to the feedback function. This Proportional-Integral scheme could effectively synchronise the transmitter and receiver and properly unmask the encoded message. Using this method both analog and digital messages could be successfully transmitted and retrieved.

The last section of this work was focussed on an equally important application of semiconductor lasers, i.e. array of lasers. In this case we employed different methods of coupling such as the open loop coupling, global coupling and nearest neighbour coupling for synchronising our system of array of chaotic semiconductor lasers. In addition we introduced a closed loop coupling scheme. The results of our study indicate that synchronisation and dynamical properties are dependent on the coupling strength and also on the number of elements that are present in the array.

Open loop coupling was the least effective in this group and is similar to the uni-directional coupling scheme described above. This method helps only in the amplification of succeeding elements in an array and, as the coupling strength and number of array increase, there is no synchronisation or control of the outputs.

The closed loop scheme is very sensitive to the number of elements in an array. It is found that closed loop coupling can induce synchronisation and control only when there is an even number of elements in the array. In arrays with an odd number of elements this method significantly amplifies the chaotic output powers without synchronising them.

Global coupling scheme is effective in inducing synchronisation and controlling the chaotic outputs. This method is sensitive to increase in coupling strength and also to the increase in the number of elements in an array. Because all the

array elements are directly influenced by all other outputs, this is an example of collective interaction. Increase in the number of elements in an array does not affect the stability of this system but increase in coupling strength will strongly affect the stability. Therefore, whatever be the number of elements in a particular array, the choice of coupling strength should be restricted within a small range. However, this will not reduce the types of behaviours that can be expected from an array, since synchronisation and control of chaos can be achieved even for small coupling strengths in the case of arrays with even or odd number of elements.

In the case of nearest neighbour coupling scheme, synchronisation is achieved only between the outer pairs of lasers. Even higher of coupling strengths could not induce synchronisation between any of the outer and inner pairs of lasers. However, increase in the coupling strength can induce stability can be achieved through reverse period doubling for the array elements. The dynamics is weakly dependent on the number of elements in an array, in that synchronisation and stability can be achieved for relatively lower values of coupling strengths in the case of arrays with odd number of elements. This scheme is the least effective in providing amplification of the output powers.

The overall outcome of this study indicates that when the number of elements in an array is small any one of the closed loop coupling, nearest neighbour coupling or the global coupling, can be used depending on whether the number is odd or even. When the number of elements is odd either the global or the

nearest neighbour coupling can be used and the range of coupling strength is to be chosen depending on the desired dynamics. However, when the number of elements in an array is even, closed loop coupling can be used and in this case closed loop coupling can prove to be the best since this can provide exact synchronisation between all pairs of lasers for a wide range of coupling strengths. When the number of elements is odd global coupling would be the choice with special note on the coupling strength. Thus the choice of coupling scheme and number of elements depend on the particular choice of application.

As our concluding remarks we would like to add a note on the possibility of future investigations in this direction. Other types of feedback functions can be used and the effectiveness of these methods on synchronisation can be studied. In the field of secure communication the level of security of the encoded message signal can be investigated and for improving the level of security methods like using cascaded systems or hyper chaotic systems as the message transmitter^[128,129] can be employed. Coherence of the amplified synchronised outputs can be studied and effect of each of the coupling schemes on coherence properties can be investigated. Effect of parameter mismatch on synchronisation properties of the current model can be investigated^[130].

REFERENCES

The literature which was reviewed and which served as the background for our studies are cited in the following pages. The scientific papers which were published based on the outcome of the present work are also included.

REFERENCES

1. E. N. Lorenz. J. Atmos. Sci, **20** (1963) 130
2. Foundations of Synergetics II Complex Patterns. A. S Mikhailov & A.Yu. Loskutov. Series ed. H. Haken; Springer-Verlag, (1991)
3. H. Poincaré. Foundations of Science: Science and Method, English Translation, The Science Press, (1946)
4. Chaotic Dynamics, G. L. Baker & J. P. Gollub. Cambridge Univ. Press, II Ed, (1996)
5. Introduction to Chaos and Coherence. J. Froyland, Intst. of Phys. Publ. (1992.)
6. Deterministic Chaos. N. Kumar, Univ. Press.(1996)
7. R. May. Nature, **261**, (1976) 459
8. Order Within Chaos. P. Berge, Y. Pomeau & C. Vidal. Herman and, John Wiley & Sons Inc., (1984)
9. Deterministic Chaos-An Introduction, H. G. Schuster, VCH, Verlag Sgesellschaft, (1995)
10. Chaos in Laser- Matter Interactions. P. W. Milonni, M- L Shih & J. R. Ackerhalt. World Scientific Publishing Co Pte Ltd. (1987)

-
11. Chaos in Dynamical Systems. Edward Ott. Cambridge Univ. Press (1993)
 12. Lasers-Principles and Applications. J. Wilson & J. F. B. Hawkes. Prentice Hall (1987)
 13. Fundamentals of Photonics. B.E.A.Saleh & M.C.Teich. John Wiley & Sons Inc.(1991)
 14. Essentials of Optoelectronics. A. Rogers. Chapman & Hall (1997)
 15. Long Wavelength Semiconductor Lasers. G. P. Agrawal & N. K. Dutta, Van Nostrand Reinhold Co (1986)
 16. H. Haken. Phys. Lett A **53** (1975) 77
 17. F. T. Arecchi, R. Meucci, G.Pucconioni & J. Tredicce. Phys. Rev. Lett **49** (1982) 1217
 18. R. S. Gioggia & N. B. Abraham. Phys. Rev. Lett. **51** (1983) 650
 19. W.Klische, H. R. Telle & C. O. Weiss. Opt. Lett. **9** (1984) 561
 20. M. F. H. Jarroja, N .B. Abraham, D. K. Bandy & L. M. Narducci. Phys. Rev. A. **34** (1986) 3148
 21. M. A. Dupertius, R. R. E. Saloma & M. R. Siegrist. Opt. Comm. **57** (1986) 410
 22. H. Kawaguchi. Appl. Phys. Lett. **45** (1984) 1264
 23. J. Sacher, W. Elsasser & E. O. Gobel. Phys. Rev. Lett. **63** (1989) 2224
 24. M. Tang & S. Wang. Appl. Phys. Lett. **48** (1986) 900
 25. H. G. Winful, Y. C. Chen & J. M. Liu. Appl. Phys. Lett. **48** (1986) 616
 26. Y. H. Kao & H. T. Lin. IEEE. J. Quan. Elec. **29** (1993) 1617
 27. G. P. Agrawal. Appl. Phys. Lett. **49** (1986) 1013

-
28. N. F. Rulkov, M. M. Suschik & L. S. Tsimring. *Phys. Rev. E.* **51** (1995) 980
 29. L. M. Pecorra & T. L. Carroll. *Phys. Rev. Lett.* **64** (1990) 821
 30. L. M. Pecorra & T. L. Carroll. *Phys. Rev. A.* **44** (1991) 2374
 31. T. L. Carroll & G. A. Johnson. *Phys. Rev. E.* **57** (1998) 1555
 32. L. M. Pecorra, T. L. Carroll, A. Johnson & D. Mar. *Phys. Rev. E.* **56** (1997) 5090
 33. Anil. Maybhate & R.E.Amritkar. *Phys.Rev. E.* **59** (1999) 284
 34. A.L.Gelover-Santiago, R.Lima & G.Martinez-Mekler. *Int.J.Bifur.Chaos.* **10** (2000) 453
 35. Y.Hong, H.Qin & G.Chen. *Int. J. Bifurc. Chaos.* **11** (2001) 1149
 36. B.Cannas, S.Cincotti & E. Usai. *IEEE Trans. Circ.& Sys.* **49** (2002) 1000
 37. A.Volkovski. *IEEE Trans. Circ.& Sys.* **44** (1997) 913
 38. C.K.Duan & S.S.Yang. *Phys. Lett. A.* **229** (1997) 151
 39. J.Guemez & M.A. Matiaz. *Phys. Lett. A.* **246** (1998) 289
 40. R.Wang & K.Shen. *Phys. Rev. E.* **65** (2001) 016207
 41. H.Fujisaka & T.Yamada. *Prog. Theor. Phys.* **69** (1983) 32
 42. N. F. Rulkov, A.R.Volkovski, A.Rodriguez-Lozano,E.Del Rio & M.G.Velarge. *Int. J. Bifurc. Chaos.* **2** (1992) 669
 43. O.Morgul & M.Feki *Phys. Rev. E.* **55** (1997) 5004
 44. O.Morgul. *Phys. Lett . A.* **247** (1998) 391
 45. K.Pyragas. *Phys. Lett. A.* **170** (1992) 421
 46. S.Kaart, J.C.Schouten & Corr.M.V.Bleck. *Phys. Rev. E.* **59** (1999) 5303

-
47. M.G.Rosenblum, A.S.Pikovsky & J.Kurths. *Phys. Rev. Lett.* **76** (1996) 1804
 48. M.G.Rosenblum, A.S.Pikovsky & J.Kurths. *Phys. Rev. Lett.* **78** (1997) 4193
 49. R.Femat & G. S. Perales. *Phys. Lett. A.* **262** (1999) 50
 50. H.G.Winful & L. Rahman. *Phys. Rev. Lett.* **65** (1990) 1575
 51. R.Roy & K.S.Thornburg Jr. *Phys. Rev. Lett.* **72** (1994) 2009
 52. T.Sugawara, M.Tachikawa, T.Tsukamoto & T.Shimizu. *Phys. Rev. Lett.* **72** (1994) 3502
 53. C.R.Mirasso, P.Colet & P.Garcia-Fernandez. *IEEE Phot. Tech. Lett.* **8** (1996) 299
 54. V.Annavozzi-Lodi. *IEEE J. Quan. Elec.* **32** (1996) 953
 55. A.Hohl, A.Gavrielides, T.Erneux & V.Kovanis. *Phys. Rev. Lett* **78** (1997) 4745
 56. J.P.Godgebuer, L.Larger & H.Porte. *Phys. Rev. Lett.* **80** (1998) 2249
 57. G.D.Van Wiggeren & R.Roy. *Science.* **279** (1998) 1198
 58. G.D.Van Wiggeren & R.Roy. *Phys. Rev. Lett.* **81** (1998) 3547
 59. S.Sivaprakasam & K. A. Shore. *IEEE J. Quan. Elec.* **36** (2000), 35
 60. *Controlling Chaos Through Parametric Excitations, Dynamics and Stochastic Processes.* M.Pettini. Eds. R.Lima, L.Streit, M.Pettini & R.V.Mendes (Springer-Verlag, New York) (1988) 242
 61. E.Ott, C.Grebogi & J.A.Yorke. *Phys. Rev. Lett.* **64** (1990) 1196
 62. E.R.Hunt. *Phys. Rev. Lett.* **67** (1991) 1953

-
63. K.Murali & M.Lakshmanan. *J. Circ. Sys. Comp.* **3** (1993) 125
 64. J.Gao, X.Wang, G.Hu & J.Xiao. *Phys. Lett. A.* **283** (2001) 342
 65. W.Huang. *Phys. Rev. E.* **65** (2001) 010215
 66. R.Femat, J.A Rameirez & J.Gonzales. *Phys. Lett. A.* **224** (1997) 271
 67. R.Femat, J.Tobias & G.S.Perales. *Phys. Lett. A.* **252** (1999) 27
 68. W.L.Ditto, S. M. Rausco & M.Spano. *Phys. Rev. Lett.* **65** (1990) 3211
 69. R.Roy, T.W.Murphy, T.D.Maier, Z.Gills & E.R.Hunt. *Phys. Rev. Lett.* **68** (1992) 1259
 70. Y.Liu, L.C.Barbosa & J.R.Riosleite. *Phys. Lett. A.* **193** (1994) 259
 71. T.Kuruvilla & V.M.Nandakumaran. *Phys. Lett. A.* **59** (1999) 254
 72. T.Shinbrot, E.Ott, C.Grebogi & J.A.Yorke. *Phys. Rev. Lett.* **65** (1990) 3215
 73. T.Shinbrot, W.L.Ditto, C.Grebogi, E.Ott, M.Spano & J.A.Yorke. *Phys. Rev. Lett.* **68** (1992) 2863
 74. Y.Nagai & Y.C.Lai. *Phys. Rev. E.* **51**(1995) 3842
 75. J.L.Chern & J.K. Mc-Iver. *Phys. Lett. A.* **151** (1990) 150
 76. D.E.Postnov, A.G.Balnov, O.V.Sosnovpseva & E.Mosekilde. *Phys. Lett. A.* **283** (2001) 195
 77. J.N.Blakely & D.J.Gautier. *Chaos.* **10** (2000) 738
 78. M.Nan, K.Tsang, C.Wong & X.Shi. *Phys. Rev. E.* **60** (1999) 5439
 79. Y.L. Maestrenko, V.L.Maestrenko, O.Popovych & E.Mosekilde. *Phys. Rev. E.* **60** (1999) 2817
 80. G.L.Baker, J.A.Blackburn & H.J.T. Smith. *Phys. Lett. A.* **252** (1999) 191

-
119. S.S.Wang & H.G.Winful. *Appl. Phys. Lett.* **52** (1988) 1774
 120. M.Chabanol & V.Zehle. *Phys. Rev. A.* **63** (2001) 053809
 121. S.Dasgupta & D.R Anderson. *J. Opt. Soc. Am. B.* **11** (1994) 290
 122. J.R.Terry, K.S.Thornburg,D.J.De shazer, G.D.Wan Wiggeren,S.Zhu, P.Ashwin & R.Roy. *Phys. Rev. E.* **59** (1999) 4036
 123. D.J.De Shazer, R.Breban, E.Ott & R.Roy. *Phys. Rev. Lett.* **87** (2001) 044101
 124. J.G.Ojalvo, J.Casatemont, M.C.Torrent, C.R.Mirrasso & J.M.Sancho, *Int. J. Bifurc. Chaos.* **9** (1999) 2225.
 125. V.Bindu & V.M.Nandakumaran. *Nat. Laser Symp.* (2000)
 126. V.Bindu & V.M.Nandakumaran. *Recent Advances in Nonlinear Science*(2002)
 127. V.Bindu & V.M.Nandakumaran. *Int. Con. Stochastic Optimisation & Adaptation.* (2000)
 128. K.Murali. *Int. J. Bifurc. Chaos.* **10** (2000) 2489
 129. V.Ahlers, U.Parlitz & W.Lauterborn. *Phys. Rev. E.* **58** (1998) 7208
 130. A.Jalnine & S.Kim. *Phys. Rev. E.* **65** (2002) 026210

G 8535

-
63. K.Murali & M.Lakshmanan. *J. Circ. Sys. Comp.* **3** (1993) 125
 64. J.Gao, X.Wang, G.Hu & J.Xiao. *Phys. Lett. A.* **283** (2001) 342
 65. W.Huang. *Phys. Rev. E.* **65** (2001) 010215
 66. R.Femat, J.A Rameirez & J.Gonzales. *Phys. Lett. A.* **224** (1997) 271
 67. R.Femat, J.Tobias & G.S.Perales. *Phys. Lett. A.* **252** (1999) 27
 68. W.L.Ditto, S. M. Rauseo & M.Spano. *Phys. Rev. Lett.* **65** (1990) 3211
 69. R.Roy, T.W.Murphy, T.D.Maier, Z.Gills & E.R.Hunt. *Phys. Rev. Lett.* **68** (1992) 1259
 70. Y.Liu, L.C.Barbosa & J.R.Riosleite. *Phys. Lett. A.* **193** (1994) 259
 71. T.Kuruvilla & V.M.Nandakumaran. *Phys. Lett. A.* **59** (1999) 254
 72. T.Shinbrot, E.Ott, C.Grebogi & J.A.Yorke. *Phys. Rev. Lett.* **65** (1990) 3215
 73. T.Shinbrot, W.L.Ditto, C.Grebogi, E.Ott, M.Spano & J.A.Yorke. *Phys. Rev. Lett.* **68** (1992) 2863
 74. Y.Nagai & Y.C.Lai. *Phys. Rev. E.* **51**(1995) 3842
 75. J.L.Chern & J.K. Mc-Iver. *Phys. Lett. A.* **151** (1990) 150
 76. D.E.Postnov, A.G.Balnov, O.V.Sosnovpseva & E.Mosekilde. *Phys. Lett. A.* **283** (2001) 195
 77. J.N.Blakely & D.J.Gautier. *Chaos.* **10** (2000) 738
 78. M.Nan, K.Tsang, C.Wong & X.Shi. *Phys. Rev. E.* **60** (1999) 5439
 79. Y.L. Maestrenko, V.L.Maestrenko, O.Popovych & E.Mosekilde. *Phys. Rev. E.* **60** (1999) 2817
 80. G.L.Baker, J.A.Blackburn & H.J.T. Smith. *Phys. Lett. A.* **252** (1999) 191

-
81. I.V.Koryukin & P.Mandel. *Phys. Rev. E.* **65** (2002) 026021
 82. I.Wedekind & U.Parlitz. *Int. J. Bifurc. Chaos.* **11** (2001) 1141
 83. T.Kuruvilla & V.M.Nandakumaran. *Pramana. J. Phys.* **54** (2000) 393
 84. T.Kuruvilla & V.M.Nandakumaran. *Phys. Lett. A.* **254** (1999) 59
 85. V.Bindu & V.M.Nandakumaran. *Int.Con.Laser Materials & Devices.* 1999
 86. V.Bindu & V.M.Nandakumaran. *Phys. Lett. A.* **277** (2000) 345
 87. T.C.Newell, V.M.Alsing, A.Gavrielides & V.Kovanis. *Phys. Rev. E.* **49** (1994) 313
 88. J.M.Liu & T.B.Simpson. *IEEE Phot. Tech. Lett.* **4** (1993) 380
 89. B.C.Buchler, E.H.Huntington, C.C.Harb & T.C.Ralph. *Phys. Rev. A.* **57** (1998) 1286
 90. M.K.Ali. *Phys. Rev. E.* **55** (1997) 4804
 91. V.Bindu & V.M.Nandakumaran. *Nat. Laser Symp.* (1999)
 92. J.A.K.Suykens, P.E.Curran & L.O.Chua. *IEEE Trans. Circ & Sys.* **46** (1997) 891
 93. T.L.Carroll. *IEEE Trans. Circ & Sys.* **42** (1995) 105
 94. K.M.Cuomo & A.V.Oppenheim. *Phys. Rev. Lett.* **71** (1993) 65
 95. T.L.Liao & N.S.Huang. *IEEE Trans. Circ & Sys.* **46** (1999) 1144
 96. C.W.Wu & L.O.Chua. *Int. J. Bifurc. Chaos.* **3** (1993) 1619
 97. Y.C.Lai, E.Bollt & C.Grebogi. *Phys. Lett. A.* **255** (1999) 75
 98. A.A.Minai & T.Anand. *Phys. Rev. E.* **59** (1999) 312
 99. M.Nan, C.Wong, K.Tsang & X.Shi. *Phys. Lett. A.* **268** (2000) 61
 100. K.Murali. *Phys. Lett. A.* **272** (2000) 184

-
101. K.Murali & M.Lakshmanan. Phys. Rev. E. **49** (1994) 4882
102. Lj.Kocarev, K.Halle, Keckert, L.O.Chua & U.Parlitz. Int. J. Biifurc. & Chaos. **2** (1992) 709
103. O.Morgul & M.Feki. Phys. Lett. A. **251** (1999) 169
104. K.M.Cuomo, A.V.Oppenheim & S.H.Strogatz. Int. J. Bifurc & Chaos. **3** (1993) 1629
105. P.Celka. IEEE Trans. Circ & Sys **42** (1995) 455
106. K.S.Halle, C.Wu, M.Itoh & L.O.Chua. Int. J. Biifurc. & Chaos. **3** (1993) 469
107. K.Murali & M.Lakshmanan. Phys. Rev. E. **56** (1997) 251
108. K.Murali & M.Lakshmanan. Phys. Lett. A. **241** (1998) 303
109. H.F.Chen & J.M.Liu. IEEE J. Quan. Elec. **36** (2000) 27
110. S.Sivaprakasam & K.A.Shore. Opt. Lett. **24** (1999) 1200
111. V.Bindu & V.M.Nandakumaran. J. Opt. A. Pure. & Appl. Opt. **4** (2002) 115
112. C.W.Wu & L.O.Chua. IEEE Trans. Circ.& Sys. **42** (1995) 430
113. G.V.Osipov & M.M.Suschik. Phys. Rev. E. **58** (1998) 7198
114. A.A.Minai. Phys. Lett. A. **251** (1999) 31
115. J.K.Butler, D.Eackley & D.Botez. Appl. Phys.Lett. **44** (1984) 293
116. L.Rahman & H.G.Winful. Opt. Lett. **18** (1993) 128
117. J.K.Ehlert, W.J.Cossarly, J.M.Finlan & K.M.Flood. Appl. Phys. Lett. **64** (1994) 1478
118. Y.Twu, K.L.Chen, S.Wang, J.R. Whinnery & A.Diens. Appl. Phys. Lett. **48** (1986) 16



-
119. S.S.Wang & H.G.Winful. *Appl. Phys. Lett.* **52** (1988) 1774
 120. M.Chabanol & V.Zehle. *Phys. Rev. A.* **63** (2001) 053809
 121. S.Dasgupta & D.R Anderson. *J. Opt. Soc. Am. B.* **11** (1994) 290
 122. J.R.Terry, K.S.Thornburg,D.J.De shazer, G.D.Wan Wiggeren,S.Zhu, P.Ashwin & R.Roy. *Phys. Rev. E.* **59** (1999) 4036
 123. D.J.De Shazer, R.Breban, E.Ott & R.Roy. *Phys. Rev. Lett.* **87** (2001) 044101
 124. J.G.Ojalvo, J.Casatemont, M.C.Torrent, C.R.Mirrasso & J.M.Sancho, *Int. J. Bifurc. Chaos.* **9** (1999) 2225.
 125. V.Bindu & V.M.Nandakumaran. *Nat. Laser Symp.* (2000)
 126. V.Bindu & V.M.Nandakumaran. *Recent Advances in Nonlinear Science*(2002)
 127. V.Bindu & V.M.Nandakumaran. *Int. Con. Stochastic Optimisation & Adaptation.* (2000)
 128. K.Murali. *Int. J. Bifurc. Chaos.* **10** (2000) 2489
 129. V.Ahlers, U.Parlitz & W.Lauterborn. *Phys. Rev. E.* **58** (1998) 7208
 130. A.Jalnine & S.Kim. *Phys. Rev. E.* **65** (2002) 026210

G 8535